1994

Correlation of locally-based performance of asphalts with their physicochemical parameters

Sang-Soo Kim
Iowa State University

Order Number 9424233

Correlation of locally-based performance of asphalts with their physicochemical parameters

Kim, Sang-Soo, Ph.D.

Iowa State University, 1994

U·M·I
300 N. Zeeb Rd.
Ann Arbor, MI 48106

Correlation of locally-based performance of asphalts with their physicochemical parameters

by

Sang-Soo Kim

A Dissertation Submitted to the

Graduate Faculty in Partial Fulfillment of the

Requirements for the Degree of

DOCTOR OF PHILOSOPHY

Department: Civil and Construction Engineering
Major: Civil Engineering (Civil Engineering Materials)

Approved:

Signature was redacted for privacy.

In Charge of Major Work

Signature was redacted for privacy.

For the Major Department

Signature was redacted for privacy.

For the Graduate College

Iowa State University
Ames, Iowa

1994

DEDICATION

In loving memory of my brother, Min-Soo Kim

TABLE OF CONTENTS

LIST OF FIGURES

LIST OF TABLES

ACKNOWLEDGMENTS

The author wishes to extend the most sincere appreciation to his major professor Dr. Dah-Yinn Lee. His caring, patient, and enthusiastic guidance and instruction throughout this research and the author's graduate study at the Iowa State University are gratefully acknowledged. The author would also like to extend sincere gratitude to his committee members: Dr. Richard L. Handy for serving as chair for the author's minor in Geotechnical Engineering, and also Dr. Kenneth L. Bergeson, Dr. Herbert T. David, and Dr. Glen A. Russell for their guidance and for many helpful suggestions.

The author wishes to express sincere appreciation to Dr. B. Vedat Enustun for helping many parts of this study.

The author would like to thank the engineers of the Iowa Department of Transportation for their support and cooperation. The author would also like to thank Dr. Bernard C. Gerstein, Professor of Chemistry, Iowa State University for the NMR work.

Special thanks are rendered to Dr. Jan F. Branthaver and Dr. John F. McKay, the Western Research Institute, for many helpful discussions on asphalt chemistry and to Dr. John J. Duvall, the Western Research Institute, for many good suggestions and a thorough review of this manuscript.

Finally, the author would like to extend sincere appreciation to his parents in Korea and to his wife, Hyunsun, for their encouragement and support during the course of this study.

ABSTRACT

This research was undertaken to study the relationships between the performance of locally available asphalts and their physicochemical properties under Iowa conditions with the ultimate objective of development of a locally and performance-based asphalt specification for durable pavements.

Physical and physicochemical tests were performed on three sets of asphalt samples including: (a) twelve samples from local asphalt suppliers, (b) six core samples of known service records, and (c) a total of 79 asphalt samples from 10 pavement projects including original, lab aged, and recovered asphalts from field mixes and lab aged mixes. Tests included standard rheological tests, HP-GPC, and TMA. Some specific viscoelastic tests at 5°C were run on the (b) samples and some (a) samples. DSC and X-ray diffraction studies were performed on the (a) and (b) samples. In addition, NMR techniques were applied to some (a), (b), and (c) samples.

Efforts were made to identify physicochemical properties which are correlated to physical properties known to affect field performance. The significant physicochemical parameters were used as a basis for an improved performance-based trial specification for Iowa to ensure more durable pavements.

I. INTRODUCTION

Current specifications for asphalt cement contain limits on physical properties based on correlations established in the past with field performance of asphalt pavements. Recently, however, concerns have arisen that although current asphalts in use meet these specifications, they are not consistently providing the long service life once achieved.

There are a number of logically possible explanations of this situation:

(1) A considerable concern is associated with the changes in the world crude oil supply and the economic climate after the 1973 oil embargo which may have affected the properties of asphalt of certain origin [47]. Blending several crudes, as routinely practiced in refineries to produce asphalts meeting current specifications, may have upset certain delicate balances of compatibility between various asphaltic constituents, which may manifest itself in their long-term field performance but not in original physical properties specified in the specifications [37,82].

(2) The increased volume and loads of traffic on highways, which have occurred over the decades, may have shortened the life span of pavements, indicating the necessity of revising specification limits and/or imposing new provisions to maintain desired durability.

(3) Inadequate mixture design, particularly gradation of aggregates, changing construction practices and improper use of additives may also be responsible for early deterioration of asphalt pavements [4,47].

(4) Specifications based only on physical properties of asphalts do not guarantee

adequate performance. The physical properties currently being used in specifications have been empirically developed and can not be considered as fundamental properties. The Strategic Highway Research Program (SHRP) [101] showed that the physical properties of asphalts are governed by chemical composition. A physical state at a given temperature can be achieved by several different combinations of chemical compositions which result in widely different physical states at different temperatures. Furthermore, some performance characteristics, such as resistance to moisture damage, are directly related to chemical makeup of asphalt and aggregate.

The selection of asphalts based on performance-related properties, tests, and specifications is one of the key factors for durable asphalt pavements. The performance of pavements could also be improved by judicious application of improved mix design techniques, more rational thickness design procedures, and better construction methods and quality control measures.

Asphalts used in the state of Iowa were collected and their physical properties were determined. The asphalt samples were also analyzed by high performance gel permeation chromatography (HP-GPC), thermomechanical analyzer (TMA), differential scanning calorimetry (DSC), X-ray diffraction (XRD), and nuclear magnetic resonance (NMR). The results were correlated with properties known to affect field performance. On the basis of the correlations, trial performance-based specifications for the state of Iowa were developed.

II. LITERATURE REVIEW

Asphalt is a complex mixture of chemical compounds. Chemical composition of asphalt governs physical and engineering properties of asphalt which, in turn, determine performance or distresses of asphalt pavements. Major distress modes in asphalt pavement failure are low temperature thermal cracking, fatigue cracking, rutting, and moisture damage. Pavements crack when asphalts do not have enough viscous properties to accommodate thermal contraction and expansion resulting from temperature fluctuations or repeated deformation by traffic. Pavements rut when asphalts do not possess enough elasticity or stiffness at high pavement temperatures. Certain combinations of asphalt and aggregate are very susceptible to water invasion and result in stripping problems (moisture damage). In these kinds of pavement failures, chemical composition of asphalt plays a significant role. In this chapter, some conventional physical tests, physical parameters, and specifications often used by asphalt technologists to build asphalt pavements and to estimate performance of pavements are reviewed. Chemical properties of asphalt and characterization techniques used in this dissertation research are also discussed. The relationships between the chemical properties of asphalt and their physical properties are also reviewed in this chapter.

A. Physical Properties of Asphalt

1. Historical development of asphalt testing methods

At the beginning of asphalt paving history from the 1870s to the 1890s, Trinidad Lake asphalt and Bermudez Lake asphalt were the primary sources of the asphalt used

for pavement construction in the United States. The promoters of these native asphalts exercised a monopoly and attempted to restrict the use of other asphalts, especially petroleum asphalts refined from crude oils. In this period, merely to identify the source of an asphalt and to restrict the use of petroleum asphalts or untried sources, simple asphalt specifications were used. These specifications consisted of the appearance of the crude asphalt and analytical tests to determine amounts of bitumen, organic insolubles, and inorganic matter. Because these solid native asphalts were blended with fluxes to reduce their consistency, volatility and hardening of fluxed asphalts during construction and in service became a great concern. To determine and control the volatility and hardening of asphalts, oven heat tests were developed. As more various sources of asphalt were used in construction, specifications were needed to control the quality of asphalts. Penetration tests were developed to determine and control consistency of asphalt. Several other test methods for determining the rheological properties of asphalt also had been developed and used on a local basis [41,78].

Schweyer [93] discussed dozens of test methods and equipment developed over several decades from a simple penetration test device to a very complicated instrument to characterize the viscoelastic properties of asphalt.

Along with the penetration test, softening point and viscosity measurements became the most commonly employed standard physical tests for an asphalt study and specification. These three test methods are briefly reviewed as follows.

In the penetration test (ASTM D 5 and AASHO T 49), penetration depth of a specific needle into an asphalt is recorded in tenths of a millimeter under a specific

temperature, load, and period of time.

Softening point (ASTM D 36 and AASHO T 53) represents the approximate melting point of asphalt. Softening point is used because melting of asphalt does not take place at a definite temperature. As the temperature rises, asphalt gradually changes from an extremely viscous and slow-flowing material to a softer and less viscous liquid. Softening point is determined by an arbitrary and closely defined method. A ring filled with asphalt and loaded with a steel ball is heated in a bath and the temperature at which the asphalt reaches a certain deformation is reported as the ring and ball softening point, $T_{R\&B}$.

For determining absolute or kinematic viscosity of asphalt at 60°C or higher, precisely manufactured and calibrated vacuum tubes or capillary tubes are used (ASTM D 2170, D 2171 and AASHO T 201, T 202). At temperatures of 25°C or lower, a cone and plate viscometer (ASTM D 3205) is used where viscosity is determined as a function of the shear rate. Asphalt placed between the cone and plate is simply sheared by a constant torque and the shear rate is determined from the angular velocity. Shear index, the slope of the log viscosity versus log shear rate plot, and complex flow, the slope of the log shear stress versus log shear rate plot, can be determined.

These three rheological properties, penetration, softening point, and viscosity, are very closely related with one another. Although there are some discrepancies [30,92], generally at ring and ball softening point, asphalts are considered to have a penetration of 800 (25°C, 100g, 5sec) and a viscosity of 1,300 Pa·s [43,83].

Low temperature properties of asphalt have received a great amount of attention

due to their significant influence on pavement cracking. To study low temperature rheological properties of asphalt, the Schweyer constant stress rheometer and the Fraass brittle point test are commonly employed [93]. The Schweyer constant stress rheometer allows measurement of rheological properties at -10°C or lower. Shear modulus, stiffness and viscosity can be determined from creep response of asphalt in a tube [103].

In the Fraass brittle point test, a thin film of asphalt coated on a metal plaque is cooled and flexed in accordance with specified conditions. The temperature at which the asphalt first becomes brittle as indicated by the appearance of cracks is referred to as the Fraass breaking point. This temperature can be -26°C or lower for some asphalts. At this breaking point, asphalts are believed to have a viscosity of about 4×10^8 Pa·s and a stiffness of 1.1×10^8 Pa at an 11 second loading time [107].

After five years of study (1987-1992), the Strategic Highway Research Program proposed new asphalt specifications utilizing very complex and delicate asphalt testing equipment [101]. For example, a dynamic shear rheometer measures dynamic responses of asphalt samples placed between two parallel plates to sinusoidally applied shear stress or strain. In the strain controlled test, dynamic modulus can be calculated using the following equation:

$$|G^*(\omega)| = |\tau(\omega)| / |\gamma(\omega)|$$

where, $|G^*(\omega)|$ = dynamic shear modulus at frequency ω,
$|\tau(\omega)|$ = absolute magnitude of shear stress response, and
$|\gamma(\omega)|$ = absolute magnitude of applied shear strain.

In viscoelatic materials such as asphalts, the response lags behind the applied shear strain or stress. The amount of lagging is expressed by the phase angle, δ. Purely elastic materials have a 0° phase angle while purely viscous materials have a 90° phase angle. For presentation of viscoelastic properties measured by the dynamic shear rheometer, the dynamic shear modulus is divided into two components; one, in-phase with the applied strain (storage modulus, $G'(\omega)$, an elasticity measure) and another, out-of-phase with the applied strain (loss modulus, $G''(\omega)$, an viscosity measure). Calculations of these two modulus are as follows:

$$G'(\omega) = |G^*(\omega)| \cos \delta$$

$$G''(\omega) = |G^*(\omega)| \sin \delta, \text{ and}$$

$$G''(\omega) / G'(\omega) = \tan \delta$$

The ratio of the moduli, $\tan \delta$, is an important indicator describing viscoelastic properties of asphalt. The strain levels in the dynamic shear rheometer measurement must be within the linear region and at a frequency which represents highway traffic loading. A frequency of 10 rad/sec is used for specification purposes. This equipment measures viscoelastic properties of asphalt at intermediate to upper temperature ranges.

For low temperature characterization, asphalts are subjected to both a bending beam rheometer and a direct tension device. The bending beam rheometer measures creep stiffness at an 8 to 240 seconds loading time scale. For the measurement, a constant load is applied at the mid point of an asphalt beam with dimensions of 127 mm

x 12.7 mm x 6.35 mm (5 inch x 0.5 inch x 0.25 inch). The device can measure creep stiffnesses from 2.8 x 10^3 kPa to 2.8 x 10^6 kPa which typically occur in the temperature range from -40°C to 25°C. The direct tension device measures tensile failure properties in the temperature region where asphalt behaves in a brittle manner. An asphalt specimen cast in a dog-bone shape is elongated at a specified rate until rupture occurs. This procedure determines strain-to-failure as an asphalt performance indicator at low pavement temperatures. All of the above SHRP tests are performed at varying temperatures related to the region where the asphalt pavement will be placed. Details of the significance of these tests will be discussed in Section E of this chapter.

2. Temperature susceptibility of asphalt properties

Viscoelatic properties of asphalt (for example, viscosity) change drastically with temperature. In practice, asphalt cement is required, at high temperatures, to retain its consistency in order to hold the aggregate matrix together and to resist traffic loading without permanent deformation. At low temperatures, asphalt cement must be soft enough to prevent cracking induced by thermal and traffic action. This temperature dependency of asphalts is expressed by a term 'temperature susceptibility'. The temperature susceptibility is the rate at which the consistency of an asphalt changes with a change in temperature [87].

Several parameters for characterizing the temperature susceptibility of asphalt have been proposed for use as indicators of asphalt performance. Penetration ratio (PR), for example, is the simplest way to determine temperature susceptibility which has had

local application [76].

$$PR = \frac{\text{Penetration at 4°C, 200g, 60sec}}{\text{Penetration at 25°C, 100g, 5sec}}$$

Pfeiffer and van Doormaal [83] found a linear relationship between the logarithm of the penetration and temperature. They presented an expression, the so-called penetration index (PI) for temperature susceptibility, which becomes about zero for road paving asphalt.

$$PI = \frac{20 - 500\,A}{1 + 50\,A}$$

where, A = temperature susceptibility parameter and is defined as follows:

$$A = \{\text{Log } 800 - \text{Log (pen at } 25°C)\}/(T_{R\&B} - 25)$$

$T_{R\&B}$ = ring and ball softening point, °C

Heukelom [43] modified the equation for A using penetrations at two different temperatures, T_1 and T_2;

$$A = \{\text{Log (pen at } T_1) - \text{Log (pen at } T_2)\}/(T_1 - T_2)$$

McLeod [74-76] presented the penetration-viscosity number (PVN) based on an

empirical correlation among penetration at 25°C, viscosity at 60 or 135°C, and Pfeiffer and van Doormaal's PI for a few carefully selected 'wax free' asphalts. PVN is represented as:

$$PVN = \frac{\text{Log L - Log X}}{\text{Log L - Log M}} (-1.5)$$

where

X = measured viscosity in centistokes (10^{-6} m^2/s) at 135°C,
L = viscosity at 135°C for PVN = PI = 0, and
M = viscosity at 135°C for PVN = PI = -1.5.

Viscosity-temperature susceptibility (VTS) is another measure used to determine temperature susceptibility [7,76].

$$VTS = \frac{\text{Log Log10}\eta_1 - \text{Log Log10}\eta_2}{\text{Log}T_1 - \text{Log}T_2}$$

where, η_1 and η_2 are the viscosities in Pa·s at temperatures T_1 and T_2 in degrees Kelvin.

To describe the relationship between viscosity and temperature, Heukelom [43] used the Williams, Landel and Ferry (WLF) equation [112] and developed the bitumen test data chart (BTDC) where the viscosity-temperature relationship of straight run asphalts is represented by a single straight line. Based on BTDC plot, asphalts are categorized by three classes: Class S for straight run bitumen, Class B for blown

asphalts and Class W for waxy bitumen. In the BTDC plot, Class B and Class W deviate from the straight line of Class S.

Bell [7] presented a numerical procedure which classified asphalts into Classes S, B and W by comparison of predicted and measured penetration at 25°C and derived the Class Number (CN). Positive CN indicates Class W and negative CN indicates Class B. When CN is within the range of ±2, the asphalt belongs to Class S. He noted that high positive or negative values of CN indicated a large difference between high and low temperature susceptibility. Lower PR, PI and PVN and greater VTS indicate greater temperature susceptibility.

3. Asphalt rheology

Asphalt rheology is characterized by time-temperature dependent response to applied stresses and has been described by the structural concept, empirical power law, and mathematical representations [72,77] which are reviewed in this section. A mathematical descriptions of stress-strain relationships in asphalt defined by Heukelom [45] are also reviewed. The mathematical representation of viscoelasticity of asphalt mostly rely on the time-temperature superposition principle [112] and generalize the time and temperature dependency of asphalt. Van der Poel's [107] and SHRP's [101] generalizations are reviewed. Some practical uses of van der Poel's procedure are also reviewed.

In the structural representation of flow behavior, the deformation of asphalt is considered to be the result of the movement of flow units, that is, groups of molecules.

The application of shear stress may result in the degradation of these flow units. Considering the thermodynamics of an asphalt system, the associated complexes (flow units) are probably spherical in shape. On application of shear stress, the complexes elongate and flow through the oily medium. As the stress increases, the association bonds in the complexes start to break and continue breaking until the extent of the breakup is in equilibrium with the applied stress. An increase in temperature also reduces the size of the flow units. These changes in the flow units affect the rheological properties of asphalt [72,77].

The empirical power law of flow behaviors is represented by a linear relationship between log shear stress and log shear rate. As a simple example, a typical creep test is used as shown in Figure 1. Under static load at constant temperature, asphalt exhibits linear elastic response, delayed elastic response, and creep behavior. The initial elastic response can be used to calculate elastic or shear modulus of asphalt. The slope of the creep response is the strain or shear rate corresponding to a given stress and test temperature. Viscosity can be calculated from the relationship, shear stress = viscosity x shear rate. Upon unloading, there is an immediate elastic strain recovery and then a delayed elastic strain recovery. Creep results in nonrecoverable strain or permanent deformation [103]. Changing applied shear stress results in a different shear rate and a different creep curve. From a series of creep tests, shear stress and rate can be plotted as a straight line on a log-log plot. The slope of the line, c, changes in log shear stress divided by changes in log shear rate, is referred to as the degree of complex flow or the shear susceptibility. Schweyer et al. [95] demonstrated the importance of shear

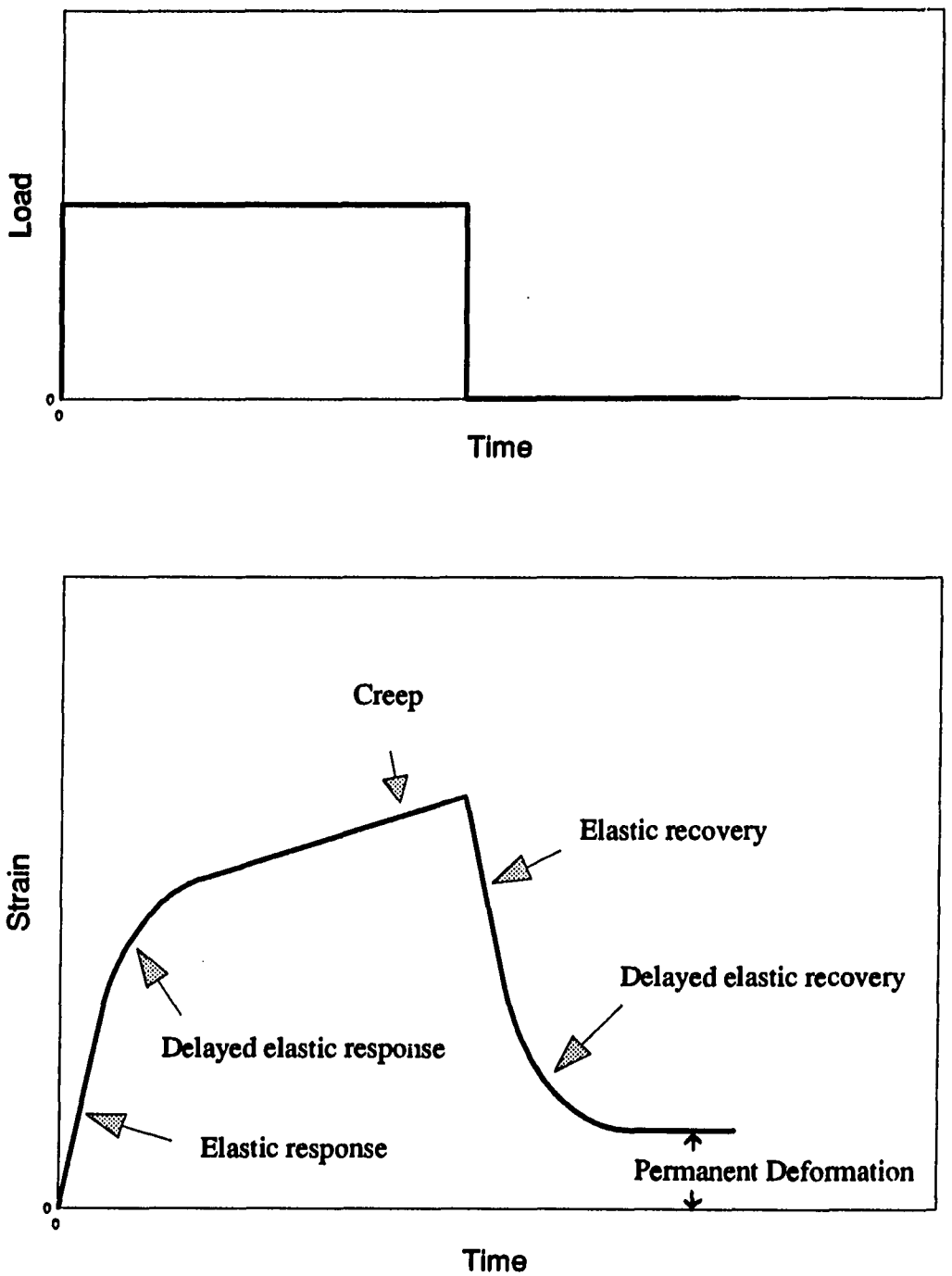

Figure 1. Typical responses of creep experiment

susceptibility in determining the viscosity of asphalt. Depending on the selection of shear rate for the viscosity calculation, the viscosity of an asphalt may be greater than, equal to, or less than that of another asphalt having a different shear susceptibility. Changing the test temperature will result in a different response.

In general, flow behaviors of asphalts are categorized into three types: Newtonian, pseudoplastic, and dilatant behaviors [64,103]. At high temperatures in excess of 25°C or near mixing temperature (~135°C), paving asphalts often exhibit Newtonian flow behavior, that is, having a linear relationship between stress and strain rate without elastic response (shear susceptibility, c, equal to 1). At low temperatures and low shear stresses, asphalts exhibit pseudoplastic or shear thinning behavior. As shear stress or shear rate increases viscosity decreases ($c<1$). Age hardening of asphalt results in more pseudoplastic behavior with a smaller c value [64,82]. For highly air blown asphalt, yield point may exist as in Bingham plastic behavior. At high temperature and high shear rate levels, asphalts can exhibit shear thickening, that is, an increase of viscosity with increased shear rate or shear stress. This condition is referred to dilatant behavior ($c>1$). A large deviation of the c value from one indicates high shear susceptibility of asphalt. For some asphalts, flow behavior may change from pseudoplastic to Newtonian and to dilatant as the shear stress is increased [103].

Heukelom [45] described the rheological behavior of asphalt as the summation of individual elastic, viscous and delayed elastic behaviors and defined the stiffness modulus of bituminous material, S, as the ratio of stress, σ, and strain, ε, and as a function of temperature, T, and loading time, t.

$$S(t,T) = \frac{\sigma}{\varepsilon}$$

Modulus of elasticity (E) is described as a bulk effect of all the hydrocarbon molecules of an asphalt instantaneously being deformed by an applied load. Asphalts have a nearly constant experimental value of $E = 2.7 \times 10^9$ Pa. Elastic strain, ε_e, caused by external stress, σ, is defined by

$$\varepsilon_e = \frac{\text{stress}(\sigma)}{\text{elastic modulus}(E)}$$

In a colloidal system of asphalt, applied stress would be transmitted through the liquid phase to the molecular agglomerates. For constant stress, σ, viscous strain of an asphalt having viscosity, η, is

$$\varepsilon_v(t,T) = \frac{\sigma t}{3\eta}$$

and depends on loading time, t, and temperature, T.

The molecular agglomerates cause delayed elastic behavior, the bulk effect of which is described by a modulus of delayed elasticity D(t,T). Delayed elastic strain is

$$\varepsilon_d = \frac{\text{stress}(\sigma)}{\text{delayed elastic modulus}(D)}$$

When these three characteristic strains are assumed to be independent of one another, the total strain, ε, becomes

$$\varepsilon = \varepsilon_e + \varepsilon_v + \varepsilon_d$$

Then, the stiffness of asphalt, S, can be expressed as

$$\frac{1}{S} = \frac{1}{E} + \frac{t}{3\eta} + \frac{1}{D}$$

At very short loading time and low temperature, asphalt essentially behaves as an elastic solid. At very long loading time, the term with viscosity in the above equation is the largest so that the behavior becomes viscous. At moderate loading time, the delayed elastic effects influence the transition from elastic to viscous behavior [5].

A number of attempts have been made to generalize the viscoelastic properties of asphalt over wide ranges of temperature and time variables by use of the time-temperature superposition principle [13,14,19,22,31,56,77,91,96,98,99,107,108]. Rheological properties derived from dynamic measurements or from steady flow measurements are represented by two generalized curves: (a) the dependence of rheological properties on reduced time variables, such as frequency or shear rate and (b) the dependence of the shift factor on temperature. These generalizations allow prediction of viscoelastic properties of asphalt at any conditions. Van der Poel [107] and Brodnyan [13] proposed procedures that determined the viscoelastic properties of asphalt with a penetration at 25°C and the softening point. Based on the Williams-Landel-Ferry (WLF) equation [112], Schmidt and Santucci [91] presented a method to

predict viscosities at various shear rates and temperatures from a measured glass transition temperature and viscosity determined at 60°C.

Simple instruments capable of measuring asphalt stiffness at low temperatures have not been available and accurate stiffness measurements obtained from some instruments have been considered to be too complex and expensive for routine pavement design and analysis procedures. In practice, asphalt stiffness at low temperature has usually been predicted by a generalized procedure discussed above, such as van der Poel's procedure [5]. In van der Poel's procedure [107], a nomograph is used to determine the stiffness at temperature, T, and loading time, t, for a given bitumen with known PI and softening point. In his nomograph, hardness is expressed by temperature and ring and ball softening point, $T_{R\&B}$, is used as a reference temperature at which all asphalts are considered to have the same viscosity. The temperature difference from the softening point, $T_{R\&B}$-T, is used for a hardness parameter. Temperature dependent properties are expressed by penetration index, PI [45]. Van der Poel's nomograph has been revised by Heukelom [43] and McLeod [76] using modified PI and PVN discussed earlier. Generally, Heukelom's procedure is believed to give more accurate stiffness prediction than others [5].

Using this procedure, pavement cracking temperature can be predicted. Asphalt pavements crack when asphalts reach a limiting or critical asphalt stiffness. By using this limiting stiffness as an input in van der Poel's nomograph together with $T_{R\&B}$ or T_{800pen} (temperature where penetration is 800 at 25°C, 100g, and 5sec), PI and selected loading time, cracking temperature can be determined. This temperature is sometimes

referred to as temperature of equivalent stiffness (TES).

Another commonly used procedure, together with the van der Poel's procedure, to predict pavement cracking temperature is that of Hills'. He [46] reported a critical thermal stress of $5x10^5$ Pa (72.5 psi) to induce pavement cracking. Based on that, he developed a nomograph to estimate cracking temperature from only two penetration values, penetration at 25°C and penetration at 5°C.

Among several explicit mathematical models characterizing master curves of viscoelastic properties of asphalt is one developed through SHRP [17,101]. In this model, master curves for the dynamic modulus of asphalts are characterized by four characteristic parameters which are defined as follows:

> The glassy modulus, $|G^*_g|$: the value that the dynamic modulus approaches at low temperatures and high frequencies and is very close to 1 GPa in shear loading for most asphalt cements.
>
> The steady-state viscosity, η_o: the steady-state or Newtonian viscosity as the phase angle approaches 90°. The 45° slope that the dynamic master curve approaches at low frequencies is frequently referred to as the viscous asymptote, and is indicative of the steady-state viscosity of a given asphalt.
>
> The crossover frequency, ω_c: the frequency where the storage modulus and the loss modulus are equal ($\tan \delta = 1$). This parameter is believed to be related to the hardness of asphalt.
>
> The rheological index, R: the difference between $\log |G^*_g|$ and $\log |G^*(\omega_c)|$. This parameter is believed to be related to the width of the relaxation spectrum.

These parameters are illustrated in Figure 2.

The temperature dependency of viscoelastic properties above the glass transition temperature is characterized by the William-Landel-Ferry (WLF) equation;

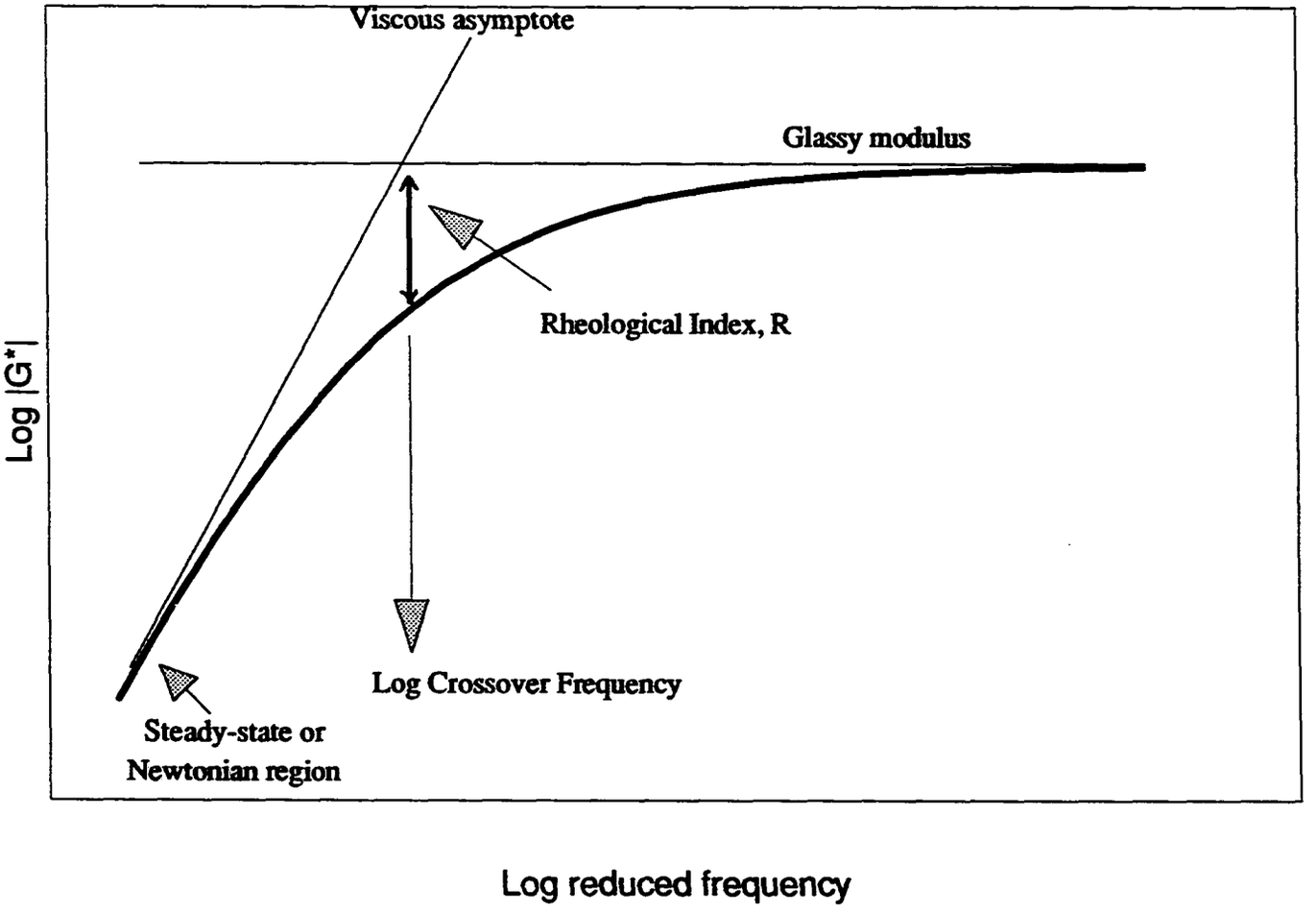

Figure 2. Characteristic parameters of dynamic master curve

$$\log \alpha(T)/\alpha(T_g) = C_1(T-T_g)/(C_2+T-T_g)$$

where, $\alpha(T)/\alpha(T_g)$ = the shift factor relative to the glass transition temperature, T_g,

C_1, C_2 = empirically determined constants which can be fixed, for all asphalts studied, to -19 and 92, respectively, and

T, T_g = the selected temperature and the glass transition temperature in °C, respectively.

Below the glass transition temperature, an Arhennius function is used;

$$\log \alpha(T)/\alpha(T_g) = 2.303\ E_a/R_{gas}\ (1/T - 1/T_g)$$

where, E_a = the activation energy for flow below T_g which can be fixed to 261 kJ/mol,

R_{gas} = the ideal gas constant, 8.314 J/mol-°K.

When linear viscoelasticity is assumed, by knowing these three of the four characteristic parameters, e.g. η_o, ω_o, and R ($|G^*_g|$ is already known, 1 GPa) , the dynamic modulus of asphalt cement at any temperature and frequency can be determined using following equation and using the shift factor equations discussed above. At the reference temperature, the dynamic modulus at the frequency ω can be determined as follows:

$$|G^*(\omega)| = |G^*_g|\ \{1+ (\omega_o/\omega)^{(\log 2)/R}\}^{-R/(\log 2)}$$

and the phase angle at frequency ω can be determined by

$$\delta(\omega) = 90/\{1 + (\omega/\omega_o)^{(\log 2)/R}\}$$

The variables are the same as defined previously.

B. Chemical Properties of Asphalt

Asphalt is defined as a dark brown to black cementitious material in which the predominating constituents are bitumens which occur in nature or are obtained in petroleum processing. Bitumen is a mixture of hydrocarbons of natural or pyrogenous origin, or a combination of both and is completely soluble in carbon disulfide [6]. Chemical studies have shown that asphalt is a complex mixture of organic molecules containing from simple hydrocarbons to highly condensed aromatic ring systems. While carbon and hydrogen are the predominant elements in asphalt, heteroatoms (oxygen, nitrogen and sulfur) are present together with trace amount of metals, mainly vanadium and nickel [82].

1. Asphalt chemical model

Generally, asphalt has been considered to be a colloidal system [40,70,84]. The three main constituents of the asphalt colloid system are asphaltenes, asphaltic resins and oily constituents. The asphaltenes are the dispersed phase in the dispersion medium of the asphaltic resins and the oily constituents. According to the description of this

system by Pfeiffer [84], the asphaltenes are the center of micelles which are formed by adsorption and absorption of the resins on the surfaces or the interiors of the asphaltenes. The resins with the greatest molecular weight and with the strongest aromatic nature are arranged the most closely to the nuclei of the micelles. Again, these are surrounded by lighter resins of less aromaticity and so on, until a gradual transition to the intermicellar phase is formed. When there are not enough resins, part of the forces causing the formation of the micelle are not compensated by adsorption of asphaltic resins. The micelles will be subjected to mutual attraction and finally form a gel structure. This gel structure is responsible for complex flow of asphalt, such as elasticity and thixotropy.

Recently, through the Strategic Highway Research Program (SHRP), a new asphalt model has been proposed [101]. According to the model, named the microstructural model, asphalts consist of a solvent moiety and dispersed moiety. The solvent moiety is composed of relatively aliphatic and non-polar molecules while the dispersed moiety is composed of polar and aromatic molecules. A large number of the molecules comprising the dispersed moiety are believed to be multifunctional and can be associated through molecular forces including hydrogen bonds, dipole interaction, and π-π interactions. These interactions allow formation of microstructure. The microstructures, structural units formed by molecular association, are dispersed by the solvent moiety. In paving asphalts, it is believed that the microstructures associate into three-dimensional structuring or networks. Both, the microstructure and the three-dimensional structures, may be broken up or dissociated by heat and shear. Oxidative

aging will promote more structuring by increasing the number of polar molecules and will also increase the solvent power of the dispersing moiety.

2. Separation of asphalt into fractions

Because of extremely large number of molecules in asphalt with different chemical structures and reactivities, asphalt is usually fractionated into less complex and more homogeneous fractions for further characterization. A classical analytical procedure separating asphalt into asphaltenes, resins, and oils is Hubbard-Stanfield method [48]. In this procedure, asphaltenes are separated as n-pentane insolubles. Remaining fraction (maltene, n-heptane soluble) is adsorbed on alumina. Oils and resins are obtained by washing with n-pentane and with methanol-benzol 10:90 solution, respectively.

Schweyer and Traxler [94] presented a procedure of asphalt partitioning with partial solvents. By use of n-butanol and acetone, asphalt is divided into asphaltics, paraffinics and cyclics. Because the fractions separated are not clearly different in their chemical nature, this procedure has not been widely used [82].

Corbett [19] presented a fractionation method using adsorption-elution chromatography on alumina. First, asphaltene fraction is separated as an n-heptane insoluble fraction. Then, the remaining maltene fraction is adsorbed on a chromatographic column and sequentially desorbed with solvents with increasing polarity. Saturates, naphthene aromatics and polar aromatics are obtained in the order of elution. Corbett described the asphaltenes as solution thickeners. The saturate and

naphthene aromatic fractions were considered as a plasticizer for the polar aromatic and asphaltene fractions. The polar aromatics were believed to be responsible for the ductility of the asphalt. This separation procedure has been adopted as an standard by American Society for Testing and Materials (ASTM D 4124).

The Rostler fraction method is based on chemical precipitation [89]. After separation of asphaltenes (A) as an n-pentane precipitate, the remaining fraction is further separated into fractions based on their reactivity with sulfuric acid. With increasing acid strength, nitrogen base (N), first acidaffin (A1) and second acidaffin (A2) fractions are separated. The remaining fraction is called paraffin fraction (P). Rostler described the asphaltenes as the solid components of asphalts and said they are primarily responsible for asphalt viscosity and colloidal behavior due to their limited solubility in the balance of components. The asphaltenes dispersed by the nitrogen bases were solvated by the acidaffins and gelled by the paraffins. He found that on oxidation, the nitrogen base and the first acidaffin fractions underwent the greatest change while the second acidaffin and paraffin fractions were changed very little. He believed that much of the nitrogen base changed into the asphaltenes and the first acidaffins into the nitrogen bases on oxidation. Changes from the first acidaffins to the asphaltenes were limited due to insufficient chemical reactivity of the first acidaffin to form large size molecules.

During SHRP [101], two separation techniques have been developed for asphalt cements. First, ion exchange chromatography (IEC) separates asphalt in fractions of molecules having similar functionalities [11,101]. In this procedure, asphalts are

dissolved in solution and separated with anionic and cationic resins. By using solvents with different polarities, asphalt was separated into neutrals, weak acids, weak bases, strong acids, strong bases, and amphoterics. The neutrals are relatively small in size and free of functional groups and the amounts in asphalts ranged from 50 to 60%. The amphoterics are molecules which, by definition, possess both acidic and basic functionalities and are the other major components in asphalt. By infra-red functional group analysis, it was found that the amphoterics are highly aromatic species containing strongly polar functionalities such as carboxylic acids and 2-quinolones. The amounts of amphoterics in asphalt ranged from 15 to 20%.

Second, a size exclusion chromatography (SEC) separation in preparative scale was developed to separate asphalts into fractions having different hydrodynamic volumes in solution [101]. In this procedure, asphalt is dissolved in toluene and pumped into a column containing SEC gel with a pore size of 170 Å. Gravimetrically obtained chromatograms show bimodal peaks. It was found that the materials of the first peak (emerging earlier) were nonfluorescing under 350-360 nm UV lamp indicating large associations of aromatic polar molecules. The nonfluorescing materials are denoted as SEC fraction-I which comprise 10 to 30% of the asphalts tested. Molecular weights of these fractions, measured in toluene at 60°C by vapor phase osmometry (VPO), ranged from 5,000 to 11,000 daltons. The materials of the second peak, denoted as SEC fraction-II, was fluorescing under the UV light. Their molecular weights determined by VPO are much smaller than those of SEC fraction-I and are believed to be solvent moieties.

3. Asphaltenes

Asphaltenes are soluble in benzene and insoluble in low-molecular weight n-paraffin hydrocarbons, usually n-pentane or n-heptane. The solubility of the polar components in pentane or heptane depends on many variables such as functional group type and content, molecular weight, and molecular structure. Many polar components of the resin fraction have been found to have functionality similar to that of asphaltenes [85]. A gel permeation chromatography study of asphaltenes (n-pentane insoluble) and maltenes or petrolenes (n-pentane soluble) indicated considerable overlap in their size distributions [39]. Long [68] indicated that precipitation of asphaltenes by alkane solvent was dependent on the polarity and molecular weight of the asphaltene component. Less polar materials of higher molecular weight and more polar materials of lower molecular weight both would precipitate as asphaltenes. Boduszynski [10] found that the initial composition of an asphalt was another important factor determining the amount of asphaltene precipitation. When one asphalt was treated with pentane and heptane, he obtained 17% and 10.6% of asphaltenes, respectively. The pentane asphaltenes were further treated with heptane and 87% of asphaltenes (14.8% of whole asphalt) were obtained. Similar results were shown for decane asphaltenes (5.9%) and heptane-decane asphaltenes (9.7%). He concluded that treatment with a normal alkane upset the solubility equilibrium of a very complex mixture of various compounds comprising asphalt or its fraction.

Speight and Moschopedis [100] reported that for several asphalts from different sources, H/C ratios of n-pentane asphaltenes were about 1.15 with very small variation.

The average n-heptane precipitate had a higher degree of aromacity, having lower H/C ratios, than the average n-pentane precipitate. Higher concentrations of heteroatoms (O, S and N) were also found in the n-heptane precipitates. Based on these data and data from spectroscopic studies of asphaltenes, they described asphaltenes as condensed polynuclear aromatic ring systems with alkyl side chains. The number of rings may vary from 6 to 20. A study of the thermal decomposition of asphaltenes indicated that 81% of oxygen, 23% of sulfur and 1% of nitrogen in asphaltenes were lost [100]. Nitrogen and sulfur are believed to have stability due to their location in heterocyclic ring systems while oxygen is located mostly on the alkyl sidechains in the form of thermally labile carboxylate groups.

Yen [114] studied asphaltenes using X-ray diffraction and found stacking of planar aromatic molecules with five or six layers. This stacking was considered to occur via the π-π association. Metals could be coordination centers for the stacking by locating defective centers (gaps and holes) of the aromatic portions of the sheet.

Experimentally determined molecular weights of asphaltenes vary very widely in part due to the technique used in their determination. In addition, the nature of the solvent and the solution temperature used in the determination of asphaltene molecular weight affect asphaltene association and observed molecular weight [100].

4. Effects of asphalt composition on physical properties

Polar functionality of molecules and interactions of various components determine the rheology and durability of asphalt. Mack [70] concluded that high

relative viscosity of asphalt was caused by association rather than by solvation. He defined solvation as a chemical combination between solute and solvent or as some form of attachment of the solvent to the dispersed phase. Association of the solute molecules, however, results in high relative viscosity due to the inability of the solvent to overcome the space lattice forces which cause the polymeric bond. The maximum degree of association is obtained at a certain concentration of asphaltenes, which differs with different temperatures and is different for different asphalts.

Altgelt and Harle [3] studied the effects of asphalt composition on asphalt rheology. They chromatographed an asphalt using SEC and separated it into seven fractions based on molecular weight. Asphaltenes were obtained from each fraction by precipitation with n-pentane. They found the viscosity of asphaltene-benzene solutions increased with increasing molecular weight of asphaltenes. It was believed that asphaltenes of low molecular weight consisting of single sheets of condensed aromatic and naphthenic rings with attached short side chains, had less flow resistance than asphaltenes of very large molecular weight which formed extended networks with highly compacted sheets. When a heavy asphaltene fraction was dissolved in a number of solvents having different solvent powers, the viscosity of the solutions increased with decreasing solvent power. While the solvent power effects on heavy asphaltenes were extremely significant, the effects on low-molecular weight asphaltenes were minimal.

Petersen [82] pointed out that intermolecular forces and the geometry of molecules are significant chemical properties governing rheological properties of asphalt. At high temperatures, flow behaviors of asphalts are nearly Newtonian and are similar.

Polar interactions among molecules are the dominating factor in this situation. However, as the temperature is decreased, the asphalt molecules start to associate and form a more or less arranged structure. This ordered arrangement is greatly influenced by the geometry of the molecules as well as the polar functionality [82]. For these reasons, differences in chemical composition can result in significantly different flow properties at low temperatures. In 1966, Welborn et al. [111] reported that at temperatures higher than 60°C, there were relatively small differences in temperature susceptibility of asphalts being used in the United States but significant differences occurred in the temperature range between 4°C and 60°C.

During SHRP [101], the relationship between the chemical composition of asphalts and physical properties of asphalts were studied. A statistical study was performed so that the fundamental chemical properties of asphalt were used to explain important physical properties that determine asphalt pavement performance. The three basic chemical properties considered were aromaticity, molecular size (and distribution), and polarity. The aromaticity (A) was represented by the ratio of hydrogen to carbon. The average molecular weight was expressed by the carbon number (C) at peak maximum of supercritical fluid chromatography (SFC) of IEC neutral fractions. The size distribution was represented by the width of the SFC peak (W) at its one-half height. Polarity was expressed by heteroatom content (H), the relative molar concentration of the sum of nitrogen, oxygen, and sulfur in asphalt. The physical properties studied were viscosity, temperature susceptibility, and aging index, a viscosity ratio before and after an aging procedure. Though only eight asphalts were used in the

statistical analysis, the results have a significant meaning showing trends between an asphalt's chemistry and its physical properties. The viscosity of the IEC neutral fraction, η_N, at 25°C was strongly related to its molecular weight and aromaticity:

$$\log \eta_N = 5.23 + 0.0606\,(C) - 3.69\,(A)$$

$$r^2 = 0.971 \qquad \text{P-value} < 0.001$$

where, C = carbon number at SFC peak maximum of the IEC neutral fraction,
A = the ratio of hydrogen to carbon for the IEC neutral fraction.

As molecular weight increases (higher C) or as aromaticity increases (lower A), the viscosity of the IEC neutral fraction increases. The variable C, the carbon number at SFC peak maximum, was much more significant than variable A, the hydrogen to carbon ratio, indicating the IEC neutral fraction is chemically simple so that the classic viscosity-molecular weight relation is observed.

A regression equation to predict viscosity (η_{AC}) of whole asphalt at 25°C is as follows:

$$\eta_{AC} = 10.9 + 5.64\,(H) + 0.0663\,(C) - 6.52\,(A)$$

$$r^2 = 0.950 \qquad \text{P-value} = 0.005$$

Unlike the IEC neutral factions, whole asphalts contain different amounts and different kinds of polar functional groups which involve one or more of heteroatoms. At 25°C,

the association of the polar functional group would be quite extensive and would become one of the major factors affecting asphalt rheology. Thus, the amounts of heteroatoms present in asphalts should appear in the equation to predict their viscosity.

An equation for energy of activation of viscous flow (E_a), a parameter related to temperature dependency of viscosity, has been derived as follows:

$$E_a = 74.4 + 0.937\,(C) + 65.6\,(H) - 55.5\,(A) - 0.204\,(W)$$

$$r^2 = 0.996 \qquad \text{P-value} = 0.001$$

This relationship indicates the temperature dependency of asphalt as related to all aspects of chemical composition.

The study also showed aging properties were equally related to the chemical composition of asphalt as were viscosities and activation energies for viscous flow as discussed above. For high temperature short term aging, a regression equation for the aging index, AI_{TFO}, is obtained as follows:

$$AI_{TFO} = -5.13 + 0.323\,(C) + 2.43\,(A_{Whole}) + 9.91\,(H)$$

$$r^2 = 0.925 \qquad \text{P-value} = 0.010$$

where, AI_{TFO} = ratio of viscosities at 60°C after thin film oven aging and before aging.
A_{Whole} = hydrogen to carbon ratio for whole asphalt

For asphalts containing large molecules (lager C), effects of aging is greater than for asphalts made up of small molecules. An asphalt containing more polar functional groups (larger H) will be more easily oxidized and will result in a larger AI_{TFO}. More aromatic asphalts (lower A_{Whole}) will be able to dissociate some of the polar groups formed during oxidation and this will prevent large increases in viscosity caused by aging.

For low temperature long term aging, as when TFO aging is followed by low temperature pressure aging, the aging index, a regression equation for $AI_{TFO\text{-}PAV}$, is obtained as follows:

$$AI_{TFO\text{-}PAV} = 82.4 + 1.14\,(C) - 65.9\,(A) + 138\,(H) - 10.6 \log \eta_{AC}$$

$$r^2 = 0.940 \qquad \text{P-value} = 0.035$$

In low temperature aging, the mobility of oxidizable sites becomes a factor in determining oxidation rate. That would explain why the viscosity of the whole asphalt, η_{AC}, appeared in the regression equation. For the same reason, the sign for aromaticity was changed.

During SHRP [101] it was also found that the amount of the associated fraction separated by SEC (SEC fraction I) is related to tan delta (tan δ). Asphalt containing more SEC fraction I shows lower tan δ (higher elasticity). This indicates that an asphalt with more associated molecular structure has the ability to recover from deformation caused by traffic loads and will perform better in terms of rutting

resistance.

5. Oxidative aging

To explain the effects of oxidation and compositional change on rheological properties of asphalt, Altgelt and Harle [3] used asphalts from three different sources. Asphalt A consists of a high concentration of high molecular weight asphaltenes in maltenes (solvent phase) of strong solvent power. Asphalt B, with the same penetration grade of asphalt A, consists of a low concentration of high molecular weight asphaltenes in a less strong solvent phase. Asphalt C has an intermediate concentration of asphaltenes of intermediate molecular weight in maltenes of poor solvent power containing mainly paraffins. On oxidation, asphalt C hardens most rapidly since the asphaltenes become larger in size and even less soluble in that poor solvent phase. Asphalt B hardens least because, although the amount of asphaltenes increased on oxidation, maltenes are the major fraction controlling the rheology of this asphalt. The addition of a paraffinic fraction softens asphalts B and C by diluting their maltene fractions. However, the dilution effect of the paraffinic solvent in asphalt A is offset to some extent by increased agglomeration of the asphaltenes shown by the reduced solvent power of the maltenes. For this reason, viscosities of blended asphalts are often widely different from the expected or that linearly calculated from the viscosities of the original asphalts.

For a given asphalt, oxidative aging increases the amount of asphaltenes and increasing the amount of asphaltenes increases viscosity. Plancher et al. [85] found that

this relationship between the amount of asphaltenes and viscosity was widely different for asphalts from different sources. For example, with the same asphaltene content, asphalt from one source showed 100 times higher viscosity than asphalt from another source. This indicates that the asphaltene-viscosity relationship was determined by chemical makeup which varied from one asphalt source to another. They also found that lime treatment reduced the hardening rate of asphalt and reduced asphaltene formation. It was believed that the lime removed reactive functionality in the asphalt which reduced formation of asphaltenes and, therefore, reduced the interaction among polar functional groups which caused increased asphalt viscosity.

Many researchers have devoted their efforts to understand oxidation mechanisms in asphalts. Petersen [82] explained the oxidation mechanism of asphalt as the formation of ketones as major products via hydroperoxide intermediates. During SHRP [101], formation of peroxy free radicals in the bulk asphalt was evidenced by observing chemiluminescence emission in the near uv/visible region when asphalts were heated in air. It was also found during SHRP [101] that, in all asphalts studied, there were significant amounts of free radical inhibitors (mostly phenols) distributed almost equally between maltene and asphaltene fractions. Oxidation in asphalt, therefore, is believed to be a non-chain process that probably involves radical intermediates at some stage. Most sulfur in asphalt exists as sulfide or thiophenic sulfur and only aliphatic sulfide sulfur is oxidized during thermal oxidation. The sulfur compounds do not react directly with oxygen to form sulfoxide at pavement service temperature but are oxidized by intermediates formed by reaction of substances in asphalt with oxygen [101].

Aging studies performed during SHRP also show that the aging properties of asphalts are a function of the physical state of the asphalt and, therefore, are temperature dependent. For this reason, the maximum temperature to which the pavement is exposed is an important factor in determining the long term hardening of the asphalt pavement [101].

The effects of aggregate on asphalt aging were also studied during SHRP [101]. For most asphalt, the effects was not very significant. However, asphalt containing large amounts of associated fractions or polar species, such as asphaltenes, SEC fraction I, or IEC amphoteric fraction, tends to harden slightly less when coated on an aggregate. This was explained by asphalt-aggregate interaction which limits the availability of oxidation reactive species in asphalt similar to the effects of lime mentioned previously.

The results from nonaqueous potentiometric titration studies of asphalt indicate that aging increases the amounts of total bases in asphalt. The largest increase occurred in the weak bases by formation of ketones and sulfoxides upon aging [101].

6. Molecular structuring

Molecular structuring or steric hardening is a reversible phenomenon which can cause significant changes in asphalt rheology with time. This property is different from irreversible oxidative hardening and is believed to be the result of molecular reorganization within asphalt on a long time scale [101]. The original flow properties can almost be restored by mechanical work or heat. In spite of its importance in the setting of asphalt in a mix and also in low temperature properties, molecular structuring

is not well understood because of its slow process going on days and even years and it is destroyed during solvent recovery of aged asphalt in pavement [82]. In asphalt-aggregate mixes, the aggregate surface can promote molecular structuring by adsorption and induced dipole-dipole interactions [24]. It has also been found that the molecular structuring has relationships with complex flow and oxidative aging. An asphalt with a greater degree of molecular structuring potential exhibits a higher degree of complex flow [105]. The degree of molecular structuring of oxidized asphalt is much greater than that of unoxidized asphalt. Oxidative hardening and molecular structuring are believed to be synergistic [82].

Physical hardening of asphalt at low temperature was reported during SHRP [18,101]. By storing asphalt at -15°C for 24 hours, a creep master curve was shifted about $10^{0.7}$ seconds. This kind of phenomenon has previously been reported in polymer rheology [27]. As the temperature is lowered to near the glass transition temperature, there will be a delayed voluminal equilibrium. The lower the temperature, the longer the time required to reach that equilibrium.

C. Durability of Asphalt

Desirable asphalt pavements should have proper (a) stability, (b) durability, (c) flexibility, (d) fatigue resistance, (e) skid resistance, (f) imperviousness, and (g) fracture or tensile strength [64]. While the skid resistance is an important property for highway safety, lack of one or some of the other characteristics may lead to the pavement failure in the form of (a) cracking, (b) disintegration, and/or (c) excessive deformation. Major

contributors to pavement deterioration are material properties which include asphalt durability, shape and gradation of aggregate, aggregate durability, and volumetric composition and aggregate-asphalt interaction [28]. Air voids and asphalt film thickness in the mixture are also important variables affecting the performance of asphaltic pavement.

Although asphalt represents only about 5% by weight of the mixture, hardening of the asphalt is generally believed as the most important single factor that causes cracking and disintegration of pavement [82,106]. Vallerga et al. [106] listed six factors causing asphalt hardening as follows:

1. Oxidation - reaction of oxygen with asphalt,
2. Volatilization - evaporation of the lighter constituents from asphalt,
3. Polymerization - combining of like molecules to form larger molecules, causing a progressive hardening,
4. Thixotropy - progressive hardening due to formation of a structure within the asphalt over a period of time,
5. Syneresis - exudation reaction where the thin oily liquids are exuded to the surface of the asphalt film, and
6. Separation - removal of oily constituents, resins, or asphaltenes from the asphalt as caused by selective absorption into porous aggregate.

The effects of light, water, chemical reaction of asphalt with the aggregate, microbiological deterioration, and adsorption of asphalt on the aggregate surface also have been suggested as influencing factors in asphalt hardening [104].

As a relative durability measure, the degree and rate of asphalt hardening during a laboratory accelerated test have been used since the early 1900s. The durability of asphalt is expressed in terms of changes in weight, penetration, ductility, softening point and/or viscosity. In some instances the changes in asphalt were measured by physical tests on compacted asphalt-aggregate mixtures. The studies using mixtures and recovered asphalt have been found to be too complex to be used for routine control [110].

The test methods that have been developed can be divided into two groups: (a) tests on neat asphalts and (b) tests on asphalt-aggregate mixtures. An excellent review on the development of the durability tests can be found in the state-of-the-art report by Lee [63] and in reference 25. In the 1890s, weight loss and decrease in penetration due to oven heating of asphalt (loss on heating) were used to determine the relative durability of asphalt. Around 1940, the U. S. Bureau of Public Roads conducted a series of investigations on oven heating tests and the thin film oven test using a film thickness of 1/8 inch was proposed including requirements for percent weight loss, retained ductility, and penetration. In the 1950s, it was observed that changes in asphalt due to atmospheric exposure were limited to a depth of a few microns from the asphalt surface and use of thin asphalt film in the durability test was studied. With the development of the microviscometer [37,44,97], so-called microfilm durability tests began to be used. In these tests, hardening of 5 to 15 μm of asphalt film due to heat and air is measured by change in viscosity. Aging index, the ratio of viscosities before and after aging procedures, has been widely used as a durability parameter. For routine

control testing purposes, the rolling thin film oven test (RTFOT) was developed. In the RTFOT, 5 to 10 μm of asphalt film is exposed in an oven at 163°C for 75 minutes, a relatively short period of time compared with the 2 to 5 hour exposure times of other test methods.

Of the various methods for testing and evaluating the durability of asphalt, only the thin-film oven test (TFOT) and the rolling thin-film oven test (RTFOT) both run at 163°C have been adopted as standard methods by AASHTO and ASTM. Both methods provide the estimated age hardening due to hot-plant mixing. Long-term asphalt durability, for 5 to 10 years or more service in pavement, is usually estimated by severe aging procedures having extended exposure time and/or reduced asphalt film thickness. However, it has been realized that the hardening during service in pavement at relatively lower temperatures and lower rates could have a quite different hardening mechanism from that occurs during hot-plant mixing at higher temperatures and higher rates. For long-term aging evaluation, pressure oxidation (pressure oxidation bomb, POB) procedures have been used at relatively low temperatures (50-66°C), the extreme temperatures encountered in the field [9,23,49,62,64]. Lee [62,64] developed a two-stage durability test: 1) thin film oven test at 163°C for hot-plant mixing followed by 2) pressure oxidization at 65.6°C and 20 atm (2,027 kPa) oxygen pressure for service in pavement.

Chemical properties of asphalt also have been used to evaluate durability of asphalt. It is generally agreed that a proper balance of chemical components is important for compatibility and for durable asphalt [3,82,89]. To predict the durability

of asphalt, Rostler and White [89] proposed a parameter estimating the compatibility of asphalt. In this, the balance of the components was indicated by the ratio of the most reactive fractions (nitrogen base plus first acidaffin) to the least reactive fractions (paraffin plus second acidaffin). The abrasion resistance of sand-asphalt mixture was found to decrease as the value of the parameter increased.

As a measure of durability, Heithaus [42] proposed internal compatibility between maltenes and asphaltenes. He found asphalt with more stable internal phase hardened more slowly.

Oxidative aging produces polar functional groups in asphalt and causes more extensive intermolecular association or embrittlement of asphalt. This embrittlement of asphalt upon oxidation has been considered as one of the major factors causing pavement failure. Inverse gas-liquid chromatography (IGLC) was developed by Davis et al. [21] to study polar functional groups formed on oxidation and to relate with the pavement performance. In this test, asphalt is coated as a thin film on inert fluorocarbon particles and aged in a gas chromatographic (GC) column. Then, polar test compounds are passed through the GC column using an inert gas carrier at 130°C. Retention times are determined as a measure of the interaction between the test compounds and the polar groups formed by oxidation. An asphalt having a greater concentration of polar groups interacts more strongly with the test compound functionalities, giving larger interaction coefficients (I_p). Studies indicated excellent correlations with laboratory durability and pavement performance when phenol was used as the test compound with better durability correlating with lower I_p [20].

D. Characterization of Asphalt by Chemical Methods

1. High pressure gel permeation chromatography (HP-GPC)

High pressure gel permeation chromatography (HP-GPC) is a technique by which the molecular size distribution of asphalt is determined by means of gels of selected pore sizes as in sieve analysis. Reports from a Montana asphalt quality study using this technique have shown considerable promise and led the Montana State Department of Highways to institute special provisions based on requirements based on HP-GPC [50,52,54]. While there were unresolved exceptions, it has been concluded that large molecular size asphaltic constituents contribute to low temperature cracking of asphalt pavements. Other studies [16,115] have related the amounts of small molecular size fractions to rutting and tender mixtures. Garrick and Wood [29] reported correlations between asphalt chemical composition by HP-GPC and performance characteristics of asphalts and asphalt mixtures. Elder et al. [23] found correlations between pavement deformation and bleeding and asphalts of certain molecular profiles as determined by HP-GPC. Goodrich [34] found association between asphalts with wide distribution of molecular sizes as determined by HP-GPC, aging, and desirable mix characteristics with respect to low-temperature creep (rutting resistance). Researchers have also shown that the HP-GPC technique can be used as a reliable test to relate chemical composition and aging characteristics of asphalts [8,61,80]. Pribanic et al. [86] reported an improved technique in which the wavelength of detection light used is as variable. Using a multichannel UV-visible detector, this method makes it possible to obtain GPC chromatograms at eight different wavelengths simultaneously in one run. As wavelength

scanning provides information on distribution of aromaticity and the functional groups over the molecular size range, this sophistication may prove to be valuable in asphalt characterization. Polar and non-polar association of molecules also have been studied by this technique [54].

2. Thermal analyses

Thermal analysis techniques have been used extensively by chemists to identify and characterize polymers. Breen and Stephen [12] and Schmidt and Santucci [91] recommended the use of the glass transition temperature (T_g) from thermal analysis data for predicting low-temperature cracking of asphalt pavements.

The glass transition point, which is known to depend to some extent on the scanning rate, is identified by a discontinuity in the expansion coefficient versus temperature plot or in the specific heat versus temperature plot [73]. In actual practice, the former discontinuity is reflected in a thermomechanical (TMA) plot, i.e., a plot of linear dimension of sample versus temperature, as a rounded break. The latter discontinuity manifests itself as an inflection point in a differential scanning calorimetry (DSC) plot. Both methods are in use to determine glass transition points.

The application of DSC to asphalts has also revealed another transformation that takes place as they are heated from a low temperature. It is an endothermic transformation which may be interpreted as melting of crystallizable components [79], dissolution of these components in the liquid matrix [1], or dissociation of agglomerates of asphaltene micelles [67]. The presence of these species in an asphalt is believed to

affect its low-temperature performance adversely. The enthalpy change associated with these transformations measurable by DSC may measure the amount of these species in the sample [1]. Claudy et al. [18] found that the enthalpy change, defined as crystallized fraction (CF), is strongly related to the isothermal volume shrinkage and isothermal physical hardening. As asphalt contains more CF and have lower T_g it hardens faster. They also observed the growth of the endothermic peak upon isothermal conditioning at -15°C. They believe that the CF is composed of paraffinic species capable of forming microscopic crystalline or amorphous domains within the solvent phase of asphalt.

During SHRP [101], T_g was measured by two different ways; one using a dynamic mechanical analyzer (DMA) and the other using a home-built thermomechanical analyzer (TMA). The values obtained were very close between these two different instruments. In the previous discussion, it was shown that the glass transition temperature is the sole parameter determining the shift factor in the viscoelastic master curve. The shift factor describes the temperature dependency of asphalt. During SHRP [101], it was also found that the activation energy of viscous flow, E_a(a kind of temperature susceptibility measure), is strongly related to T_g. For eight asphalts studied during SHRP, it was found that T_g is closely related to the mobility of asphalt solvent phase expressed by the viscosity of the IEC neutral fraction which, in turn, is closely related to its average molecular weight.

Claudy et al. [18] used the same asphalts used in the SHRP study [101] and showed that T_g determined by DSC is not consistent with T_g measured by DMA and

TMA. T_g measured by DMA or TMA is always higher by 1°C to 20°C. From a careful review of two sets of data for eight asphalts, the following relationship was found:

$$T_g(DMA) - T_g(DSC) = 7.14 + 3.1\ CF$$

$$r^2 = 0.948 \qquad \text{P-value} = 0.000$$

An interpretation of this relationship might be that DSC detects the glass transition at the molecular level at a lower temperature. However, in the bulk asphalt, the rapid changes in volume expansion are restricted by the presence of CF.

3. X-ray diffraction (XRD)

X-ray diffraction spectra of asphalts have been used for their structural characterization in relation to their quality [66,113]. According to Williford [113], the height of the shoulder of the spectral curve at low angles is a measure of the quality of asphalt. The higher the shoulder the better the asphalt. In an asphalt additive study, Lee and Demirel [66] concluded that XRD can be used for studying asphalt structure based on low-angle scattering intensities and the shape of amorphous peak. They also found a preferred orientation in the horizontal direction with about 4.7 Å spacing in asphalts.

4. Nuclear magnetic resonance (NMR)

Nuclear magnetic resonance (NMR) spectroscopy is a powerful tool and is used in a broad array of disciplines to describe the character of atoms, molecules, and assemblies of molecules [102].

Hagen et al. [38] characterized asphalt using ^{13}C NMR. A large effort has been devoted to assignments of NMR peaks which were classified into 17 groups for interpretation of data. They found that the amounts of aromatic and aliphatic carbons can be quantified and polar functionality also can be quantified by the NMR technique. Upon aging, increases in aromaticity and polar functionalities were also observed. Rose and Francisco [88] reported a procedure characterizing polar functionalities in heavy petroleum fractions by NMR. By a methylation procedure, acidic oxygen, nitrogen, and sulfur functional groups can be tagged with an isotopically enriched methyl group. Any changes occurring due to this methylation can be detected by NMR.

During SHRP, an extensive NMR study on asphalt cements was performed at Montana State University [102]. From a solution state NMR study, aromaticity, concentrations of phenol and carboxylic acids, degree of branching, and length of aliphatic chains were estimated. Together with information obtained from elemental analysis and VPO molecular weight of asphalts [101], NMR results provided average molecular structures for asphalts. These average molecular structures of asphalts are in good agreement with the observed rheological properties of the asphalts [101] and the viscoelastic theory [27]. A solid state NMR was also used in the SHRP study [102] to investigate structure in asphalt on a small-distance scale ranging from a few angstroms

to 30 nm. This study indicates that the eight asphalts studied differ in molecular mobility at any given temperature. Molecular mobility for a given asphalt at any given temperature has a wide distribution. This finding supports the idea that the glass transition phenomena in asphalts will occur over a broad temperature range. Upon aging, the viscosity of asphalt increased 7 to 40 times while proton mobility decreased by only a few percent. Mixing of asphalt and aggregate fines did not change any NMR responses.

E. Current Asphalt Cement Specifications

In this section, the rationale and weakness of current asphalt specifications are reviewed. New asphalt specifications proposed by SHRP are also reviewed.

1. Rationale of the current specification

AASHTO specification M 266 grades asphalt cements into six ranges of viscosity at 60°C. Suitable asphalts for a given project may be chosen using this specification. Highly viscous asphalts (AC-20 or AC-30), for example, may be used for heavy traffic or warm climates and less viscous asphalts (AC-5) for light traffic or cold climates. It is believed that the viscosity grading gives a more uniform consistency at temperatures above 60°C than penetration grading and a more uniform behavior of a given paving mixture during construction where asphalts from different sources are used [109].

The way the viscosity of asphalt varies with changing temperature varies among asphalts. The viscosity-temperature susceptibility, therefore, is limited to a workable

range by establishing a minimum viscosity at 135°C and a maximum consistency measured by penetration at 25°C. The temperature, 25°C, for the penetration test together with its simple procedure, enables this test to be run virtually anywhere. The minimum viscosity at 135°C can also be used to estimate the rheological behavior of asphalt during storage and hot mix manufacturing [35].

Other tests included in the specification include a minimum solubility in trichloroethylene is used to control insolubles (asphalt additives or contaminants) in asphalt which may damage equipment [26]. During handling, storage, and construction, a minimum flash point becomes important in terms of safety as in preventing a fire hazard and for environment concerns. In addition to these tests, a ductility test on thin film oven test (TFOT) residue is used to ensure sufficient internal compatibility and homogeneity. By setting a minimum limit for ductility, the use of excessively waxy crudes and excessive oxidation during production can be limited [35].

The overall behavior of asphalt is controlled by the quantitative amount of each component and the interaction of these components. A lack of component compatibility causes excessive component phase separation and leads to nondurable asphalts. For this reason, the spot test has been adopted in the specification; this ensures homogeneity of asphalts by checking the stability of asphalt constituents in three different solvents [40].

Asphalts in mixes age harden in two manners; first, during hot-mix manufacturing and second, during pavement service life at ambient temperature. Hardening by hot-mix manufacturing is simulated by TFOT. The maximum rate of hardening is set in the specification by the ratio of viscosity at 60°C before and after

TFOT [35].

Major causes of hardening in asphalt are oxidation and loss of volatiles. The loss of volatiles is measured in terms of weight loss during TFOT and the maximum limit is set in the specification. Since weight loss is related to the front end of distillation as well as the smoke point, undesirable blending of asphalts at refineries may be prevented by specifying a weight loss limit on TFO residue [35].

2. Weaknesses of the current specification

Recently, although asphalts used met the specification, a number of early pavement life problems were reported. A significant number of these problems are believed to come from the use of inadequate asphalt cements [26].

The weaknesses of the current specification are summarized as follows:

a) The current specification is not performance based Test methods and limiting values used in the current specification had been empirically developed for mainly ease and uniformity of construction. Thus it does not guarantee adequate performance of the resulting asphalt paving mixture.

b) Lack of control on long term age hardening properties Pavement failure is more closely related to the properties of asphalt at the time of failure (aged) rather than initial properties. TFOT estimates age hardening during mixing at high temperature for a short period of time. However, the age hardening mechanism during service is believed to be quite different from that during TFOT. The former occurs at lower temperatures for a longer period of time. Thus, the age hardening tendency

estimated from TFOT could be different from the actual one. For example, blending stiff asphalts with very soft asphalts is common in current practice to meet the specifications. In the TFOT of these asphalts, a large proportion of the age hardening is due to loss of volatiles mainly from the soft asphalt. Consequently, the long term age hardening tendency, where slow oxidation is predominant, will be different from TFOT result.

c) Lack of knowledge on low temperature properties Understanding low-temperature properties of asphalt is critical for understanding thermal cracking of pavement. Low temperature (less than -20°C) properties obtained by extrapolation from the properties at high temperatures (25, 60, and 135°C in the specification) would not be appropriate [35,40].

d) Lack of knowledge on chemical properties Chemical properties govern physical properties. The fundamental behavior of asphalts is related to their chemical composition and their interactions. Significantly different chemical properties for the same grade asphalts in the current specification are possible and could result in a significant difference in long term performance [26].

3. SHRP asphalt specifications

SHRP [101] proposed an asphalt cement specification based on consideration of four major distress modes in asphalt pavement failure. These failure modes are low-temperature thermal shrinkage cracking, thermal fatigue, load-associated fatigue cracking, and plastic deformation in the upper hot-mix layers that leads to rutting. Five

pieces of asphalt testing equipment are used to grade asphalt; the dynamic shear rheometer, the bending beam rheometer, the direct tension device, the pressure aging vessel, and the Brookfield rheometer. In the specification, the asphalt to be used in a specific project will be determined by the minimum and maximum pavement temperatures expected for the region. For an asphalt to meet a certain grade in the specification, the performance related tests must be performed at the temperature relevant to the grade and must pass the specified limits. For short-term aging, the rolling thin film oven test (RTFOT) is used and a maximum mass loss is specified at one percent. For the long-term aging test, a two-step pressure aging procedure is used at varying temperatures depending on the grade or the regional climate. For safety and workability controls, flash point and a maximum viscosity at 135°C are specified, respectively. For the viscosity at 135°C, the Brookfield rheometer is used.

Rutting is more prevalent at the upper range of service temperature and right after construction. Therefore, rheological properties of asphalt are measured using the dynamic shear rheometer at the upper range of the service temperature on the RTFOT residue at 10 radian/sec, a frequency closely related to the traffic speed. A truck tire traveling at 50 MPH gives about 0.1 second loading time which corresponds to 10 radian/sec sinusoidal loading. To control rutting, the loss compliance, J", of the RTFOT residue is used. The loss compliance, J", is numerically equal to $|G^*|/\sin\delta$. A wheel tracking experiment shows a significant relationship between $|G^*|/\sin\delta$ and rutting potential. The minimum $|G^*|/\sin\delta$ value is 2.2 kPa at 10 radian/sec.

Several parameters (creep stiffness, slope of the creep curve, and failure strain)

are used to control low temperature shrinkage cracking. Since these phenomena are prevalent in aged pavement, use of a long-term aged residue in testing is required. Creep properties are obtained using the bending beam rheometer at low temperatures corresponding to the grade or the regional climate. Based on the limiting stiffness concept, below which asphalt reaches a critical stiffness value and the pavement cracks, the maximum creep stiffness is set at 300,000 kPa. For the consideration of time dependency of asphalt even at low temperatures, the slope of the creep curve, m = dlog J(t)/dlog t, is also required to have a minimum of 0.30. Often, modification of asphalt with polymer makes the limiting stiffness concept invalid. For this reason, the strain at failure at the minimum pavement temperature is specified at a minimum of one percent. This failure strain can be used as an alternative to creep stiffness criterion.

Load-associated fatigue cracking is also prevalent in aged asphalt pavement. This distress is controlled by using the dissipated energy concept. Dissipated energy in a dynamic shear test can be expressed by $|G^*|\sin\delta = G''$. In the specification, the maximum value of $|G^*|\sin\delta$ for a long-term aged residue, measured by dynamic shear rheometer at average pavement temperature and 10 radian/sec, is 5,000 kPa.

Control of tenderness of newly constructed pavement is obtained by measuring $|G^*|/\sin\delta$ before and after RTFOT at the upper range of service temperature at 10 radian/sec using the dynamic shear rheometer. Asphalts causing tender mixes will not pass the minimum requirement after RTFOT of $|G^*|/\sin\delta = 2.2$ kPa.

III. OBJECTIVES

Objectives of this study are fourfold: (1) to examine the variability of properties of asphalts used in Iowa between suppliers and between times of supply, (2) to evaluate the feasibility or applicability of characterizing asphalts by HP-GPC, TA, XRD, and NMR, (3) to correlate the measured physicochemical properties of asphalts with field performance, and (4) ultimately, to develop locally-based asphalt cement specifications for the State of Iowa.

IV. METHODS OF STUDY

This study consists of two phases, a preliminary study and a main study. The preliminary study was performed to investigate variability of locally used asphalts and applicability of HP-GPC, XRD, and DSC techniques for asphalt characterization and specification use. In the main study, asphalt samples were collected from actual construction sites and their physicochemical properties were measured and used for development of performance-related specifications.

A. Materials

In the preliminary study, asphalt cement samples representing those commonly used in Iowa were obtained from Koch Asphalt Co., St. Paul, Minnesota and Jebro, Inc., Sioux City, Iowa. Two sets of asphalt samples were supplied by each of the two suppliers: each set of samples consisted of one AC-5, one AC-10, and one AC-20. The two sets of samples from Jebro were received in February, and September, 1987; those obtained from Koch were received in June, and October, 1987. A total of 12 virgin asphalt cements were used in this preliminary study. They were identified as J0501-O, J0502-O, J1001-O, J1002-O, J2001-O, J2002-O, K0501-O, K0502-O, K1001-O, K1002-O, K2001-O, and K2002-O.

In addition, two sets of asphalt samples recovered from pavement cores, taken in April, 1987, were provided by the Materials Laboratory, Iowa Department of Transportation (DOT). These samples were taken from seven-year old pavements of known performance with respect to cracking [71]. They were identified as Sugar Creek

(surface, binder, and base) and Wood River (surface, binder, and base), respectively.

For the main study, ten hot mix field pavements were selected by the engineers of the Iowa Department of Transportation to represent a range of asphalt source, asphalt grade, and type of construction projects in Iowa. The selected projects included four AC-5s, two AC-10s, and four AC-20s. The projects consisted of two Interstate projects, three primary, and five secondary highways, three of which were placed as surface, two as binder, and five as base courses. A summary of these projects is given in Table 1.

For each project, one gallon of original asphalt cement, 15 to 25 kg of virgin aggregates, and 15 to 25 kg of plant mix were collected. In addition, 2 to 3 core samples were taken after compaction. These samples were obtained between August, and November, 1988. Between September, 1989 and January, 1990, an additional 8 to 10 core samples were taken by Iowa DOT engineers at each project.

B. Procedures

For the preliminary study, the 12 original asphalts (O samples) were first aged following the thin-film oven test procedure (ASTM D 1754) and identified as R samples (J0501-R, J0502-R, etc.). The O and R samples were characterized by rheological properties, HP-GPC, DSC,and XRD.

In the main study, for each of the 10 sets of field samples, the following asphalt cement samples were derived for characterization by rheological properties, HP-GPC, TMA, and NMR:

· PAO: Virgin or original asphalt.

Table 1. Summary of field projects

Project	County	AC Source & Aggregate	Pavement Type
1	Monona	AC-10 KOCH, Algona, IA 70% 3/4" gravel, 30% crushed gravel	surface, S[1]
2	Story	AC-20 KOCH, Tama, IA 65% 3/4" crushed limestone, 10% 3/8" chips, 25% sand	binder, P[2]
3	Dallas	AC-20 KOCH, Dubuque, IA 50% 3/4" crushed gravel, 35% 3/4"quartzite, 15% concrete sand	surface, I[3]
4	Grundy	AC-5 KOCH, Dubuque, IA 70% 3/4" gravel, 12% 3/4" crushed gravel, 18% 1/2" crushed limestone	base, C
5	Hardin	AC-5 KOCH, Dubuque, IA 70% 3/4" gravel, 30% 3/4" crushed limestone	base, S
7	Webster	AC-5 KOCH, Algona, IA 60% 3/4" crushed limestone, 40% 3/4" gravel	base, S
8	Plymouth	AC-5 KOCH, Algona, IA 17% 3/4" wash rock, 83% 3/4" pit run	base, S
10	Harrison	AC-20 JEBRO, Sioux City, IA 35% 3/4" quartzite, 14% concrete sand, 51% 3/4" crushed rock	surface, P
11	Harrison	AC-10 KOCH, Algona, IA 30% 3/4" limestone, 30% 3/8" limestone, 40% scushed gravel	binder, P
12	Pottawattamie	AC-20 KOCH, Omaha, NE 50% 3/4" stone, 35% 3/8" stone, 15% sand	binder, I

[1] Secondary road
[2] Primary road
[3] Interstate highway

- PAR: Thin-film oven test residue following ASTM D 1754.
- PO: Laboratory aged asphalt following pressure-oxidation procedure (20 atm of oxygen at 65.6°C for 46 hours) developed by Lee [62,65]. This procedure was developed to simulate field in-service aging for five years under Iowa climatic conditions.
- PO5: Laboratory aged asphalt following pressure-oxidation procedure (20 atm of oxygen at 65.6°C for 5 hours).
- PM: Asphalt cement extracted and recovered from plant mix.
- PC: Asphalt cement extracted and recovered from core samples taken right after compaction.
- PC1: Asphalt cement extracted and recovered from core samples taken after one year of service.
- LM: Asphalt cement recovered from laboratory prepared hot mix following plant job mix formula using virgin aggregates and asphalt cement from the project.
- L35: Asphalt cement recovered from laboratory mix, compacted by 35-blow Marshall procedure and aged in oven at 60°C for 12 days [33,81]. This procedure was developed to simulate in-service asphalt aging in pavement with high air voids.
- L75: Asphalt cement recovered from laboratory mix, compacted by 75-blow Marshall procedure and aged in oven at 60°C for 12 days [33,81]. This procedure was developed to simulate in-service asphalt aging in pavement with low air voids.

In the following discussion, these asphalt sample codes will be preceded by a project number identified in Table 1.

1. Rheological properties

Penetration at 5°C (100 g, 5 sec), penetration at 25°C (100 g, 5 sec), penetration at 4°C (200 g, 60 sec), viscosity at 25, 60, and 135°C, and ring-and-ball softening point tests were performed. From these data, penetration ratio (PR), penetration index (PI), pen-vis number (PVN), viscosity temperature susceptibility (VTS), cracking temperature (CT), critical stiffness, and critical stiffness temperature were calculated. Based on viscosity data at 25°C, shear index (SI, the slope of log viscosity versus log shear rate plot) and complex flow (CF) were determined.

To correlate with low temperature field performance, the dependence of viscoelastic properties of selected asphalt samples on their thermal history was studied at a low temperature. Newtonian viscosities and elastic shear moduli of these samples were determined at 5°C after cooling from 25°C as well as after warming from a quenching temperature of -30°C at a rate of 0.7°C/min. Asphalt samples were conditioned for 24 hours at 25°C or 1 hour at -30°C. The reasons for choosing 5°C were: 1) It was the lowest temperature at which rheological tests were manageable with the equipment on hand. 2) It may reasonably be considered as an intermediate winter temperature which prevails after a warm spell or after a severe cold. 3) It is within a temperature range in which most asphalts suffer a thermal (endothermic) transition upon heating [1,79]. The instrument used for these measurements was a cone and plate

viscometer modified to measure rotational displacements as small as 1/100 degree. The Newtonian viscosity and the elastic shear modulus were estimated from the slope and the intercept of the linear asymptotic section of the rotation versus time plot. Details of the instrumentation, procedure, and theory were described in reference 67.

2. HP-GPC

A high performance gel permeation chromatography system (Waters) was used for this study. This system consisted of a solvent reservoir, a dual head high pressure pump (Waters 510), an injector (Waters U6K), three 'Ultrastyragel' columns (Waters, one 1,000 Å followed by two 500 Å units), a UV absorbance detector set at 340 nm (Waters 481), and a data module (Waters 745).

Asphalt samples of 0.02 to 0.05 grams were accurately weighed to prepare a 0.5% (w/v) solution with tetrahydrofuran (THF). Prior to injection, the sample solution was centrifuged to remove foreign particles capable of plugging columns. The carrier solvent was THF, flow rate was 0.9 ml/min, and sample size was 100 µl. The columns were maintained in a constant temperature water bath at 27°C. To establish the relationship between molecular weight and retention time, eight standard materials of known molecular weight were analyzed using the HP-GPC system described above.

3. Thermal analyses

For the differential scanning calorimetry (DSC) measurement, 10 to 20 mg of asphalt sample sealed in an aluminium pan was scanned from -80°C to 80°C with a

heating rate of 5°C/min using a DuPont 1090 system. The precooling rate was 10°C/min.

For the thermomechanical analyses (TMA), a Dupont 943 thermomechanical analyzer was used. Dimensions of the asphalt samples used in TMA were 3 mm thickness and 5 x 5 mm square. Samples were quench-cooled to -70°C, conditioned for 10 minutes, and then heated at a rate of 5°C/min up to 25°C. An expansion probe with contact diameter of 2.54 mm was used.

4. XRD

All 12 original asphalt samples (O samples) and their TFOT aged residues (R samples) used in the preliminary study were subjected to X-ray diffraction analysis by θ-2θ scanning, using a monochromatized CuK_α beam with a 1.54 Å wavelength. The samples were molded in circular Plexiglas holders exactly flush with their brim.

In a θ-2θ scan, both θ and 2θ vary. Whenever the Bragg equation is satisfied, a diffraction peak is obtained. The Bragg equation [2] is

$$\lambda n = 2d \sin \theta$$

where, λ = wavelength of X-ray used,
n = integer (1,2,3 ...),
d = interplaner spacing, and
θ = angle of incidence.

5. NMR

Four samples were subjected to ^{13}C and ^{1}H NMR analyses using a home-built solid state NMR spectrometer, situated in the Department of Chemistry, Iowa State University, operating at 100 MHz for ^{1}H and 25 MHz for ^{13}C. This unit has been extensively used for studies of pyrolyzed pitches and coals supplied by Mobil Oil Research, the Argonne Coal Bank, and Iowa and German coals. To fingerprint the heteroatom functionality by NMR, labeling with a ligand containing phosphorus was attempted.

Solution ^{13}C NMR was employed for the two recovered field asphalts [64], two project asphalts, and asphaltenes of the two project asphalts. A Bruker WM-200 operating at 50 MHz for ^{13}C was used for this purpose. This unit is a research grade multi-nuclear NMR spectrometer for both routine and long-term experiments. The relaxation constant, $T_{1\rho}$ [32], was measured by ^{1}H NMR using a Bruker MSL-300, a high performance dedicated solid-state NMR spectrometer operating at 300 MHz for ^{1}H.

6. Water-sensitivity of mixes

Pavement performance of the one-year old core sample against moisture damage was evaluated by measuring resilient modulus (RM) and indirect tensile strength (ITS) before and after an accelerated Lottman conditioning procedure [69] as follows. A set of three randomly selected cores, among the 8 to 10 cores from each project, was subjected to RM measurement followed by ITS measurement. Another set of three random cores was subjected to RM and ITS measurements after the Lottman

conditioning procedure. This procedure consisted of the following steps in order: 1) 30 minute vacuum saturation at 88 kPa (26 inch Hg) gage vacuum, followed by 2) 30 minute submerging under water at atmospheric pressure, 3) 15 hours sealed in a wet atmosphere at -18°C, 4) 24 hours at 60°C water bath, and finally 5) 3 hours at 25°C water. RM was measured with a Retsina Mark IV resilient modulus device at 25°C, 0.33 Hz frequency, and 0.1 second load duration [90]. ITS was measured at 25°C and a loading rate two inches per minute [60].

7. Aging of asphalts

Age hardening characteristics of asphalt samples was studied in the laboratory by use of three different aging procedures; the thin film oven test (TFOT), the Iowa durability test (IDT), and asphalt-aggregate mix aging. As mentioned previously, TFOT simulates age hardening due to conventional batch mixing [35]. The IDT or pressure-oxidation procedure, also discussed earlier, consists of two aging stages; TFOT to simulate hardening during hot-plant mixing followed by pressure-oxidation under 20 atm of oxygen at 65.6°C for oxidative hardening during field pavement service [62,65]. In this study, two different durations of pressure-oxidation, 46 and 5 hours, were used. The IDT studies previously performed [62,65] indicated that 5 and 46 hours of IDT on asphalt were equivalent to 1-year and 5-year aging, respectively, for in-service pavement under Iowa climatic conditions.

Aging characteristics of asphalts were determined based on a theory that the changes in physical properties of asphalt are hyperbolic functions of time and, therefore,

approach a definite limit with time. An equation to express the hardening of asphalts in the field has been suggested as follows [15]:

$$\Delta Y = \frac{T}{a + bT}$$

where, ΔY = change in physical property with time T,
a,b = constants, and
1/b = the ultimate change of property at infinite time.

Constants a and b, and the ultimate change, 1/b, were determined from the measured physical property changes after 5 and 46 hours of the IDT. Through use of the above equation, physical properties after 10, 20, and 30 years of field service were estimated.

The hardening of asphalt in a mix is believed to be affected by air void content, asphalt film thickness, characteristics of the aggregate, and the durability of asphalt. To examine the age hardening of asphalt in a mix, Marshall specimens were prepared by use of the same materials and job mix formula used at each project. To simulate asphalt aging in pavement of high and low void levels, mixes were compacted by 35 blows per side or 75 blows per side. The specimens were then oven-aged at 60°C for 12 days which conditions simulate eight years of in-service asphalt aging in pavement [33,81].

V. RESULTS AND DISCUSSIONS

A. Results of the Preliminary Study

1. Rheological properties

Penetrations at 5 and 25°C, viscosities at 60 and 135°C, and softening points of the 12 original asphalt (O) samples, as well as their thin film oven test residues (R) are given in Table 2. While all 12 samples met AASHTO M226-2 specifications, variations between samples and between suppliers within given viscosity grades existed. By far, the most uniform results were observed in softening points.

Temperature susceptibility parameters including the class number (CN), the penetration index (PI), the viscosity-temperature susceptibility (VTS), the penetration-viscosity number between 25°C and 60°C (PVN60), and the penetration-viscosity number between 25°C and 135°C (PVN135) are given in Table 3. The results, in general, for temperature susceptibility, especially measured by VTS and PVNs, were remarkably uniform although a few of the samples showed somewhat higher (e.g., the second set of samples from Jebro, J2 samples) or lower (e.g., the first set of samples from Koch, K1 samples) values.

Low-temperature asphalt stiffness has been correlated with pavement cracking associated with nonload conditions. The low-temperature behavior of asphalts can be evaluated either by estimating the temperature at which asphalt reaches a certain critical or limiting stiffness or by comparing the stiffness of asphalts at low temperatures and at long loading times. Table 4 presents the results of estimated low-temperature cracking properties of the 12 asphalts. The properties include cracking temperature (CT), the

Table 2. Rheological properties (preliminary study)

Sample ID	Sp.Gravity @ 25°C/25°C	P25	P5	VIS60 Pa·s	VIS135 10^{-6} m^2/s	SP °C
J05-01-O	1.024	162	16	65.4	232.8	41.5
J05-01-R	1.027	98	15	137.0	309.3	48.0
J05-02-O	1.019	160	15	49.3	213.0	41.5
J05-02-R	1.032	79	11	152.8	336.7	50.0
K05-01-O	1.023	193	22	55.6	225.0	40.5
K05-01-R	1.026	103	13	127.3	334.7	49.0
K05-02-O	1.023	182	17	48.4	211.8	40.0
K05-02-R	1.026	95	13	116.0	321.5	48.0
J10-01-O	1.031	91	11	146.7	329.5	48.0
J10-01-R	1.034	60	8	264.0	453.9	54.0
J10-02-O	1.019	92	11	109.1	312.1	45.5
J10-02-R	1.031	59	10	264.0	469.5	53.0
K10-01-O	1.028	123	15	102.4	307.1	45.5
K10-01-R	1.030	72	9	254.1	457.4	51.5
K10-02-O	1.028	102	11	107.9	311.2	46.0
K10-02-R	1.031	61	10	273.5	461.9	53.5
J20-01-O	1.028	78	12	244.5	448.7	50.0
J20-01-R	1.029	57	10	506.3	660.7	56.0
J20-02-O	1.018	66	8	182.9	450.8	49.5
J20-02-R	1.029	50	8	392.9	592.8	54.0
K20-01-O	1.031	75	10	189.3	430.3	49.0
K20-01-R	1.034	49	8	464.8	618.2	55.5
K20-02-O	1.031	67	7	201.0	428.3	50.0
K20-02-R	1.034	43	6	500.1	581.4	55.5

Table 3. Temperature susceptibility (preliminary study)

Sample ID	CN	PI	VTS	PVN60	PVN135
J05-01-O	5.17	-0.327	3.538	-0.432	-0.510
J05-01-R	2.44	0.060	3.601	-0.462	-0.639
J05-02-O	11.00	-0.378	3.497	-0.784	-0.675
J05-02-R	6.38	-0.036	3.569	-0.689	-0.742
K05-01-O	5.09	0.028	3.497	-0.306	-0.344
K05-01-R	4.76	0.510	3.503	-0.459	-0.462
K05-02-O	8.73	-0.455	3.490	-0.580	-0.526
K05-02-R	8.30	-0.038	3.498	-0.691	-0.614
J10-01-O	3.67	-0.171	3.571	-0.509	-0.624
J10-01-R	4.67	0.206	3.540	-0.552	-0.595
J10-02-O	9.98	-0.884	3.504	-0.807	-0.694
J10-02-R	5.75	-0.072	3.515	-0.577	-0.565
K10-01-O	4.82	0.056	3.483	-0.400	-0.390
K10-01-R	1.28	0.091	3.522	-0.309	-0.393
K10-02-O	7.94	-0.414	3.494	-0.654	-0.586
K10-02-R	3.60	0.132	3.542	-0.492	-0.554
J20-01-O	-0.01	-0.072	3.524	-0.221	-0.333
J20-01-R	-3.67	0.526	3.499	0.016	-0.125
J20-02-O	11.75	-0.658	3.411	-0.778	-0.507
J20-02-R	4.10	-0.247	3.487	-0.433	-0.411
K20-01-O	6.84	-0.451	3.453	-0.548	-0.438
K20-01-R	1.08	0.039	3.514	-0.300	-0.375
K20-02-O	7.98	-0.488	3.481	-0.660	-0.564
K20-02-R	1.24	-0.264	3.589	-0.422	-0.586

Table 4. Low-temperature cracking properties (preliminary study)

Sample ID	CT °C	TES °C	S23 MPa	S29 MPa
J05-01-O	-40.5	-46.5	2.8	8.0
J05-01-R	-45.0	-47.0	9.0	18.0
J05-02-O	-40.0	-46.5	2.4	11.0
J05-02-R	-40.0	-40.0	12.0	30.0
K05-01-O	-45.0	-49.5	1.5	5.0
K05-01-R	-42.0	-43.0	7.0	12.0
K05-02-O	-40.0	-45.0	2.0	5.0
K05-02-R	-43.0	-42.0	7.0	25.0
J10-01-O	-38.0	-40.5	10.0	20.0
J10-01-R	-37.5	-37.0	20.0	30.0
J10-02-O	-38.5	-34.5	19.0	40.0
J10-02-R	-42.0	-36.0	23.0	50.0
K10-01-O	-42.5	-44.5	4.0	10.0
K10-01-R	-37.5	-38.5	12.0	40.0
K10-02-O	-38.0	-42.0	9.0	21.0
K10-02-R	-41.5	-36.5	14.0	40.0
J20-01-O	-42.5	-39.0	12.0	24.0
J20-01-R	-42.5	-36.0	15.0	30.0
J20-02-O	-36.5	-32.5	25.0	70.0
J20-02-R	-39.0	-34.5	30.0	60.0
K20-01-O	-39.5	-36.0	20.0	50.0
K20-01-R	-39.0	-34.5	30.0	60.0
K20-02-O	-34.0	-35.0	20.0	50.0
K20-02-R	-35.0	-32.5	50.0	100.0

temperature corresponding to an asphalt thermal cracking stress of 500 kPa (72.5 psi) based on penetrations at 5°C and 25°C, the temperature of equivalent asphalt stiffness of 1.38×10^5 kPa (20,000 psi) at 10,000 second loading time (TES), estimated stiffness at -23°C and 10,000 second loading time (S23), and stiffness at -29°C and 20,000 second loading time. The following can be observed:

- Softer asphalts AC-5 had lower cracking temperatures and reached a critical stiffness of 1.38×10^5 kPa (20,000 psi) at lower temperatures than harder asphalts AC-20.
- Within a given viscosity grade, cracking temperatures of asphalts can vary by as much as 5°C.
- Low temperature stiffness values for asphalts of a given viscosity grade can differ by a factor of 4.

The effects of heat, as determined by viscosity at 60°C and penetration at 25°C on the thin film oven test (TFOT) residues, are given in Table 5. Ratios of viscosities after and before TFOT were uniform between 1.8 to 3.1 (all meeting AASHTO M226, Table 2, maximum ratio of 5); penetration ratios varied between 0.49 and 0.76.

The resistance of asphalts to hardening during hot-mixing and their temperature susceptibilities are indirectly specified in AASHTO M226, Table 2. These important properties are plotted in Figure 3 in terms of PVN60 and viscosity ratio at 60°C. Except for the second set of samples from Jebro (J2 samples), asphalts supplied in Iowa appeared to be rather uniform in these properties.

The properties of recovered asphalt samples from 80 month old pavements are given in Table 6. The pavements were constructed August, 1980 at Jones County, Iowa.

Table 5. Thin film oven test hardening (preliminary study)

Sample ID	Viscosity Ratio @ 60°C	Penetration Ratio @ 25°C
J05-01	2.09	0.60
J05-02	3.10	0.49
J10-01	1.80	0.66
J10-02	2.42	0.64
J20-01	2.07	0.73
J20-02	2.15	0.76
K05-01	2.29	0.53
K05-02	2.40	0.52
K10-01	2.48	0.59
K10-02	2.53	0.60
K20-01	2.45	0.65
K20-02	2.49	0.64

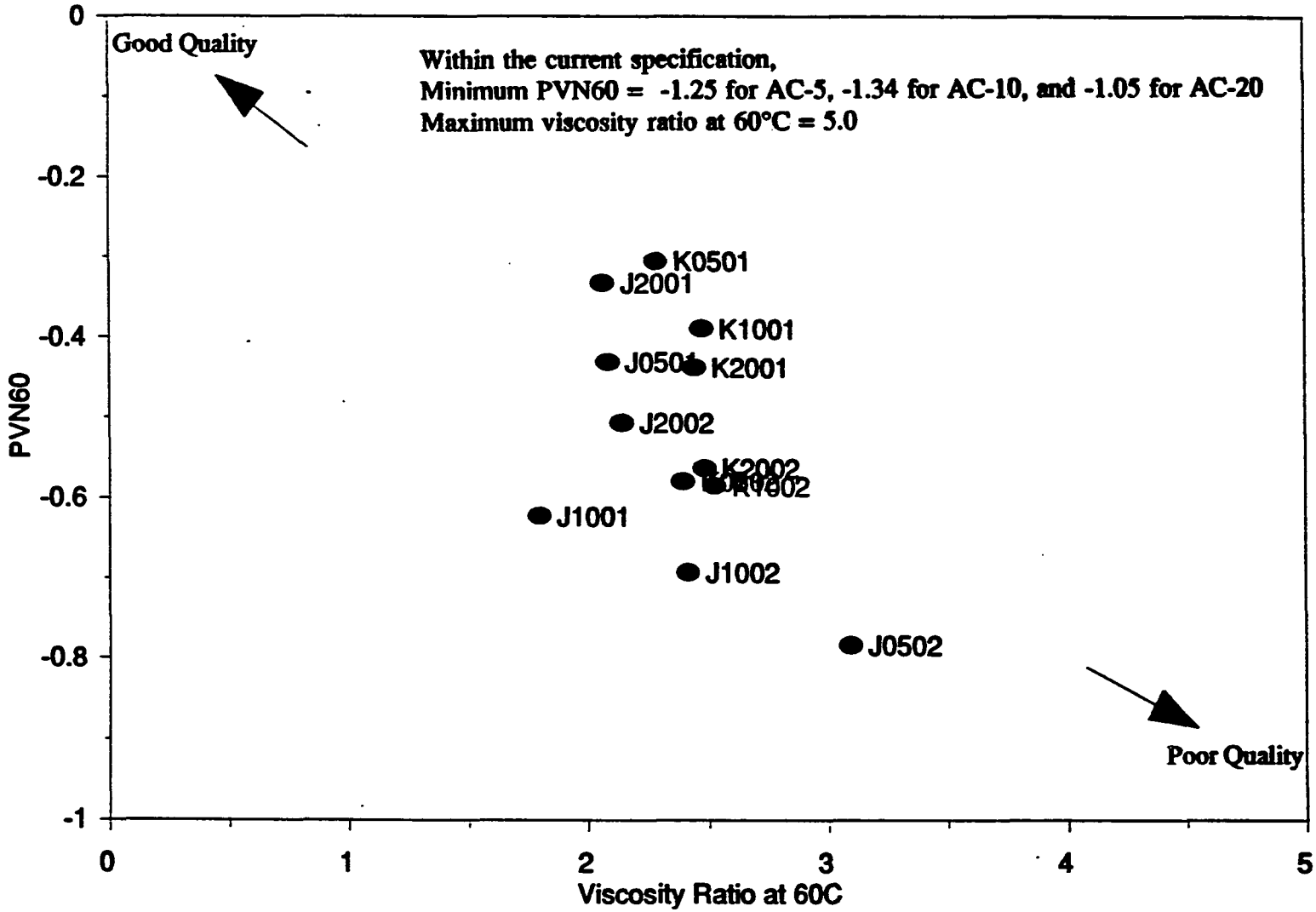

Figure 3. PVN60 versus viscosity ratio

Table 6. Properties of recovered asphalts (preliminary study)

Sample	P25	VIS60 Pa·s	PVN60
80 months after construction			
WOOD RIVER			
Surface	43	480.6	-0.460
Binder	71	170.1	-0.742
Base	56	247.1	-0.720
SUGAR CREEK			
Surface	24	826.8	-0.763
Binder	35	362.4	-1.010
Base	26	481.7	-1.137
45 months after construction (average values)[1]			
WOOD RIVER	55	291.8	-0.61
SUGAR CREEK	40	292.4	-1.04
At time of construction (average values)[1]			
WOOD RIVER	100	110.0	-0.6
SUGAR CREEK	75	90.0	-1.2

[1] Data from Marks and Huisman [71]

Visual crack surveys performed 3 1/2 years after construction indicated that the Sugar Creek asphalt pavement showed an average crack interval of 10.7 m and the Wood River asphalt pavement showed an average crack interval of 51.8 m. As shown in Table 6, the Sugar Creek asphalt had, initially and after 45 months of field service, a higher temperature susceptibility with about the same consistency as the Wood River asphalt. Based on this information, Marks and Huisman [71] concluded that the temperature susceptibility of asphalt was a key factor in understanding the transverse cracking in asphalt pavement. However, the physical properties of these asphalts, after 80 months of field service and determined during the current study, showed great differences in age hardening in these asphalts as measured by penetration at 25°C and viscosity at 60°C. A comparison of their properties after 45 month of service, showed that while the temperature susceptibilities of both asphalts, measured by PVN60, changed little, the average viscosity of the Sugar Creek asphalts increased to about twice that of the Wood River asphalts. This suggests that the chemical composition of Sugar Creek asphalts is very different from that of the Wood River asphalts. This would result in greatly different temperature susceptibility and age hardening characteristics. The effects of thermal history on the rheological properties of these recovered asphalts are discussed below.

The results of viscoelastic measurements at 5°C, after two different thermal treatments as described previously, are given in Figures 4 through 7 where viscosity and elastic shear modulus are plotted respectively against time of thermal treatment. Reviewing these figures, it can be observed that the rheological properties of these

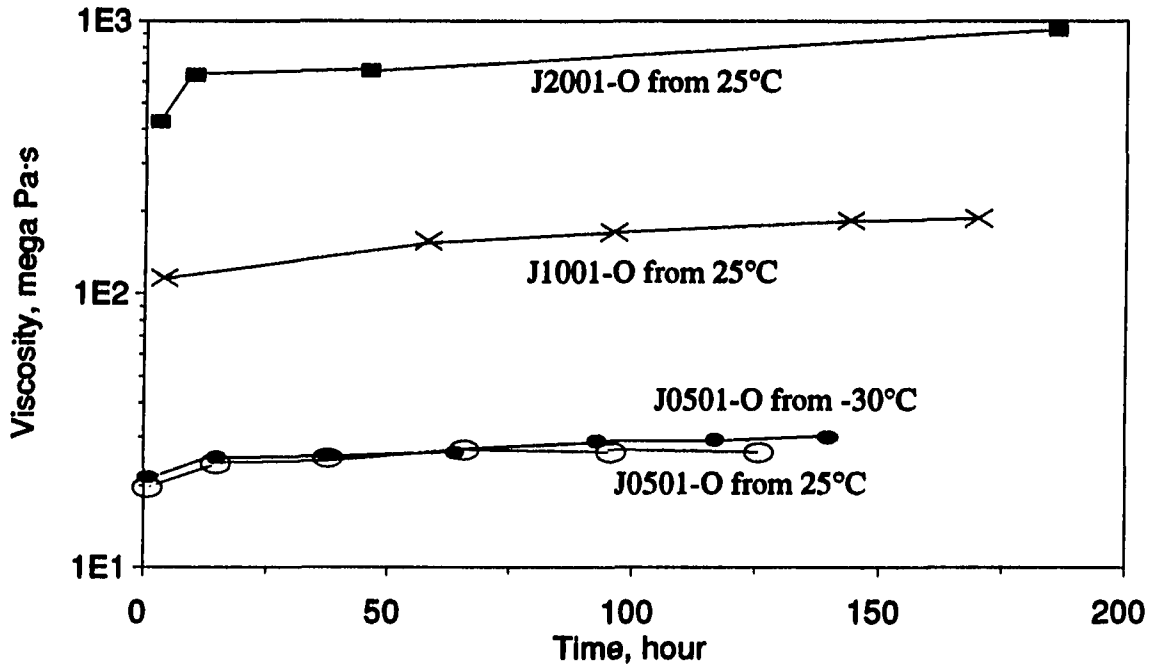

Figure 4. Effects of thermal treatment and time on viscosities of J1 samples at 5°C

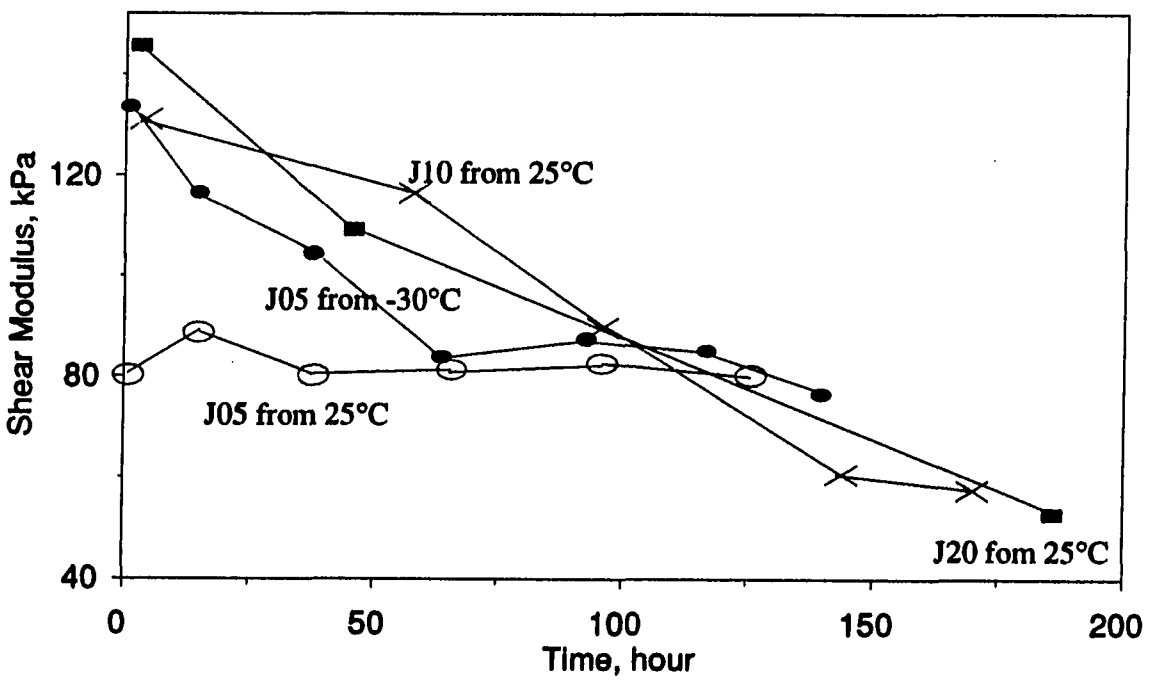

Figure 5. Effects of thermal treatment and time on shear moduli of J1 samples at 5°C

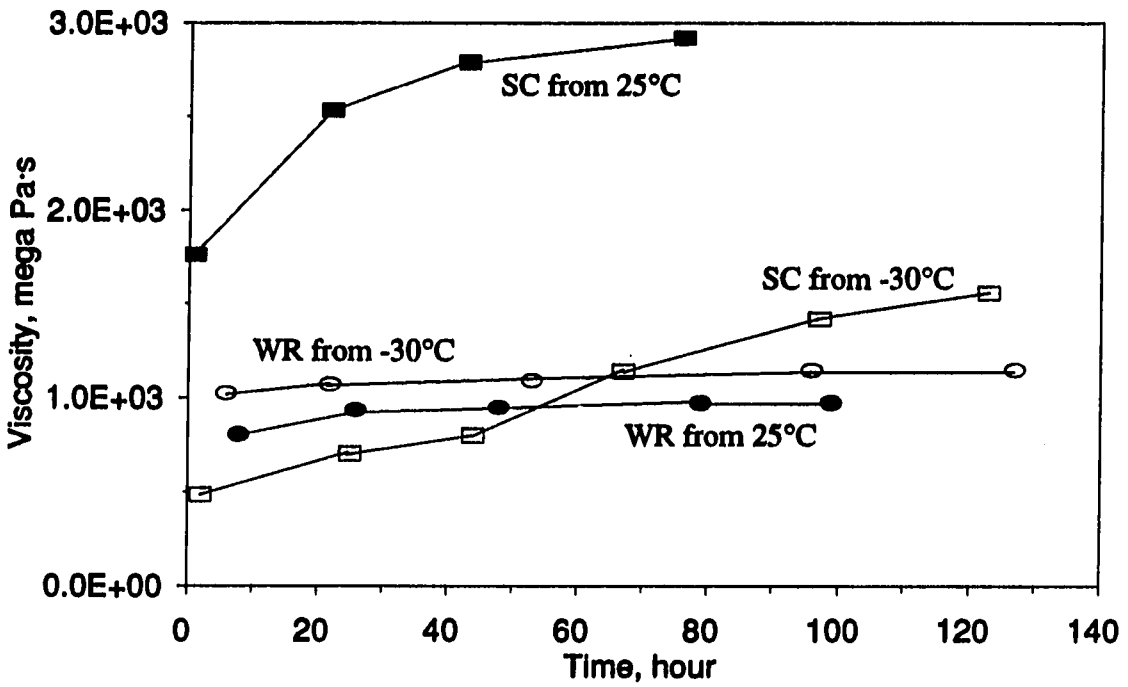

Figure 6. Effects of thermal treatment and time on viscosities of recovered samples at 5°C

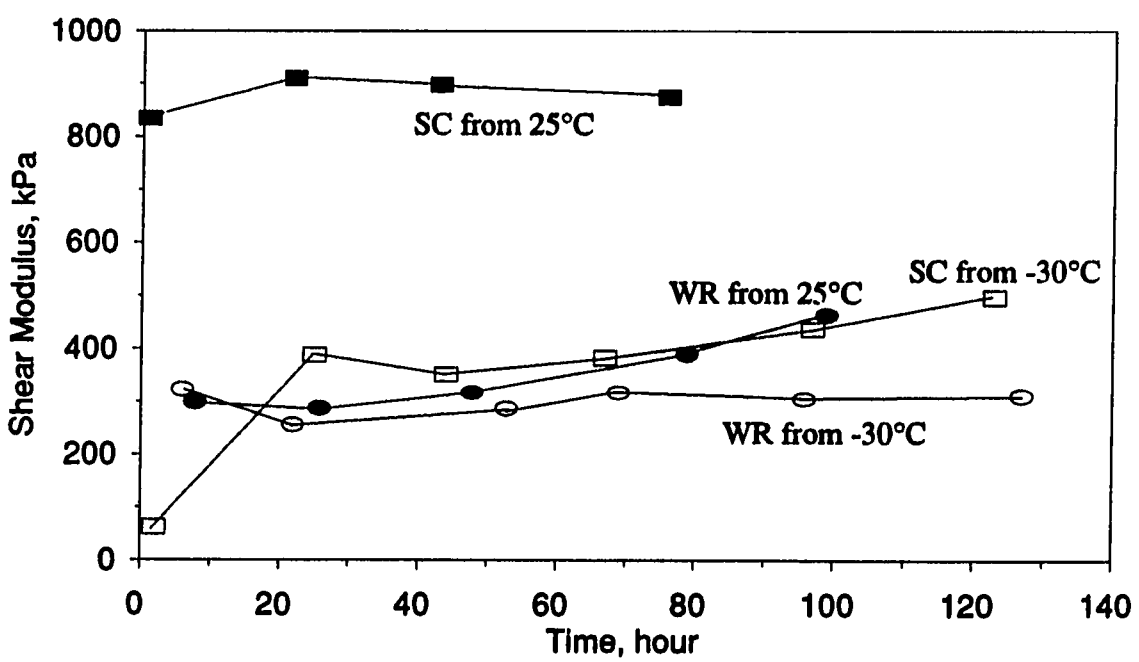

Figure 7. Effects of thermal treatment and time on shear moduli of recovered samples at 5°C

samples at 5°C exhibit strikingly different dependence on their thermal history and time. Some properties do not stabilize even after seven days as shown in Figures 4 through 7.

The viscoelastic properties shown in Figures 6 an 7 may indicate that both the Sugar Creek surface and the Wood River surface asphalts possess enough mobility at temperatures between 5°C and 25°C to remain in a minimum energy state showing stabilized viscoelastic responses on different time scales. However, when samples the Sugar Creek asphalt were conditioned at -30°C, they exhibited deviated viscoelastic responses from the stabilized responses but as time elapsed the properties approached the stabilized responses. Samples of the Wood River surface asphalt showed about the same viscoelastic responses after thermal treatment at -30°C as they did after conditioning at 25°C. This indicates that the mobility of the Sugar Creek surface asphalt is quenched at temperatures between -30°C and 5°C and remains in a thermodynamically unstable state throughout the experiment. This finding is in agreement with the observation made by Claudy et al. [18] of isothermal physical hardening. This phenomena is controlled by the glass transition temperature of an asphalt as determined by DSC and the amount of crystallizable fraction found in that asphalt.

2. HP-GPC

The Montana State University research group [50-54] divided the HP-GPC chromatogram into three slices for further data analyses using two elution cut-off times of 22.5 and 30.5 minutes. They labeled the first eluted slice as LMS (large molecular

size), the second eluted slice as MMS (medium molecular size), and the third eluted slice as SMS (small molecular size). They proposed %LMS as an index for the low-temperature susceptibility of an asphalt sample. They labeled the four slices as LMS, MMS1, MMS2, and SMS, respectively, in the order of elution. A comparative analysis of the HP-GPC size distribution curves by Lee and Enustun [67] shows that the fractional increase in the largest detectable molecular size region (earliest elution) as a results of TFOT, is the largest among the other regions of the LMS fraction defined by the Montana research group. Lee and Enustun [67] believed that most of asphaltene agglomerates in asphalt will be dissociated during HP-GPC testing and the early-eluted fraction is made up by the remnants of undissociated agglomerates. They also believed that their observation just mentioned is the results of formation of extra agglomerates induced by TFOT. Then, the early-eluted fraction content of a sample is expected to be approximately proportional to the original agglomerate concentration, and thus is a more sensitive index than LMS defined by the Montana method to characterize aging and low-temperature susceptibility. For this reason, Lee and Enustun [67] further divided the LMS defined by the Montana research group into two slices using an elution time of 18.125 minute. Changes in the LMS in Lee and Enustun's procedure, upon aging of asphalts, are expected to be more sensitively detected than changes in the slices of the Montana procedure. In this preliminary study, Lee and Enustun's coding procedure is employed. The percent of LMS plus %MMS1 (LMS+MMS1) in this method is identical to %LMS of the Montana slicing method. A typical HP-GPC chromatogram is shown in Figure 8 together with Lee and Enustun's slicing method.

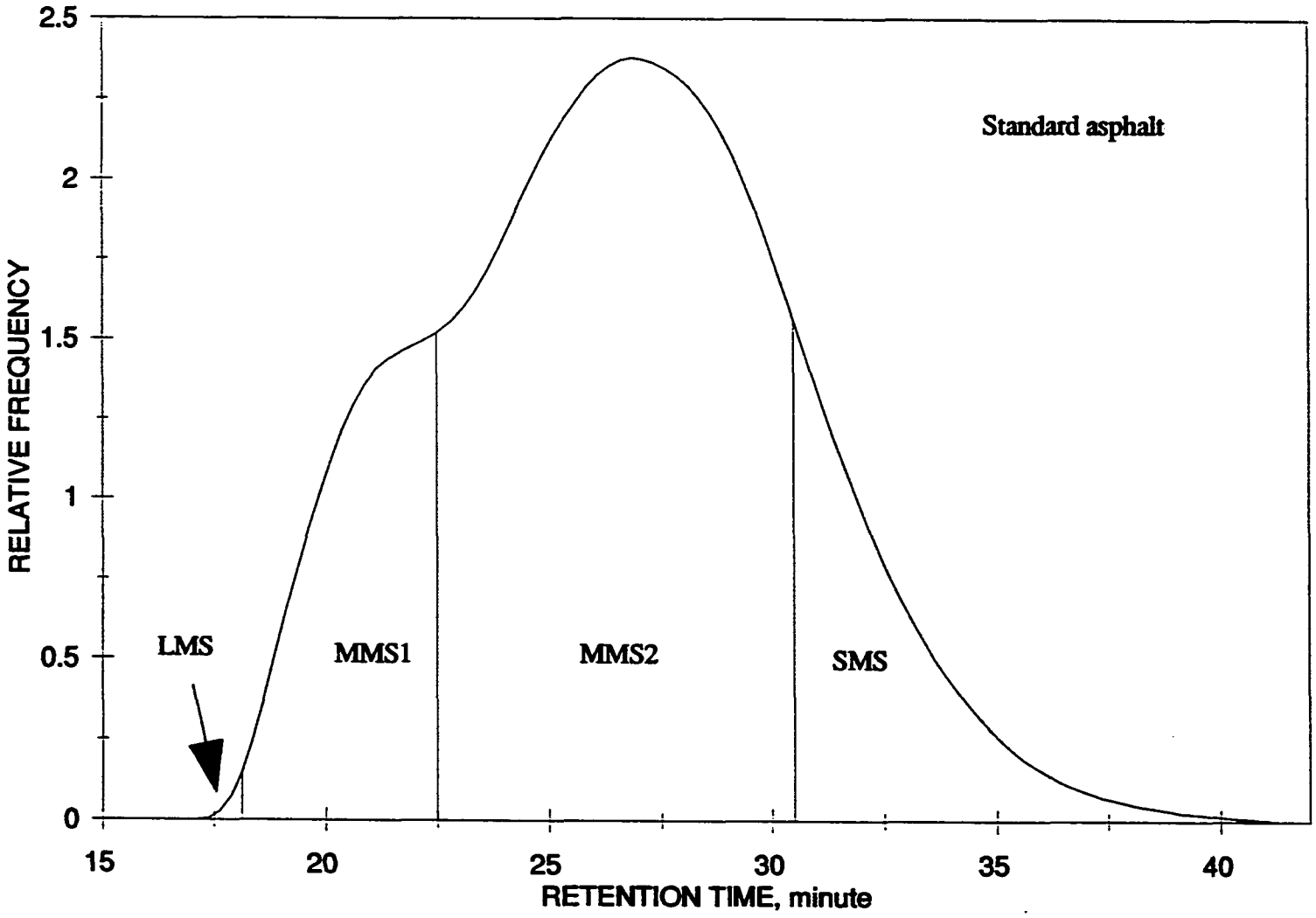

Figure 8. Typical four fraction HP-GPC chromatogram

HP-GPC runs on 12 virgin asphalts, their TFOT residues, and six recovered core samples were performed. The amounts of LMS and LMS+MMS1 for these materials before and after TFOT aging, except the recovered samples, are tabulated in Table 7. The percent changes for the recovered samples are estimated by percent differences of HP-GPC results, surface course samples compared to those of the base course samples (the surface course samples were age-hardened more severely than the base course samples). The results summarized in Table 7 showed the following:

- The %LMS+MMS1 of the original asphalt studied ranged from 20.6 to 30.9%, all higher than the maximum allowable limit of 16-17% for the Montana climates [54]. The %LMS for the original and TFOT aged samples ranged from 0.35 to 3.25 and showed a good linear relationship with the %LMS+MMS1 ($r^2 = 0.888$).
- The %LMS+MMS1 of asphalts in a given viscosity grade varied up to 7.4% between samples from the same supplier; this difference was as high as 9.6% between samples of different suppliers.
- There was no distinct relationship between viscosity at 60°C and the %LMS+MMS1 or %LMS. The samples from Koch had relatively higher %LMS+MMS1 but in a narrow range, between 27.2 and 30.8.
- Thin film oven treatment of all asphalts increased %LMS+MMS1 by an average of 2.87% (1.2 to 3.8%). The percent change in LMS due to aging was much larger as expected.
- The Wood River asphalts had larger %LMS+MMS1 and %LMS than the Sugar Creek asphalts. This might have an important bearing in temperature susceptibility and the

Table 7. Results of HP-GPC analyses (preliminary study)

Sample	LMS+MMS1, %	change, %	LMS, %	change, %
J05-01-O	22.5		0.70	
J05-01-R	26.2	+16	1.28	+83
J05-02-O	20.6		0.35	
J05-02-R	24.0	+16	0.66	+89
K05-01-O	30.2		2.26	
K05-01-R	31.4	+4	2.42	+71
K05-02-O	27.2		2.12	
K05-02-R	30.7	+13	3.25	+53
J10-01-O	21.8		0.64	
J10-01-R	24.9	+14	1.06	+66
J10-02-O	24.9		0.64	
J10-02-R	27.4	+10	1.02	+59
K10-01-O	30.8		2.26	
K10-01-R	32.8	+7	2.78	+23
K10-02-O	28.3		1.76	
K10-02-R	31.2	+10	2.57	+46
J20-01-O	30.9		1.46	
J20-01-R	33.0	+7	2.02	+38
J20-02-O	23.5		0.36	
J20-02-R	27.3	+16	0.74	+105
K20-01-O	28.8		1.85	
K20-01-R	32.3	+12	2.92	+58
K20-02-O	27.3		1.68	
K20-02-R	30.0	+10	2.37	+41
SC-Base	23.4		0.88	
SC-Binder	26.7	+19	1.50	+102
SC-Surface	27.9		1.78	
WR-Base	29.5		1.68	
WR-Binder	34.9	+2	3.34	+13
WR-Surface	30.1		1.89	

low-temperature performance of Wood River asphalt.

During SHRP [101] an SEC study showed that, for asphalts prepared from the same crude source using the same production method, increasing viscosity or changing grade (for example from AC-10 to AC-20) always increased the amount of SEC fraction I corresponding to %LMS+MMS1 or %LMS while the chemical composition determined by an elemental analysis and a functional group analysis remains the same. Table 7, however, shows that AC-20 asphalts supplied from Jebro at two different times (J1 and J2) are very different in %LMS+MMS1 (30.9% and 23.5%). For the samples first supplied by Koch (K1 samples), the AC-10 shows a larger %LMS+MMS1 than that of the AC-20 (30.8% versus 28.8%). This indicates that there might be a variation in asphalt chemical composition for materials obtained from a supplier for different grades and at different times.

Also, as shown in Table 7, aging always increases the %LMS+MMS1 or the %LMS. This means that this HP-GPC technique can be used, as concluded previously [54,61], as a reliable test to monitor aging. The increase in %LMS or %LMS+MMS1 is believed to result from the increased molecular association produced by oxidation.

3. Thermal analyses

The results of DSC runs on the 12 virgin asphalts, their TFOT residues, and the six recovered core samples are presented in Table 8. A typical DSC thermogram is shown in Figure 9. The low temperature inflexion points in the DSC thermograms, as interpreted by other researchers [1,79] as glass transition points (T_g), are determined

Table 8. DSC test results (preliminary study)

Sample	T_g °C	T_1 °C	T_2 °C	T_m °C	Enthalpy Change J/g
J05-01-O	-31	17.0	47.5	32.0	12.0
J05-01-R	-29	16.0	48.0	32.0	10.1
J05-02-O	-29	17.0	41.0	29.0	10.3
J05-02-R	-30	17.0	39.5	28.0	15.0
K05-01-O	-26	17.5	53.0	35.0	8.2
K05-01-R	-26	17.0	47.0	32.0	8.8
K05-02-O	-30	16.0	47.0	31.5	8.8
K05-02-R	-29	17.0	53.0	35.0	8.4
J10-01-O	-30	16.5	47.5	32.0	11.2
J10-01-R	-31	16.0	45.0	30.5	13.9
J10-02-O	-32	16.5	48.0	32.0	9.3
J10-02-R	-30	16.5	48.5	32.5	10.5
K10-01-O	-31	17.0	41.0	29.0	6.9
K10-01-R	-30	17.5	48.0	33.0	7.5
K10-02-O	-29	17.0	48.0	32.5	6.8
K10-02-R	-30	17.0	46.0	31.5	6.7
J20-01-O	-35	16.0	44.5	30.0	11.4
J20-01-R	-35	17.0	47.5	32.0	9.7
J20-02-O	-30	16.5	47.5	32.0	9.7
J20-02-R	-29	16.0	53.0	34.5	10.6
K20-01-O	-25	17.5	47.5	32.5	5.7
K20-01-R	-22	19.5	47.5	33.5	4.8
K20-02-O	-26	22.0	50.5	36.0	6.0
K20-02-R	-30	29.5	53.0	41.0	7.8
SC-Base	-26	17.0	50.5	34.0	9.6
SC-Binder	-31	16.0	44.0	30.0	11.2
SC-Surface	-30	16.5	48.0	32.0	10.6
WR-Baae	-37	15.0	44.5	30.0	10.8
WR-Binder	-35	14.0	44.0	29.0	13.3
WR-Surface	-35	16.0	43.5	30.0	10.7

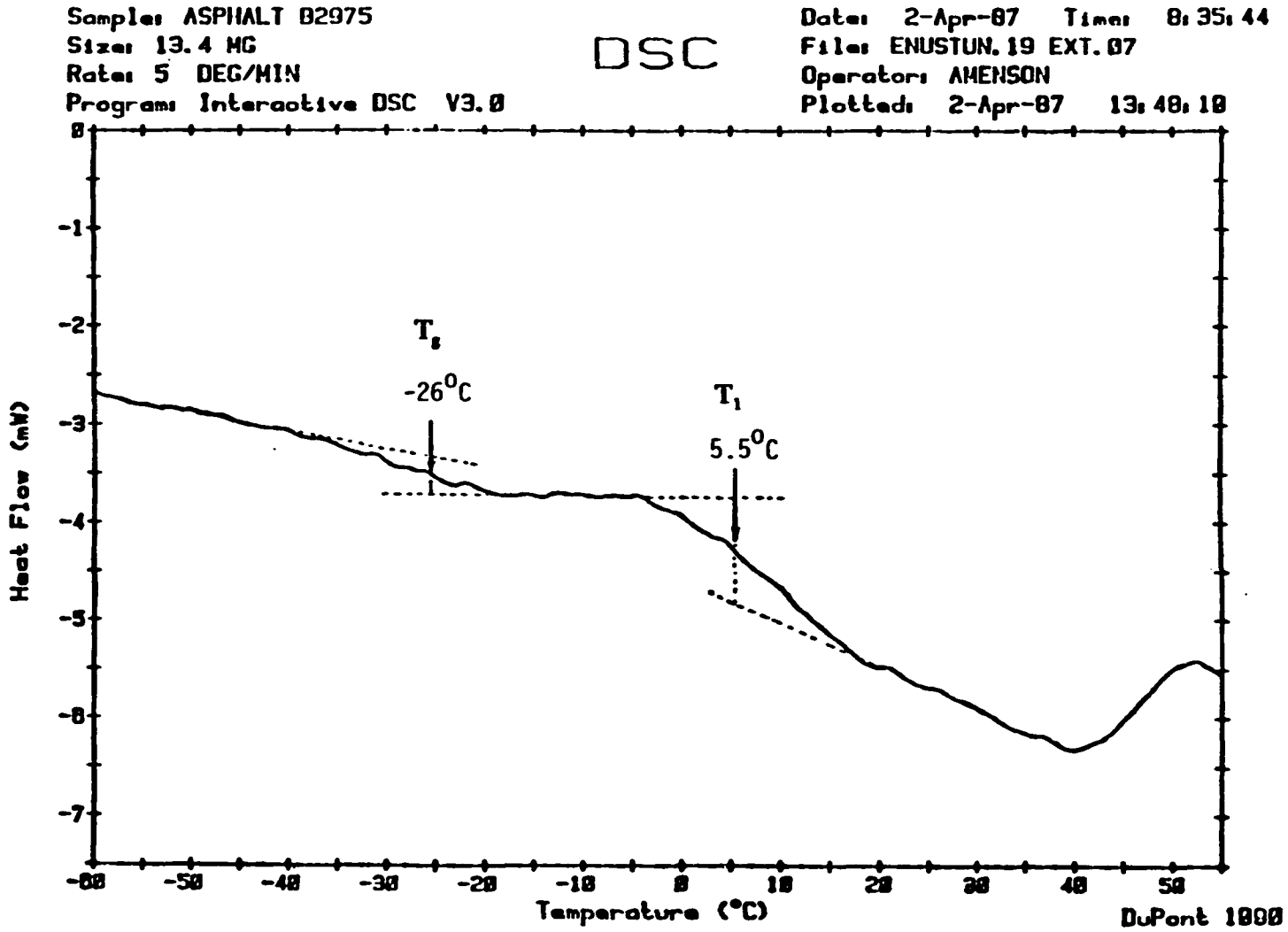

Figure 9. Typical DSC thermogram for asphalt

together with two upper temperature transition points, defined here as T_1, and T_2. The mean of T_1, and T_2, T_m, is calculated and is also shown in Table 8. Transition regions, analyzed in the manner described by Albert et al. [1] to determine the enthalpies of transformation (ΔH), are given in the last column of Table 8.

No relationship between viscosity at 60°C and transition temperatures or enthalpy change is observed. The effects of aging on transition temperatures and ΔH appear to be in random directions. However, there is a difference in ΔH between the asphalts from two suppliers. The ΔH values for the original J samples are on average 24% higher than those for the K samples. Claudy et al. [18] interpreted ΔH as a measure of the crystallizable fraction (CF) and found it to be related to isothermal physical hardening. For example, at the same low temperature, the asphalt with the lower glass transition temperature and the lower amount of CF would be less sensitive to isothermal physical hardening.

Compared with the Sugar Creek asphalts, the Wood River asphalts have about the same values for ΔH but have lower transition temperatures. The lower transition temperature of the Wood River asphalts would give a relatively higher mobility at 5°C than that of the Sugar Creek asphalts and would also give less sensitivity to the thermal treatment discussed previously.

4. X-ray diffraction

X-ray diffraction (XRD) spectra were obtained by θ-2θ scanning of the original asphalt samples and their TFOT residues. An empty sample holder was scanned over

the same range to represent background. A typical XRD spectrum is shown in Figure 10. According to Williford [113] the height of the shoulder of the spectral curve at low angles is a measure of the quality of the asphalt. This height above the background at 2θ of 4.83° for various samples and their TFOT residues is tabulated in Table 9. Also included are the qualitative changes in the shoulder height and peak height upon TFOT for each sample.

No regular trend exists in these spectra regarding the viscosity grade or supplier, nor regarding the effect of aging. In contrast to what is observed in HP-GPC, the XRD spectra are affected by TFOT in a quite random fashion and direction. At present, no explanation regarding chemical composition and change upon aging is available for these observations.

5. Correlations

As discussed previously, HP-GPC seems to be a very sensitive characterization method for asphalt cements and the changes in them upon aging. DSC can be used in characterizing asphalt but this will require a more detailed understanding of the chemical composition of asphalt. XRD may not be a suitable technique for use in asphalt characterization. In this section, the relationship of HP-GPC properties, characterized by the 3-slice and 4-slice methods to rheological properties and DSC parameters will be discussed. No relationship was found between HP-GPC and XRD properties.

Multiple regression analyses were performed between HP-GPC parameters and physical/DSC properties and the results are given in Table 10. Overall, the 4-slice

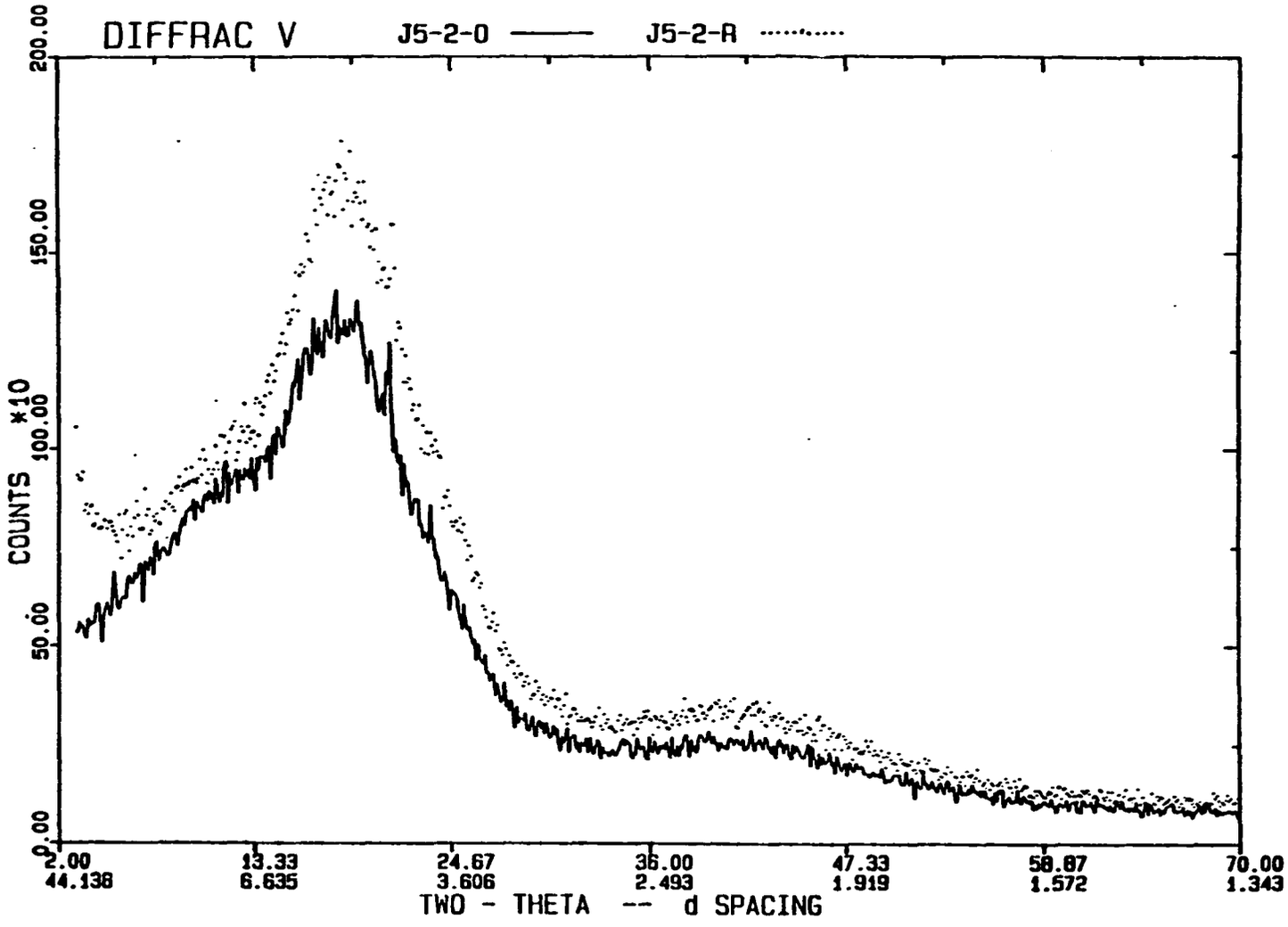

Figure10. X-ray diffraction spectra for J0502-O and -R samples

Table 9. Shoulder height of X-ray diffraction spectrum (preliminary study)

Sample	Shoulder height counts x 10	change in shoulder height	change in peak height
J05-01-O	33		
J05-01-R	37	+	0
J05-02-O	26		
J05-02-R	40	+	+
K05-01-O	26		
K05-01-R	37	+	-
K05-02-O	36		
K05-02-R	36	0	0
J10-01-O	43		
J10-01-R	37	-	-
J10-02-O	44		
J10-02-R	32	-	+
K10-01-O	34		
K10-01-R	26	-	+
K10-02-O	25		
K10-02-R	25	0	+
J20-01-O	25		
J20-01-R	41	+	-
J20-02-O	48		
J20-02-R	13	-	-
K20-01-O	36		
K20-01-R	18	-	+
K20-02-O	25		
K20-02-R	39	+	-

Note: +: increase 0: no change -: decrease

method shows better relationships than the 3-slice method.

Rheological properties show significant correlations with HP-GPC parameters. An interesting observation is that as the temperature at which the rheological properties were measured increases, a better relationship is observed, i.e., as temperature changes from 5°C to 25, 60, and 135°C, the coefficients of determination change from 0.275 to 0.420, 0.553, and 0.618 respectively using the 4-slice method. Softening points ranged from 40 to 56°C for these asphalts and also fall into this relationship. An explanation for this observation is, as pointed out during SHRP [101], that as temperature increases the degree of intermolecular association decreases within an asphalt. The solvent used in this study, tetrahydrofuran (THF), also decreases intermolecular association. Therefore, the state of dispersion of an asphalt in THF would be close to that of that asphalt at higher temperatures. At lower temperatures, polar aromatic molecules in asphalt would be involved in extensive associations and the state of dispersion would be greatly different from that in THF. This might be the reason that the HP-GPC parameter shows better relationships with high temperature rheology.

Some temperature susceptibility parameters (CN, PI, and PVN60) and the low-temperature cracking property (TES) showed weak relationships with HP-GPC parameters. Glass transition temperatures and the enthalpy changes measured by DSC show statistically significant relationships with HP-GPC parameters.

From a comparison of r^2 for the 3-slice and 4-slice methods, it can be observed that, for high temperature rheological properties and DSC properties, the 4-slice method showed a significantly better relationship (higher r^2). This indicates that high

Table 10. Results of regression analyses (preliminary study)

	Coefficient of Determination, r^2 (n=24)	
Property	4-slice method	3-slice method
Rheological properties		
Log (Sp.Gravity)	0.245	0.244
Log (P25)	0.420 *	0.205
Log (P5)	0.275	0.174
Log (VIS60)	0.553 **	0.320 *
Log (VIS135)	0.618 **	0.357 *
Log (SP)	0.423 *	0.236
Temperature susceptibility		
CN	0.418 *	0.349 *
PI	0.359	0.359 *
VTS	0.109	0.097
PVN60	0.441 *	0.398 *
PVN135	0.260	0.196
Low-temperature cracking properties		
CT	0.250	0.249
TES	0.398 *	0.206
Log (S23)	0.370	0.165
Log (S29)	0.276	0.112
Thermal properties		
T_g	0.451 *	0.313
ΔH	0.544 **	0.415 *

* significant at 5% level
** significant at 1% level

temperature rheological properties and DSC properties are related to the %LMS and the %LMS+MMS1 (the only difference between 3-slice and 4-slice methods is further division of LMS+MMS1 into two slices, LMS and MMS1).

B. Results of the Main Study

1. Rheological properties

Penetration and softening point data for the 79 asphalt samples from the ten pavement projects are given in Table 11 (numbers preceding the sample identifications are project numbers). Viscosity data, including shear index and complex flow at 25°C, are given in Table 12. Shear index or shear susceptibility (the rate of change of viscosity with rate of shear) and complex flow (the rate of change of shear stress with the rate of shear) have been found to be related to the aging characteristics of asphalts and are useful indicators for pavement performance [58,59,65]. Temperature susceptibility indices in terms of PR, PI, PVN, VTS, and CN of the asphalts studied are given in Table 13. Reviewing these tables indicates that the ten asphalts supplied in Iowa during the 1988 construction season appear to be uniform and well within the AASHTO specifications.

Table 14 presents the results of estimated low-temperature cracking properties of the 79 asphalts from the ten projects. The properties include cracking temperature (CT), temperature of equivalent asphalt stiffness of 1.38 x 10^5 kPa (20,000 psi) at 10,000 second loading time (TES), estimated stiffness at -23°C and 10,000 second loading time (S23), and stiffness at -29°C and 20,000 second loading time (S29) using van der Poel's

Table 11. Rheological properties - I

Sample ID	P5	P25	P4	SP °C
(AC-5s)				
4PAO	19	181	64	41.5
4PAR	14	100	52	45.5
4PC1	11	98	35	44.6
4PO5	11	86	31	48.8
4PO	10	52	25	54.0
4PM	18	144	56	43.5
4PC	15	105	45	46.5
4L35	15	105	54	54.0
4L75	12	55	29	55.0
5PAO	18	191	68	41.5
5PAR	13	103	40	48.0
5PC1	11	83	33	49.3
5PO5	14	105	36	46.2
5PO	11	53	25	54.0
5PM	19	156	61	45.5
5L35	12	77	39	51.0
5L75	13	86	37	50.0
7PAO	16	193	60	39.0
7PAR	12	94	38	43.5
7PC1	14	105	41	45.3
7PO5	11	84	32	49.3
7PO	10	46	24	56.0
7L35	17	105	44	45.5
7L75	14	91	39	50.0
8PAO	17	196	58	38.5
8PAR	13	95	39	46.5
8PC1	15	107	43	44.5
8PO5	11	83	30	50.2
8PO	10	46	25	56.0
8L35	15	88	36	49.5
8L75	14	84	42	50.0
(AC-10s)				
1PAO	8	82	29	47.5
1PAR	7	50	21	52.0
1PC1	7	52	21	51.4
1PO5	6	44	16	54.1
1PO	6	27	14	61.5
1PM	10	55	29	56.0
1L35	8	27	15	66.5
1L75	9	32	17	62.5

Table 11. continued

Sample ID	P5	P25	P4	SP °C
11PAO	15	133	44	44.0
11PAR	10	69	29	51.5
11PC1	11	91	36	49.0
11PO5	8	58	24	53.2
11PO	7	35	21	59.5
11L35	10	60	27	55.0
11L75	11	65	28	54.0
(AC-20s)				
2PAO	7	54	15	49.0
2PAR	6	38	17	55.5
2PC1	7	45	19	55.8
2PO5	5	36	14	52.6
2PO	6	25	14	67.0
2PM	7	35	18	59.0
2PC	6	30	17	61.0
2LM	7	39	19	60.5
2L35	5	31	16	60.5
2L75	7	35	16	58.5
3PAO	9	75	30	47.0
3PAR	8	48	22	54.5
3PC1	11	89	36	47.2
3PO5	5	41	16	55.8
3PO	6	26	14	63.0
3PM	9	41	22	58.0
3PC	9	40	24	58.0
3L35	7	30	16	66.5
3L75	6	33	18	61.5
10PAO	9	82	29	49.0
10PAR	7	47	19	50.5
10PC1	6	36	18	59.0
10PO5	5	40	16	56.5
10PO	5	24	14	62.5
10L35	8	32	19	65.0
10L75	10	81	30	48.5
12PAO	8	82	28	47.0
12PAR	6	47	20	53.5
12PC1	9	67	27	49.6
12PO5	5	40	15	56.2
12PO	4	23	14	63.0
12L35	9	54	21	56.0
12L50	10	65	27	53.0
12L75	9	51	24	54.0

Table 12. Rheological properties - II

Sample ID	VIS25 Pa·s	SI	CF	VIS60 Pa·s	VIS135 10^{-6} m²/s
(AC-5)					
4PAO	1.50E+04	0.98	0.030	58.3	250.3
4PAR	7.20E+04	0.96	0.025	157.4	368.6
4PC1	9.00E+04	0.96	0.065	173.0	343.0
4PO5	1.06E+05	0.92	0.200	204.9	394.0
4PO	4.15E+05	0.94	0.080	468.2	553.1
4PM	2.90E+05	0.60	0.330	85.6	1094.8
4PC	5.60E+04	0.92	0.050	141.0	361.5
4L35	1.75E+05	0.79	0.220	445.7	573.3
4L75	3.80E+05	0.79	0.210	680.4	707.2
5PAO	1.88E+04	0.96	0.045	63.2	247.5
5PAR	9.00E+04	0.95	0.060	147.0	395.5
5PC1	1.60E+05	0.91	0.150	235.2	540.0
5PO5	6.50E+04	0.95	0.100	145.7	348.0
5PO	4.75E+05	0.84	0.160	450.9	500.1
5PM	4.70E+04	0.91	0.066	134.1	285.9
5L35	1.21E+04	0.90	0.100	236.8	443.9
5L75	1.23E+05	0.87	0.130	252.9	447.1
7PAO	2.50E+04	0.99	0.027	73.4	250.8
7PAR	7.10E+04	0.98	0.023	174.2	398.5
7PC1	5.40E+04	0.96	0.064	84.6	346.0
7PO5	1.45E+05	0.87	0.100	236.5	414.0
7PO	5.25E+05	0.78	0.230	638.3	618.7
7L35	4.90E+04	0.89	0.070	143.1	388.9
7L75	1.44E+05	0.89	0.110	232.4	445.4
8PAO	1.86E+04	1.00	0.034	67.0	253.0
8PAR	7.15E+04	0.98	0.019	183.2	404.7
8PC1	7.00E+04	0.98	0.096	127.6	380.0
8PO5	1.10E+05	0.93	0.080	243.0	429.0
8PO	4.20E+05	0.90	0.100	508.0	550.4
8L35	1.40E+05	0.86	0.160	216.1	436.2
8L75	1.40E+05	0.89	0.090	348.4	500.8
(AC-10)					
1PAO	9.10E+04	0.95	0.045	157.6	368.7
1PAR	3.50E+05	0.90	0.100	372.2	515.3
1PC1	3.20E+05	0.85	0.108	401.5	581.0
1PO5	6.50E+05	0.84	0.160	560.3	552.0
1PO	1.55E+06	0.74	0.260	1321.0	788.4
1PM	2.80E+05	0.82	0.200	623.5	664.8
1L35	1.67E+06	0.57	0.420	5176.8	1431.3
1L75	1.12E+06	0.65	0.390	3253.4	1185.6

Table 12. contunued

Sample ID	VIS25 Pa·s	SI	CF	VIS60 Pa··s	VIS135 10^{-6} m^2/s
11PAO	3.95E+04	0.96	0.037	111.0	444.4
11PAR	1.90E+05	0.92	0.070	355.8	559.0
11PC1	1.09E+05	0.93	0.077	202.4	452.0
11PO5	2.57E+05	0.89	0.140	460.2	592.0
11PO	9.50E+05	0.82	0.190	1042.6	770.3
11L35	3.30E+05	0.83	0.180	448.1	638.5
11L75	2.70E+05	0.92	0.090	422.0	625.3
(AC-20)					
2PAO	3.40E+05	0.94	0.063	357.1	889.2
2PAR	8.20E+05	0.72	0.320	630.6	986.7
2PC1	4.30E+05	0.71	0.290	549.1	817.0
2PO5	8.00E+05	0.65	0.290	1097.7	1080.0
2PO	1.95E+06	0.55	0.460	3971.6	1654.7
2PM	8.30E+05	0.62	0.350	5232.9	1975.4
2PC	1.20E+06	0.39	0.580	1698.6	1384.5
2LM	6.50E+05	0.55	0.440	1231.5	934.1
2L35	1.40E+06	0.58	0.420	5520.2	1757.9
2L75	1.15E+06	0.66	0.340	1765.3	1063.9
3PAO	1.17E+05	0.96	0.030	273.0	477.3
3PAR	3.60E+05	0.90	0.100	610.7	713.3
3PC1	1.45E+05	0.88	0.110	248.5	495.0
3PO5	5.70E+05	0.84	0.140	894.8	810.0
3PO	1.94E+06	0.72	0.280	2140.8	1201.6
3PM	4.60E+05	0.81	0.190	1589.1	1088.2
3PC	6.70E+05	0.72	0.270	1339.8	964.6
3L35	1.05E+06	0.74	0.260	1721.8	1039.9
3L75	1.25E+06	0.72	0.290	2275.0	1183.6
10PAO	1.01E+05	0.97	0.030	210.5	459.8
10PAR	3.75E+05	0.93	0.070	633.4	732.7
10PC1	7.10E+05	0.78	0.254	1455.4	1030.0
10PO5	6.00E+05	0.90	0.170	797.7	799.0
10PO	1.85E+06	0.73	0.270	1836.0	1091.0
10L35	1.20E+06	0.69	0.360	3765.4	1630.2
10L75	1.53E+05	0.90	0.100	250.7	489.5
12PAO	1.04E+05	0.98	0.023	233.7	470.0
12PAR	4.40E+05	0.91	0.080	650.3	774.7
12PC1	2.70E+05	0.91	0.130	254.4	440.0
12PO5	6.50E+05	0.90	0.160	954.3	828.0
12PO	2.05E+06	0.73	0.260	2262.4	1139.7
12L35	5.70E+05	0.79	0.200	72.2	819.7
12L50	4.00E+05	0.89	0.120	461.1	715.7
12L75	4.90E+05	0.90	0.100	548.9	713.3

Table 13. Temperature susceptibility

Sample	PR	PI	CN	VTS	PVN60	PVN135
(AC-5)						
4PAO	0.354	0.150	7.963	3.381	-0.367	-0.243
4PAR	0.520	-0.632	2.628	3.474	-0.279	-0.347
4PC1	0.357	-0.980	-0.714	3.573	-0.210	-0.481
4PO5	0.360	-0.114	0.552	3.526	-0.247	-0.418
4PO	0.481	-0.153	-2.208	3.576	-0.203	-0.466
4PM	0.389	-0.042	27.546	2.384	-0.329	1.907
4PC	0.429	-0.166	3.981	3.445	-0.316	-0.320
4L35	0.514	1.903	-15.241	3.530	0.937	0.396
4L75	0.527	0.212	-8.185	3.527	0.252	-0.070
5PAO	0.356	0.400	4.636	3.427	-0.171	-0.190
5PAR	0.388	0.221	5.037	3.387	-0.303	-0.204
5PC1	0.398	-0.095	3.844	3.328	-0.160	0.011
5PO5	0.343	-0.274	2.422	3.490	-0.280	-0.379
5PO	0.472	-0.106	-3.780	3.641	-0.211	-0.585
5PM	0.391	0.983	-7.158	3.624	0.336	-0.211
5L35	0.506	0.153	1.697	3.487	-0.275	-0.364
5L75	0.430	0.214	-2.340	3.507	-0.025	-0.229
7PAO	0.311	-0.640	0.980	3.481	0.030	-0.153
7PAR	0.404	-1.461	2.912	3.451	-0.273	-0.300
7PC1	0.390	-0.558	16.607	3.265	-0.872	-0.388
7PO5	0.381	-0.046	-1.611	3.543	-0.134	-0.370
7PO	0.522	-0.001	-4.995	3.605	-0.089	-0.438
7L35	0.419	-0.478	4.975	3.390	-0.300	-0.207
7L75	0.429	0.388	-1.538	3.477	-0.019	-0.169
8PAO	0.296	-0.803	3.073	3.433	-0.051	-0.116
8PAR	0.411	-0.482	1.684	3.459	-0.201	-0.264
8PC1	0.402	-0.741	7.054	3.362	-0.393	-0.220
8PO5	0.361	0.162	-1.342	3.525	-0.126	-0.330
8PO	0.543	-0.001	-1.390	3.611	-0.308	-0.594
8L35	0.409	0.148	0.636	3.464	-0.153	-0.239
8L75	0.500	0.144	-7.584	3.542	0.273	-0.087
(AC-10)						
1PAO	0.354	-0.620	7.221	3.474	-0.599	-0.569
1PAR	0.420	-0.711	3.467	3.544	-0.485	-0.602
1PC1	0.404	-0.764	2.889	3.480	-0.353	-0.399
1PO5	0.364	-0.519	-2.827	3.645	-0.280	-0.633
1PO	0.519	-0.053	-5.255	3.684	-0.189	-0.626
1PM	0.527	0.434	-7.211	3.542	0.166	-0.155
1L35	0.556	0.818	-28.138	3.718	1.029	0.108
1L75	0.531	0.476	-24.338	3.697	0.875	0.044

Table 13. continued

Sample	PR	PI	CN	VTS	PVN60	PVN135
11PAO	0.331	-0.165	8.504	3.175	-0.174	0.307
11PAR	0.420	-0.026	-1.686	3.463	-0.033	-0.151
11PC1	0.396	0.113	2.210	3.409	-0.166	-0.146
11PO5	0.414	-0.080	-3.036	3.517	-0.051	-0.259
11PO	0.600	0.103	-6.383	3.618	-0.034	-0.417
11L35	0.450	0.436	-1.676	3.449	-0.024	-0.117
11L75	0.431	0.419	-2.453	3.442	0.044	-0.057
(AC-20)						
2PAO	0.278	-1.276	13.393	3.116	-0.411	0.226
2PAR	0.447	-0.534	10.235	3.255	-0.382	-0.016
2PC1	0.422	-0.095	5.292	3.341	-0.266	-0.088
2PO5	0.389	-1.278	-1.395	3.392	0.056	0.045
2PO	0.560	0.746	-16.497	3.535	0.676	0.209
2PM	0.514	0.005	-27.443	3.507	1.457	0.790
2PC	0.567	0.066	-2.815	3.372	0.187	0.173
2LM	0.487	0.534	-9.454	3.536	0.283	-0.060
2L35	0.516	0.039	-28.427	3.601	1.306	0.507
2L75	0.457	-0.093	-13.336	3.568	0.453	-0.003
3PAO	0.400	-1.008	0.067	3.485	-0.170	-0.287
3PAR	0.458	-0.230	-1.974	3.481	-0.067	-0.203
3PC1	0.404	-0.484	-0.745	3.419	0.014	-0.036
3PO5	0.390	-0.316	-5.360	3.526	0.059	-0.196
3PO	0.538	0.142	-8.030	3.548	0.187	-0.144
3PM	0.537	0.153	-14.002	3.516	0.601	0.193
3PC	0.600	0.097	-11.564	3.542	0.402	0.008
3L35	0.533	1.038	-9.235	3.575	0.199	-0.185
3L75	0.545	0.357	-16.154	3.579	0.596	0.073
10PAO	0.354	-0.199	3.939	3.411	-0.296	-0.241
10PAR	0.404	-1.211	-1.850	3.474	-0.064	-0.189
10PC1	0.500	0.066	-9.750	3.524	0.317	-0.016
10PO5	0.400	-0.222	-1.967	3.494	-0.086	-0.238
10PO	0.583	-0.100	-3.586	3.563	-0.062	-0.336
10L35	0.594	0.920	-21.449	3.528	1.009	0.446
10L75	0.370	-0.372	0.946	3.431	-0.133	-0.163
12PAO	0.341	-0.764	1.676	3.436	-0.186	-0.209
12PAR	0.426	-0.505	-1.415	3.443	-0.038	-0.114
12PC1	0.403	-0.592	2.979	3.522	-0.421	-0.526
12PO5	0.375	-0.286	-5.961	3.533	0.082	-0.192
12PO	0.609	-0.092	-7.215	3.603	0.062	-0.322
12L35	0.389	0.388	58.905	2.518	-1.981	0.114
12L50	0.415	0.181	-2.116	3.373	0.133	0.134
12L75	0.471	-0.200	-0.724	3.441	-0.077	-0.139

Table 14. Low-temperature cracking properties

Sample ID	CT °C	TES °C	S23 MPa	S29 MPa
(AC-5)				
4PAO	-43.5	-49.0	1.3	3.5
4PAR	-44.0	-38.0	12.0	25.0
4PC1	-38.0	-35.4	14.0	34.0
4PO5	-39.0	-39.2	11.0	22.0
4PO	-43.0	-33.5	30.0	65.0
4PM	-47.0	-44.5	2.7	6.0
4PC	-44.0	-40.5	7.5	15.0
4L35	-48.0	-55.0	2.5	4.0
4L75	-46.0	-36.0	20.0	37.5
5PAO	-42.5	-51.5	0.7	2.5
5PAR	-41.5	-43.0	6.5	12.5
5PC1	-39.5	-38.8	12.0	22.0
5PO5	-43.0	-39.9	8.0	16.0
5PO	-44.0	-33.5	28.0	55.0
5PM	-45.0	-54.5	1.7	2.5
5L35	-41.0	-39.5	10.0	20.0
5L75	-43.5	-41.0	7.5	16.0
7PAO	-39.0	-44.0	1.5	5.0
7PAR	-39.0	-32.0	25.0	60.0
7PC1	-43.0	-38.8	10.0	20.0
7PO5	-39.5	-39.7	9.0	20.0
7PO	-45.0	-32.5	35.0	70.0
7L35	-45.5	-39.0	9.0	20.0
7L75	-41.5	-43.0	7.5	13.0
8PAO	-40.0	-43.5	2.5	8.0
8PAR	-42.5	-38.0	8.0	20.0
8PC1	-44.0	-37.5	10.0	23.0
8PO5	-39.5	-39.8	7.5	17.0
8PO	-45.0	-32.5	33.0	60.0
8L35	-46.5	-40.5	7.5	16.0
8L75	-46.5	-40.0	8.0	18.0
(AC-10)				
1PAO	-35.0	-36.0	18.0	40.0
1PAR	-36.0	-30.5	42.0	85.0
1PC1	-36.3	-29.1	35.0	80.0
1PO5	-35.0	-28.9	50.0	95.0
1PO	-40.0	-26.0	90.0	150.0
1PM	-42.5	-37.0	20.0	40.0
1L35	-47.5	-49.5	50.0	85.0
1L75	-47.5	-48.5	50.0	80.0

Table 14. continued

Sample	CT °C	TES °C	S23 MPa	S29 MPa
11PAO	-42.5	-43.0	3.5	10.0
11PAR	-40.0	-37.0	15.0	30.0
11PC1	-38.5	-41.0	9.0	19.0
11PO5	-37.5	-34.9	22.0	46.0
11PO	-40.0	-29.5	45.0	90.0
11L35	-41.5	-38.0	16.0	35.0
11L75	-42.5	-39.0	15.0	27.0
(AC-20)				
2PAO	-36.0	-28.0	75.0	170.0
2PAR	-35.5	-28.5	75.0	150.0
2PC1	-37.5	-32.2	40.0	75.0
2PO5	-33.0	-24.4	130.0	349.9
2PO	-40.0	-30.0	60.0	100.0
2PM	-40.0	-29.5	50.0	100.0
2PC	-37.5	-28.0	65.0	150.0
2LM	-38.5	-34.0	35.0	60.0
2L35	-34.0	-28.5	70.0	130.0
2L75	-40.0	-31.0	60.0	100.0
3PAO	-37.5	-33.0	30.0	65.0
3PAR	-39.0	-32.0	35.0	75.0
3PC1	-39.0	-36.9	10.0	27.0
3PO5	-32.5	-29.3	50.0	100.0
3PO	-40.0	-27.0	80.0	140.0
3PM	-44.0	-32.0	35.0	70.0
3PC	-44.0	-31.5	37.0	72.0
3L35	-42.5	-34.0	40.0	75.0
3L75	-37.0	-31.0	50.0	90.0
10PAO	-37.0	-38.0	12.0	26.0
10PAR	-37.0	-27.5	65.0	150.0
10PC1	-36.3	-30.5	47.0	85.0
10PO5	-32.5	-29.6	50.0	95.0
10PO	-36.5	-25.0	100.0	170.0
10L35	-45.0	-34.0	36.0	60.0
10L75	-38.5	-37.0	16.0	37.0
12PAO	-35.0	-35.0	20.0	38.0
12PAR	-34.0	-31.0	38.0	75.0
12PC1	-38.5	-33.4	25.0	60.0
12PO5	-32.5	-28.9	50.0	95.0
12PO	-32.5	-24.5	110.0	170.0
12L35	-42.5	-37.0	20.0	38.0
12L50	-41.0	-37.5	15.0	30.0
12L75	-41.5	-33.0	30.0	55.0

procedure.

2. HP-GPC

The asphalt samples related to ten field samples were also analyzed by HP-GPC. For data analysis, the 3-slice and the 4-slice methods are used as discussed earlier. In addition, 8-slice method is also used as practiced by Garrick and Wood [29]. In the 8-slice method, the cut-off times used were 19.875, 21.875, 23.875, 25.375, 26.875, 28.875, and 30.875 minutes. The cut-off times were empirically determined to give about the same percent area for each slice and about the same time intervals. The eight slices were labeled as X1, X2, ... , and X8 in the same order with their elutions, i.e., the slice X1 is for the first eluted materials and so on. The 3-slice and the 4-slice data are presented in Table 15. The 8-slice data are given in Table 16. Table 17 presents average molecular weight and polydisperse index which were calculated by the data module based on relationship between elution time and molecular weight of reference materials of known molecular weights. Percent changes of 3-, 4-, 8-slice data by different aging procedures are presented in Tables 18 and 19. Discussions regarding their correlations with other properties and their potential bearing on prediction of field performance will be presented later. Other significant findings are discussed below.

Percent LMS is unidirectionally sensitive to TFOT (PAR) and pressure oxidation (PO). An example is shown in Figure 11. Therefore, the HP-GPC technique can be used to monitor and predict oxidative aging. For this purpose, all three slicing methods can be used. As recognized by others [50,54], it is likely that the aging potential, i.e.

Table 15. HP-GPC results - 3-slice and 4-slice methods

Sample ID	LMS	MMS1	MMS2	SMS	LMS+MMS1
(AC-5s)					
4PAO	4.37	28.21	57.62	9.80	32.58
4PAR	6.27	29.75	54.46	9.52	36.02
4PC1	5.81	30.67	55.57	7.95	36.49
4PO5	7.52	29.91	53.51	9.07	37.42
4PO	7.65	30.54	52.74	9.07	38.19
4PM	4.81	30.46	55.04	9.69	35.28
4PC	3.97	28.74	57.48	9.82	32.71
4L35	5.27	30.60	54.96	9.18	35.86
4L75	6.10	31.47	53.71	8.71	37.57
5PAO	4.07	27.73	58.04	10.16	31.80
5PAR	6.30	29.62	54.46	9.62	35.92
5PC1	4.82	31.62	56.37	7.19	36.45
5PO5	5.82	28.93	55.51	9.74	34.75
5PO	7.80	30.74	52.46	9.00	38.54
5PM	3.94	29.78	56.92	9.36	33.72
5L35	5.90	30.83	54.41	8.87	36.73
7PAO	1.16	22.83	62.75	13.26	23.99
7PAR	5.72	29.34	55.16	9.79	35.06
7PC1	4.09	29.43	58.67	7.83	33.52
7PO5	6.43	29.82	54.34	9.41	36.25
7PO	7.55	30.81	52.48	9.16	38.36
7L35	5.14	29.82	55.58	9.47	34.96
8PAO	3.84	28.38	57.93	9.86	32.22
8PAR	5.96	29.62	54.77	9.66	35.57
8PC1	5.91	31.57	54.36	8.16	37.48
8PO5	6.39	29.71	54.53	9.38	36.09
8PO	6.85	30.42	53.53	9.20	37.27
8L35	4.94	29.97	55.63	9.46	34.91
(AC-10s)					
1PAO	3.35	25.69	61.21	9.74	29.05
1PAR	4.53	27.49	58.48	9.51	32.01
1PC1	4.37	29.76	57.16	8.70	34.13
1PO5	5.02	27.75	57.79	9.45	32.77
1PO	5.60	29.07	56.63	8.70	34.67
1PM	3.62	28.80	57.98	9.60	32.42
1L35	4.43	29.45	56.98	9.13	33.89
1L75	3.05	28.40	58.74	9.81	31.45

Table 15. continued

Sample ID	LMS	MMS1	MMS2	SMS	LMSMMS1
11PAO	3.78	28.53	57.97	9.72	32.31
11PAR	6.07	30.23	54.48	9.23	36.30
11PC1	6.73	30.16	53.96	9.16	36.88
11PO5	6.71	30.09	54.08	9.13	36.79
11PO	7.07	30.98	52.97	8.98	38.05
11L35	5.18	29.84	55.31	9.67	35.02
(AC-20s)					
2PAO	4.56	31.34	56.89	7.21	35.90
2PAR	6.17	33.46	53.48	6.90	39.63
2PC1	6.23	33.06	52.96	7.73	39.30
2PO5	6.54	33.48	52.89	7.09	40.02
2PO	7.45	35.22	50.98	6.36	42.66
2PM	5.72	34.48	52.86	6.95	40.19
2PC	5.83	34.44	52.79	6.94	40.27
2LM	5.91	33.08	53.31	7.70	38.99
2L35	5.99	33.69	53.04	7.29	39.68
2L75	5.77	33.10	53.48	7.66	38.87
3PAO	4.44	29.25	57.40	8.91	33.68
3PAR	6.59	30.77	54.15	8.49	37.36
3PC1	6.29	30.43	54.74	8.55	36.72
3PO5	7.33	30.56	53.50	8.61	37.89
3PO	7.98	31.86	52.24	7.92	39.84
3PM	4.61	31.16	55.05	9.19	35.77
3PC	4.30	30.81	56.13	8.76	35.11
3L35	5.72	31.77	54.17	8.35	37.49
3L75	5.96	32.19	53.60	8.26	38.15
10PAO	3.93	28.75	57.96	9.37	32.68
10PAR	6.27	30.48	54.39	8.87	36.76
10PC1	4.95	31.40	54.86	8.79	36.35
10PO5	6.82	30.27	54.10	8.82	37.09
10PO	7.34	31.11	52.95	8.60	38.45
10L35	11.28	31.66	49.35	7.70	42.94
12PAO	4.33	29.53	57.06	9.09	33.86
12PAR	6.54	30.75	54.04	8.67	37.29
12PC1	5.38	29.21	56.35	9.06	34.59
12PO5	6.93	30.53	53.91	8.62	37.46
12PO	7.49	31.55	52.55	8.42	39.03
12L35	5.58	30.63	54.71	9.08	36.21

Table 16. HP-GPC results - 8-slice method

Sample ID	X1	X2	X3	X4	X5	X6	X7	X8
(AC-5s)								
4PAO	13.80	14.68	17.24	13.29	12.21	12.67	7.87	8.25
4PAR	17.14	14.88	16.49	12.56	11.50	11.91	7.50	8.02
4PC1	16.69	15.65	17.09	13.11	11.84	12.04	6.96	6.63
4PO5	18.71	14.74	16.34	12.30	11.37	11.64	7.27	7.63
4PO	19.20	15.07	16.11	12.17	11.04	11.55	7.24	7.62
4PM	15.13	15.70	17.83	12.73	11.33	11.70	7.39	8.20
4PC	13.45	15.04	17.56	13.31	12.04	12.49	7.87	8.24
4L35	16.17	15.52	17.30	12.77	11.49	11.74	7.28	7.74
4L75	17.57	15.78	17.22	12.57	11.16	11.37	7.02	7.32
5PAO	13.30	14.42	17.13	13.40	12.30	12.83	8.06	8.56
5PAR	17.12	14.82	16.44	12.55	11.44	11.98	7.53	8.11
5PC1	15.77	16.30	18.22	13.85	12.04	11.50	6.36	5.97
5PO5	15.86	14.82	16.83	12.97	11.65	12.07	7.58	8.23
5PO	19.56	15.04	16.07	12.10	10.97	11.50	7.18	7.57
5PM	13.65	15.63	18.09	13.22	11.82	12.16	7.59	7.85
5L35	17.10	15.50	16.91	12.64	11.37	11.76	7.32	7.41
7PAO	7.39	12.78	16.50	13.77	13.21	14.96	10.21	11.19
7PAR	16.20	14.83	16.67	12.76	11.61	12.10	7.58	8.27
7PC1	13.81	15.40	18.07	14.30	12.65	12.33	6.95	6.50
7PO5	17.11	15.04	16.83	12.60	11.48	11.67	7.34	7.94
7PO	19.29	15.11	16.16	12.12	11.01	11.42	7.15	7.73
7L35	15.66	15.17	17.08	12.89	11.72	12.06	7.45	7.99
8PAO	13.24	14.83	17.40	13.43	12.26	12.69	7.85	8.31
8PAR	16.63	14.93	16.58	12.68	11.51	12.00	7.52	8.16
8PC1	17.37	15.95	17.01	12.80	11.40	11.68	7.01	6.78
8PO5	17.02	15.02	16.78	12.63	11.44	11.86	7.37	7.90
8PO	18.27	15.04	16.33	12.38	11.25	11.69	7.29	7.75
8L35	15.41	15.33	17.21	12.90	11.65	12.07	7.47	7.97
(AC-10s)								
1PAO	11.65	13.44	17.23	14.34	13.29	13.73	8.16	8.16
1PAR	13.88	14.15	16.87	13.65	12.69	13.01	7.76	7.99
1PC1	14.24	15.66	17.65	13.44	12.19	12.26	7.28	7.27
1PO5	14.44	14.32	17.05	13.53	12.48	12.70	7.52	7.97
1PO	16.04	14.66	16.69	13.19	12.28	12.57	7.23	7.34
1PM	12.97	15.10	17.90	13.42	12.20	12.58	7.78	8.06
1L35	14.52	15.22	17.43	13.30	12.11	12.33	7.41	7.69
1L75	12.23	14.97	17.74	13.54	12.45	12.93	7.89	8.26

Table 16. continued

Sample ID	X1	X2	X3	X4	X5	X6	X7	X8
11PAO	13.25	14.88	17.55	13.50	12.33	12.55	7.75	8.19
11PAR	17.02	15.19	16.80	12.70	11.46	11.77	7.28	7.78
11PC1	17.72	15.09	16.64	12.56	11.42	11.65	7.17	7.75
11PO5	17.50	15.23	16.75	12.74	11.29	11.64	7.14	7.71
11PO	18.71	15.31	16.46	12.32	11.13	11.43	7.06	7.58
11L35	15.70	15.24	17.03	12.95	11.52	11.97	7.39	8.20
(AC-20s)								
2PAO	14.87	16.42	19.25	14.49	12.05	10.93	5.92	6.08
2PAR	18.02	17.04	18.60	13.53	11.25	10.22	5.50	5.85
2PC1	17.95	16.85	18.19	13.32	11.08	10.26	5.74	6.61
2PO5	18.22	17.20	18.82	13.35	11.07	9.91	5.39	6.05
2PO	20.53	17.61	18.06	12.84	10.69	9.78	5.09	5.41
2PM	17.82	17.65	18.90	13.41	10.96	9.96	5.37	5.92
2PC	18.24	17.42	18.79	13.32	10.99	9.93	5.42	5.90
2LM	17.75	16.79	18.03	13.08	11.20	10.58	6.03	6.53
2L35	18.20	17.03	18.18	13.05	11.09	10.44	5.87	6.16
2L75	17.69	16.76	18.03	13.09	11.27	10.62	6.05	6.49
3PAO	14.32	15.13	17.70	13.54	12.28	12.26	7.27	7.50
3PAR	17.85	15.44	16.90	12.80	11.59	11.45	6.82	7.15
3PC1	17.17	15.36	17.08	12.85	11.67	11.74	6.94	7.21
3PO5	18.36	15.38	16.86	12.67	11.39	11.30	6.76	7.28
3PO	20.15	15.68	16.44	12.30	11.15	11.18	6.40	6.71
3PM	15.04	16.16	18.24	12.92	11.43	11.48	6.92	7.82
3PC	14.43	16.06	18.52	13.21	11.67	11.71	7.03	7.37
3L35	17.19	16.02	17.49	12.90	11.41	11.28	6.66	7.05
3L75	17.60	16.24	17.60	12.80	11.21	11.06	6.54	6.96
10PAO	13.46	15.04	17.63	13.65	12.40	12.47	7.46	7.90
10PAR	17.35	15.31	16.92	12.77	11.51	11.64	7.02	7.49
10PC1	16.08	16.00	17.43	12.83	11.58	11.69	6.98	7.41
10PO5	17.75	15.20	17.09	12.70	11.45	11.47	6.90	7.45
10PO	19.10	15.32	16.53	12.43	11.23	11.32	6.82	7.26
10L35	23.78	15.27	15.80	11.60	10.37	10.46	6.27	6.46
12PAO	14.34	15.29	17.70	13.42	12.12	12.20	7.27	7.66
12PAR	17.76	15.40	16.94	12.74	11.45	11.51	6.89	7.32
12PC1	15.55	14.98	16.83	13.16	12.02	12.38	7.50	7.59
12PO5	17.91	15.43	17.05	12.83	11.31	11.36	6.83	7.27
12PO	19.42	15.54	16.58	12.40	11.10	11.16	6.69	7.11
12L35	16.57	15.47	17.24	12.80	11.50	11.64	7.08	7.68

Table 17. HP-GPC results - molecular weight distribution characteristics

Sample ID	Weighted Molecular Weight	Polydisperse Index
(AC-5s)		
4PAO	6.63E+03	11.484
4PAR	8.35E+03	13.857
4PC1	8.12E+03	12.472
4PO5	9.45E+03	15.183
4PO	9.61E+03	15.318
4PM	7.23E+03	12.073
4PC	6.42E+03	11.061
4L35	7.53E+03	12.270
4L75	8.35E+03	13.080
5PAO	6.33E+03	11.211
5PAR	8.35E+03	13.934
5PC1	7.37E+03	10.746
5PO5	7.93E+03	13.417
5PO	9.76E+03	15.466
5PM	6.50E+03	10.859
5L35	8.14E+03	12.989
7PAO	3.54E+03	7.596
7PAR	7.88E+03	13.359
7PC1	6.57E+03	10.230
7PO5	8.56E+03	14.070
7PO	9.50E+03	15.184
7L35	7.37E+03	12.298
8PAO	6.21E+03	10.813
8PAR	8.08E+03	13.553
8PC1	8.27E+03	12.671
8PO5	8.53E+03	14.036
8PO	8.87E+03	14.359
8L35	7.23E+03	12.055
(AC-10s)		
1PAO	5.57E+03	9.962
1PAR	6.70E+03	11.562
1PC1	6.79E+03	11.000
1PO5	7.21E+03	12.284
1PO	7.70E+03	12.537
1PM	6.10E+03	10.456
1L35	6.76E+03	11.234
1L75	5.54E+03	9.698

Table 17. continued

Sample ID	Weighted Molecular Weight	Polydisperse Index
11PAO	6.15E+03	10.625
11PAR	8.22E+03	13.410
11PC1	8.85E+03	14.320
11PO5	8.77E+03	14.152
11PO	9.15E+03	14.525
11L35	7.37E+03	12.395
(AC-20s)		
2PAO	7.21E+03	10.444
2PAR	8.74E+03	11.999
2PC1	8.87E+03	12.789
2PO5	9.17E+03	12.615
2PO	9.95E+03	12.890
2PM	8.38E+03	11.440
2PC	8.54E+03	11.640
2LM	8.47E+03	12.304
2L35	8.50E+03	11.988
2L75	8.33E+03	12.096
3PAO	6.77E+03	11.126
3PAR	8.74E+03	13.591
3PC1	8.53E+03	13.424
3PO5	9.44E+03	14.696
3PO	1.00E+04	14.840
3PM	7.13E+03	11.575
3PC	6.86E+03	10.960
3L35	8.03E+03	12.350
3L75	8.33E+03	12.623
10PAO	6.31E+03	10.686
10PAR	8.44E+03	13.464
10PC1	7.40E+03	11.775
10PO5	8.96E+03	14.176
10PO	9.37E+03	14.546
10L35	1.38E+04	19.563
12PAO	6.69E+03	11.051
12PAR	8.70E+03	13.677
12PC1	7.57E+03	12.490
12PO5	9.05E+03	14.124
12PO	9.52E+03	14.555
12L35	7.81E+03	12.625

Table 18. HP-GPC results - % changes, 3-slice and 4-slice methods

ID	LMS	MMS1	MMS2	SMS	LMS+MMS1
(AC-5s)					
4PAO	0.00	0.00	0.00	0.00	0.00
4PAR	43.35	5.47	-5.48	-2.91	10.55
4PC1	32.90	8.75	-3.56	-18.92	11.99
4PO5	71.81	6.03	-7.14	-7.44	14.86
4PO	74.83	8.28	-8.48	-7.47	17.21
4PM	10.06	8.00	-4.48	-1.16	8.28
4PC	-9.35	1.89	-0.25	0.16	0.38
4L35	20.39	8.47	-4.61	-6.37	10.07
4L75	39.48	11.58	-6.78	-11.11	15.32
5PAO	0.00	0.00	0.00	0.00	0.00
5PAR	54.60	6.85	-6.16	-5.36	12.97
5PC1	18.36	14.06	-2.88	-29.27	14.61
5PO5	42.97	4.35	-4.37	-4.11	9.30
5PO	91.55	10.86	-9.62	-11.41	21.20
5PM	-3.19	7.40	-1.93	-7.87	6.04
5L35	44.86	11.20	-6.26	-12.74	15.51
7PAO	0.00	0.00	0.00	0.00	0.00
7PAR	391.15	28.54	-12.10	-26.21	46.13
7PC1	251.20	28.92	-6.50	-41.01	39.70
7PO5	452.15	30.65	-13.40	-29.04	51.10
7PO	548.54	34.98	-16.37	-30.93	59.90
7L35	341.24	30.63	-11.43	-28.64	45.70
8PAO	0.00	0.00	0.00	0.00	0.00
8PAR	55.12	4.34	-5.45	-2.01	10.39
8PC1	53.97	11.24	-6.16	-17.21	16.33
8PO5	66.35	4.66	-5.86	-4.88	12.01
8PO	78.54	7.17	-7.59	-6.68	15.67
8L35	28.71	5.60	-3.96	-4.08	8.35
(AC-10s)					
1PAO	0.00	0.00	0.00	0.00	0.00
1PAR	34.94	6.98	-4.46	-2.39	10.21
1PC1	30.32	15.84	-6.62	-10.70	17.51
1PO5	49.61	8.00	-5.59	-3.03	12.81
1PO	66.88	13.16	-7.49	-10.65	19.36
1PM	8.05	12.10	-5.28	-1.49	11.63
1L35	32.20	14.63	-6.91	-6.26	16.66
1L75	-9.21	10.55	-4.04	0.73	8.27

Table 18. continued

Sample ID	LMS	MMS1	MMS2	SMS	LMSMMS1
11PAO	0.00	0.00	0.00	0.00	0.00
11PAR	60.65	5.94	-6.02	-5.09	12.34
11PC1	77.98	5.70	-6.92	-5.77	14.15
11PO5	77.48	5.46	-6.70	-6.14	13.88
11PO	87.19	8.58	-8.62	-7.64	17.77
11L35	37.05	4.60	-4.58	-0.50	8.39
(AC-20s)					
2PAO	0.00	0.00	0.00	0.00	0.00
2PAR	35.25	6.75	-6.00	-4.29	10.37
2PC1	36.52	5.50	-6.91	7.28	9.44
2PO5	43.36	6.82	-7.03	-1.61	11.46
2PO	63.19	12.36	-10.39	-11.82	18.83
2PM	25.22	10.01	-7.09	-3.54	11.95
2PC	27.67	9.89	-7.21	-3.75	12.15
2LM	29.45	5.55	-6.29	6.81	8.58
2L35	31.27	7.49	-6.78	1.17	10.51
2L75	26.40	5.60	-6.01	6.27	8.25
3PAO	0.00	0.00	0.00	0.00	0.00
3PAR	48.60	5.21	-5.66	-4.77	10.93
3PC1	41.79	4.03	-4.64	-4.08	9.00
3PO5	65.26	4.50	-6.79	-3.43	12.50
3PO	79.91	8.93	-8.99	-11.11	18.28
3PM	3.92	6.53	-4.09	3.05	6.19
3PC	-3.00	5.35	-2.21	-1.78	4.25
3L35	29.01	8.62	-5.62	-6.36	11.31
3L75	34.24	10.07	-6.62	-7.38	13.25
10PAO	0.00	0.00	0.00	0.00	0.00
10PAR	59.50	6.05	-6.16	-5.36	12.48
10PC1	25.91	9.22	-5.34	-6.16	11.23
10PO5	73.30	5.30	-6.65	-5.89	13.49
10PO	86.50	8.23	-8.63	-8.16	17.65
10L35	186.78	10.15	-14.84	-17.83	31.41
12PAO	0.00	0.00	0.00	0.00	0.00
12PAR	51.07	4.12	-5.28	-4.60	10.12
12PC1	24.40	-1.10	-1.23	-0.31	2.16
12PO5	60.23	3.37	-5.51	-5.13	10.63
12PO	73.08	6.81	-7.90	-7.32	15.28
12L35	29.05	3.70	-4.11	-0.07	6.94

Table 19. HP-GPC results - % change, 8-slice method

ID	X1	X2	X3	X4	X5	X6	X7	X8
(AC-5s)								
4PAO	0.00	0.00	0.00	0.00	0.00	0.00	0.00	0.00
4PAR	24.19	1.38	-4.33	-5.54	-5.81	-6.01	-4.68	-2.70
4PC1	20.97	6.63	-0.88	-1.39	-3.01	-5.00	-11.54	-19.66
4PO5	35.62	0.42	-5.21	-7.46	-6.92	-8.12	-7.55	-7.48
4PO	39.18	2.65	-6.57	-8.48	-9.57	-8.87	-7.97	-7.57
4PM	9.63	7.00	3.40	-4.27	-7.23	-7.65	-6.10	-0.52
4PC	-2.53	2.47	1.87	0.12	-1.41	-1.40	0.00	-0.05
4L35	17.18	5.72	0.37	-3.91	-5.87	-7.39	-7.46	-6.21
4L75	27.31	7.55	-0.13	-5.46	-8.63	-10.27	-10.78	-11.25
5PAO	0.00	0.00	0.00	0.00	0.00	0.00	0.00	0.00
5PAR	28.71	2.80	-4.02	-6.32	-6.99	-6.58	-6.61	-5.25
5PC1	18.58	13.04	6.35	3.38	-2.19	-10.36	-21.13	-30.24
5PO5	19.26	2.76	-1.76	-3.24	-5.29	-5.93	-6.00	-3.81
5PO	47.09	4.33	-6.19	-9.68	-10.82	-10.35	-10.91	-11.57
5PM	2.64	8.36	5.59	-1.39	-3.90	-5.22	-5.87	-8.29
5L35	28.60	7.51	-1.29	-5.69	-7.62	-8.35	-9.18	-13.45
7PAO	0.00	0.00	0.00	0.00	0.00	0.00	0.00	0.00
7PAR	119.28	16.01	1.00	-7.33	-12.15	-19.16	-25.73	-26.05
7PC1	87.00	20.51	9.54	3.86	-4.27	-17.59	-31.97	-41.91
7PO5	131.71	17.67	1.99	-8.50	-13.14	-22.02	-28.14	-29.00
7PO	161.22	18.25	-2.04	-11.97	-16.68	-23.67	-29.96	-30.87
7L35	111.98	18.68	3.49	-6.38	-11.32	-19.41	-27.03	-28.63
8PAO	0.00	0.00	0.00	0.00	0.00	0.00	0.00	0.00
8PAR	25.59	0.68	-4.71	-5.64	-6.13	-5.38	-4.21	-1.86
8PC1	31.15	7.54	-2.20	-4.70	-7.01	-7.92	-10.72	-18.38
8PO5	28.52	1.27	-3.53	-6.02	-6.71	-6.56	-6.13	-4.94
8PO	37.96	1.44	-6.11	-7.87	-8.26	-7.83	-7.11	-6.79
8L35	16.34	3.40	-1.09	-3.97	-4.99	-4.89	-4.75	-4.13
(AC-10s)								
1PAO	0.00	0.00	0.00	0.00	0.00	0.00	0.00	0.00
1PAR	19.15	5.28	-2.12	-4.82	-4.47	-5.26	-4.85	-2.11
1PC1	22.18	16.58	2.42	-6.28	-8.26	-10.71	-10.81	-10.88
1PO5	23.92	6.62	-1.09	-5.68	-6.08	-7.48	-7.87	-2.38
1PO	37.69	9.10	-3.15	-8.06	-7.55	-8.41	-11.39	-10.13
1PM	11.33	12.37	3.86	-6.48	-8.17	-8.36	-4.66	-1.31
1L35	24.61	13.30	1.15	-7.29	-8.87	-10.18	-9.23	-5.84
1L75	4.93	11.43	2.93	-5.61	-6.33	-5.81	-3.30	1.19

Table 19. continued

Sample ID	X1	X2	X3	X4	X5	X6	X7	X8
11PAO	0.00	0.00	0.00	0.00	0.00	0.00	0.00	0.00
11PAR	28.45	2.06	-4.25	-5.93	-7.00	-6.21	-6.13	-4.97
11PC1	33.79	1.38	-5.16	-6.96	-7.34	-7.23	-7.45	-5.43
11PO5	32.10	2.30	-4.52	-5.65	-8.37	-7.27	-7.88	-5.88
11PO	41.20	2.88	-6.21	-8.76	-9.68	-8.92	-8.85	-7.47
11L35	18.51	2.38	-2.92	-4.04	-6.56	-4.64	-4.63	0.12
(AC-20s)								
2PAO	0.00	0.00	0.00	0.00	0.00	0.00	0.00	0.00
2PAR	21.22	3.74	-3.39	-6.64	-6.62	-6.48	-7.00	-3.85
2PC1	20.75	2.62	-5.53	-8.08	-8.06	-6.14	-3.01	8.70
2PO5	22.56	4.71	-2.22	-7.89	-8.15	-9.35	-8.81	-0.56
2PO	38.08	7.20	-6.17	-11.39	-11.32	-10.51	-14.02	-11.03
2PM	19.88	7.50	-1.80	-7.47	-9.00	-8.85	-9.25	-2.60
2PC	22.70	6.08	-2.42	-8.12	-8.81	-9.11	-8.40	-3.01
2LM	19.43	2.25	-6.32	-9.72	-7.09	-3.17	1.94	7.30
2L35	22.45	3.68	-5.57	-9.98	-7.98	-4.46	-0.85	1.30
2L75	19.02	2.05	-6.33	-9.67	-6.50	-2.80	2.30	6.66
3PAO	0.00	0.00	0.00	0.00	0.00	0.00	0.00	0.00
3PAR	24.65	2.02	-4.48	-5.42	-5.63	-6.67	-6.11	-4.65
3PC1	19.90	1.51	-3.50	-5.10	-4.99	-4.28	-4.57	-3.89
3PO5	28.22	1.67	-4.71	-6.41	-7.25	-7.88	-6.99	-2.95
3PO	40.71	3.63	-7.13	-9.12	-9.26	-8.82	-11.90	-10.55
3PM	5.04	6.77	3.09	-4.51	-6.96	-6.41	-4.80	4.23
3PC	0.78	6.16	4.63	-2.40	-4.96	-4.54	-3.27	-1.73
3L35	20.07	5.87	-1.15	-4.70	-7.08	-8.03	-8.31	-6.00
3L75	22.89	7.35	-0.56	-5.46	-8.72	-9.86	-10.04	-7.15
10PAO	0.00	0.00	0.00	0.00	0.00	0.00	0.00	0.00
10PAR	28.94	1.82	-4.04	-6.44	-7.17	-6.62	-5.88	-5.29
10PC1	19.49	6.43	-1.16	-5.99	-6.62	-6.23	-6.47	-6.25
10PO5	31.92	1.07	-3.08	-6.97	-7.63	-7.97	-7.59	-5.76
10PO	41.98	1.89	-6.28	-8.99	-9.43	-9.22	-8.60	-8.09
10L35	76.75	1.54	-10.42	-15.07	-16.37	-16.10	-16.00	-18.26
12PAO	0.00	0.00	0.00	0.00	0.00	0.00	0.00	0.00
12PAR	23.86	0.77	-4.31	-5.10	-5.57	-5.66	-5.26	-4.53
12PC1	8.42	-2.01	-4.94	-1.95	-0.88	1.47	3.19	-0.91
12PO5	24.93	0.96	-3.71	-4.39	-6.71	-6.89	-6.04	-5.11
12PO	35.46	1.69	-6.36	-7.62	-8.44	-8.48	-7.95	-7.22
12L35	15.55	1.22	-2.60	-4.58	-5.10	-4.56	-2.55	0.23

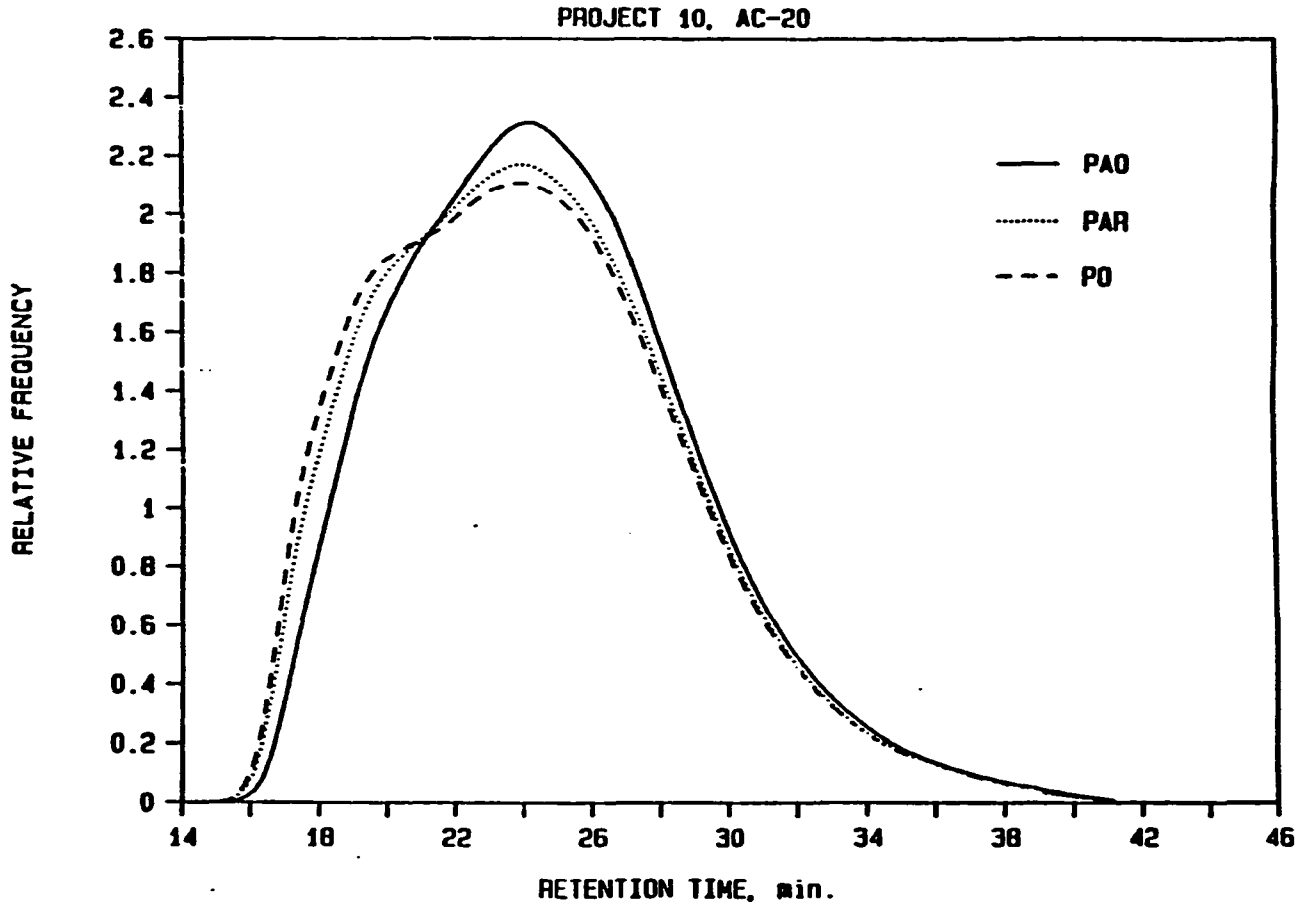

Figure 11. Effects of TFOT and pressure-oxidation on HP-GPC profile of Project 10 asphalt

the increase in LMS rating upon aging, rather than the initial LMS rating, is a performance predictor.

Aging promotes intermolecular association and thus increases the LMS content and viscosity at the same time. However, the increase of both quantities is probably not the same for all asphalts, but rather may be inversely proportional to the compatibility of asphalt. To examine this hypotheses, the quantitative aspects of these mutual shifts are tabulated in Table 20. In this table, changes in the %LMS+MMS1 and log (viscosity at 25°C), when the original asphalts (PAR) from 10 projects were pressure-oxidized for 46 hrs (PO), are presented. The last column of this table contains the ratios between these changes. Eight samples out of 10 resemble each other regardless of their types and sources. However, two of these samples (Projects 2 and 7) differ significantly from the others, as the ratio for these samples is about half of that of the other eight samples. This observation suggests that the structural and/or compositional nature of the smaller molecular size components of some asphalts may tolerate increase of polar association more and may, thereby, reduce the rate of viscosity increase upon aging. These kinds of asphalts have been referred to as compatible asphalts [3,42,101].

3. Thermal analyses

A total of 79 samples of virgin, laboratory aged, and recovered asphalts from 10 different paving projects in Iowa were subjected to thermomechanical analysis (TMA) in the heating mode to determine their glass transition temperatures (T_g). Figure 12 illustrates how T_g was determined. In addition to T_g, three other parameters associated

Table 20. Effects of 46 hour pressure oxidative aging on LMS+MMS1 and Log VIS25

Project	AC grade	Source	Δ(LMS+MMS1), %	ΔLog VIS25	ΔLog VIS25/Δ(LMS+MMS1)
4	AC-5	Koch, Dubuque	5.61	1.44	0.26
5	AC-5	Koch, Dubuque	6.74	1.40	0.21
7	AC-5	Koch, Algona	14.37	1.32	0.09
8	AC-5	Koch, Algona	5.05	1.35	0.27
1	AC-10	Koch, Algona	5.62	1.23	0.22
11	AC-10	Koch, Algona	5.74	1.38	0.24
2	AC-20	Koch, Tama	6.76	0.76	0.11
3	AC-20	Koch, Dubuque	6.16	1.22	0.20
10	AC-20	Jebro, Sioux City	5.77	1.26	0.22
12	AC-20	Koch, Omaha, NE	5.17	1.29	0.25

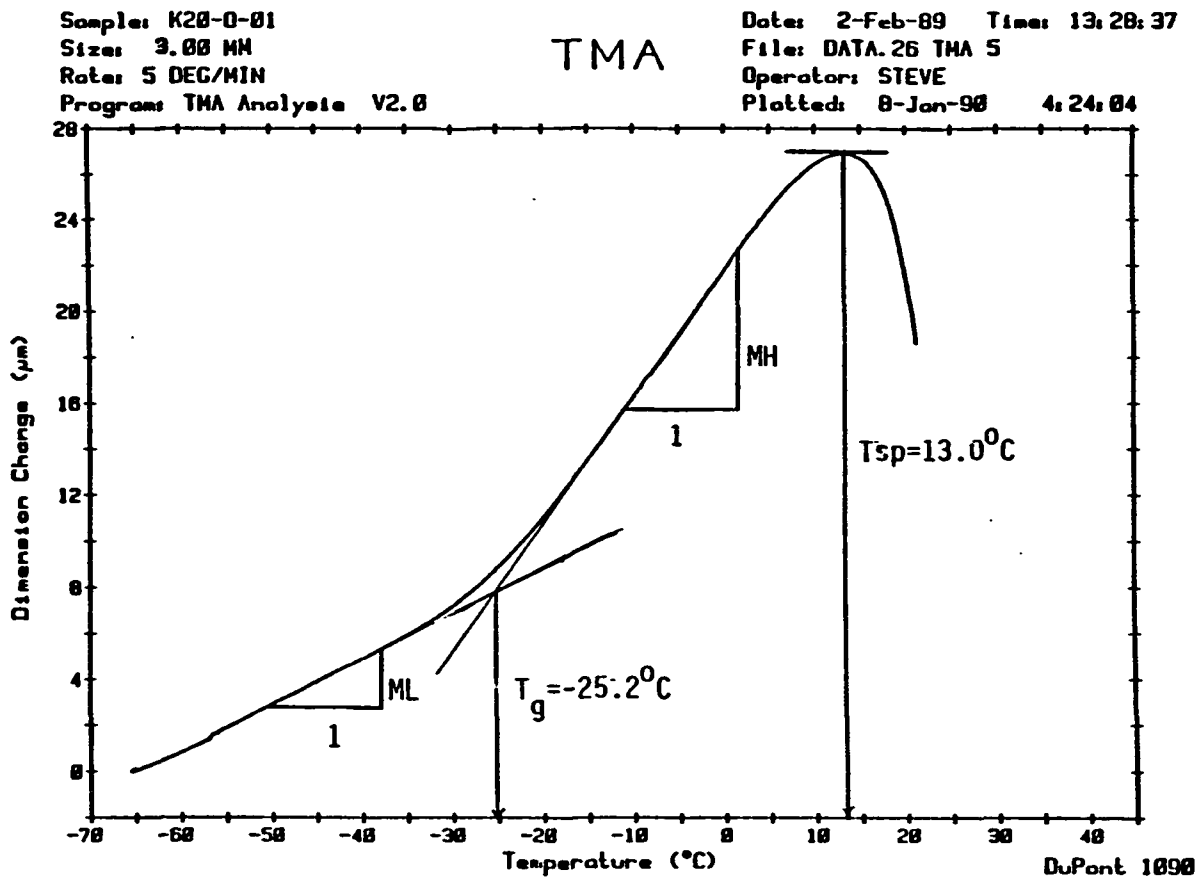

Figure 12. Typical TMA thermogram and related parameters

with TMA thermograms were also determined for the above mentioned 79 samples. These are also illustrated in Figure 12 and are the following:

1. ML: The slope of the initial straight line which measures the low-temperature thermal coefficient of expansion of the sample at the glassy state. This slope has been proposed as an index to predict the performance quality of an asphalt [60].
2. MH: The slope of the nearly straight adjacent section of the plot at higher temperature, which measures the coefficient of expansion above glass transition.
3. Tsp: The softening temperature at which the displacement of the TMA probe reaches a maximum.

These TMA parameters together with T_g are given in Table 21. The glass transition temperature, T_g, of the original asphalts ranged from -34°C to -22.5°C, increasing with viscosity from AC-5 to AC-20. In general, aging at high temperature (from PAO to PAR) reduced T_g, Tsp, ML, and MH while aging at low temperature (from PO5 to PO) increased these thermal responses. This different trend of thermal responses suggests a different aging mechanism for materials aged at different temperatures.

Glass transition temperatures of 12 asphalts used in the preliminary study were also determined by TMA and these data are compared with DSC results in Table 22. A weak correlation was observed between the glass transition temperatures determined by the two methods. The coefficient determination was 0.35, significant at 5% level.

Table 21. Summary of TMA results

Sample ID	T_g °C	Tsp °C	ML µm/°C	MH µm/°C
(AC-5s)				
4PAO	-31.3	7.0	0.176	0.466
4PAR	-30.3	5.0	0.189	0.441
4PC1	-37.7	3.9	0.127	0.559
4PO5	-28.8	7.3	0.132	0.422
4PO	-27.3	13.0	0.213	0.532
4PM	-29.5	6.0	0.158	0.441
4PC	-29.3	8.0	0.249	0.512
4L35	-33.5	7.0	0.162	0.547
4L75	-33.3	12.5	0.162	0.487
5PAO	-30.0	14.5	0.149	0.510
5PAR	-36.3	7.0	0.039	0.407
5PC1	-36.7	6.9	0.047	0.433
5PO5	-32.4	6.3	0.148	0.507
5PO	-34.0	13.0	0.162	0.503
5PM	-31.3	5.0	0.106	0.451
5L35	-30.5	10.5	0.160	0.561
5L75	-32.5	10.5	0.167	0.510
7PAO	-34.0	15.0	0.195	0.494
7PAR	-26.8	10.5	0.215	0.571
7PC1	-36.5	5.2	0.051	0.380
7PO5	-29.4	7.0	0.193	0.452
7PO	-28.5	14.5	0.231	0.577
7L35	-31.0	3.0	0.249	0.603
7L75	-37.0	12.5	0.225	0.618
8PAO	-26.8	15.0	0.209	0.577
8PAR	-29.9	12.0	0.264	0.695
8PC1	-32.1	4.2	0.079	0.331
8PO5	-29.2	6.8	0.141	0.464
8PO	-30.9	12.5	0.174	0.392
8L35	-32.0	9.5	0.113	0.441
8L75	-33.3	7.0	0.240	0.630
(AC-10s)				
1PAO	-33.0	-4.0	0.094	0.299
1PAR	-22.5	14.0	0.208	0.682
1PC1	-35.3	10.1	0.182	0.374
1PO5	-30.9	12.2	0.105	0.435
1PO	-27.5	12.5	0.264	0.647
1PM	-31.9	12.0	0.235	0.566
1L35	-28.0	25.0	0.249	0.483
1L75	-28.0	14.5	0.216	0.477

Table 21. continued

Sample ID	T_g °C	Tsp °C	ML µm/°C	MH µm/°C
11PAO	-27.5	3.5	0.126	0.488
11PAR	-28.0	12.0	0.259	0.687
11PC1	-34.9	4.5	0.139	0.454
11PO5	-29.8	9.4	0.182	0.386
11PO	-24.0	13.5	0.180	0.451
11L35	-34.0	4.0	0.251	0.732
11L75	-25.5	25.0	0.141	0.505
(AC-20s)				
2PAO	-25.0	17.5	0.167	0.477
2PAR	-28.5	16.0	0.240	0.508
2PC1	-30.6	14.9	0.213	0.380
2PO5	-29.0	15.5	0.268	0.490
2PO	-28.3	25.0	0.231	0.481
2PM	-27.8	17.5	0.224	0.514
2PC	-32.5	18.0	0.235	0.503
2LM	-29.9	12.0	0.260	0.503
2L35	-33.3	17.5	0.244	0.440
2L75	-33.9	19.5	0.138	0.429
3PAO	-22.5	12.0	0.117	0.499
3PAR	-27.0	7.0	0.154	0.367
3PC1	-34.4	7.0	0.114	0.404
3PO5	-24.5	12.2	0.198	0.431
3PO	-22.0	17.5	0.231	0.545
3PM	-29.4	17.5	0.214	0.510
3PC	-33.0	12.5	0.186	0.465
3L35	-27.5	16.0	0.220	0.521
3L75	-25.3	25.0	0.211	0.507
10PAO	-23.5	13.0	0.204	0.523
10PAR	-22.5	13.5	0.244	0.601
10PC1	-34.9	8.8	0.109	0.375
10PO5	-27.8	9.2	0.109	0.388
10PO	-28.5	14.0	0.212	0.508
10L35	-31.0	15.0	0.245	0.477
10L75	-32.0	19.5	0.160	0.444
12PAO	-24.0	13.0	0.222	0.625
12PAR	-25.0	11.5	0.195	0.521
12PC1	-30.1	11.0	0.123	0.402
12PO5	-23.1	13.4	0.211	0.483
12PO	-21.5	25.0	0.203	0.554
12L35	-28.0	25.0	0.268	0.657
12L50	-27.3	12.5	0.182	0.521
12L75	-28.3	11.5	0.191	0.525

Table 22. Glass transition temperature by TMA and DSC

	DSC		TMA
Sample ID	T_g °C	ΔH J/g	T_g °C
J0502-O	-29.0	10.3	-29.0
J0502-R	-30.0	15.0	-30.1
K0501-O	-26.0	8.2	-30.0
K0501-R	-26.0	8.8	-32.1
J1001-O	-30.0	11.2	-27.8
J1001-R	-31.0	13.9	-29.5
K1001-O	-31.0	6.9	-31.0
K1001-R	-30.0	7.5	-32.5
J2001-O	-35.0	11.4	-28.8
J2001-R	-35.0	9.7	-35.0
K2001-O	-25.0	5.7	-25.2
K2001-R	-22.0	4.8	-25.0

Inclusion of the enthalpy change did not improve the relationship ($r^2 = 0.36$).

The correlation between TMA parameters and other properties will be discussed in Section 7.

4. NMR

The samples studied by nuclear magnetic resonance (NMR) spectroscopy were the original asphalt J1002-O, its oven treated version J1002-R, the core sample Sugar Creek binder, and the Wood River binder. The ^{13}C NMR and the ^{1}H NMR spectra of these samples are shown in Figure 13 and Figure 14, respectively. The ^{13}C NMR spectra indicate that the line-width of the Sugar Creek sample is significantly larger than those of other samples meaning that this sample is considerably more rigid than the others. The ^{1}H NMR spectra indicate that oven aging decreases the amount of aliphatic quaternary carbon in the virgin asphalt and also indicate that the quaternary carbon content of the Sugar Creek sample is much less than those of all other three samples as shown in Figure 14.

Other NMR procedures investigated are as follow. Efforts were made to ligate the asphalt samples with the phosphorus marker. However, a lack of useful results suggests that the small amount of heteroatoms in asphalt made this a nonviable technique. Solution ^{13}C NMR spectra of the Sugar Creek binder, the Wood River binder, 7PAO, and 7PO did not indicate any significant difference among them. The spectra of the n-pentane insoluble asphaltenes of 7PAO and 7PO showed no significant difference between them either. Removal of the n-pentane soluble portion of asphalts

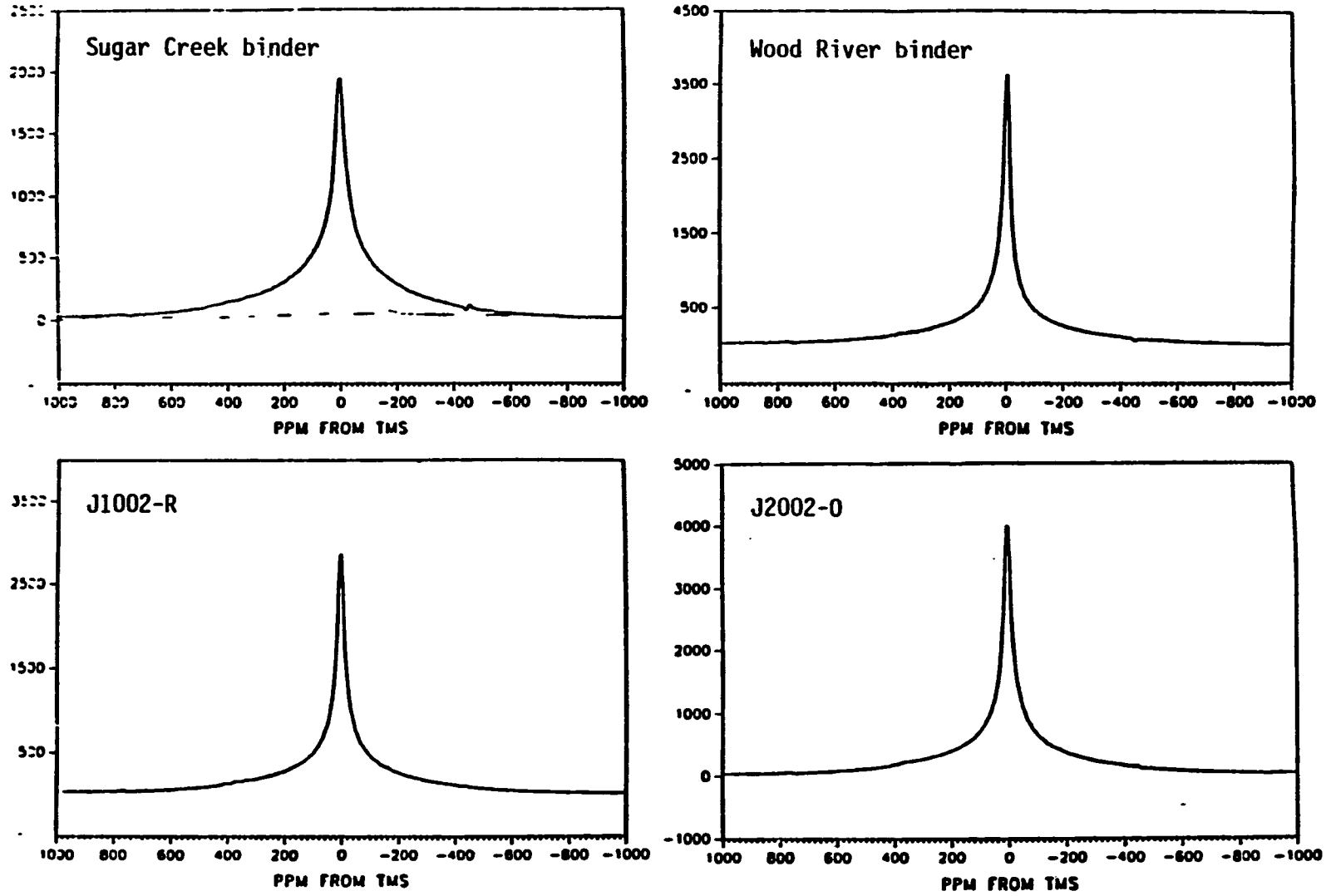

Figure 13. Carbon 13 NMR spectra

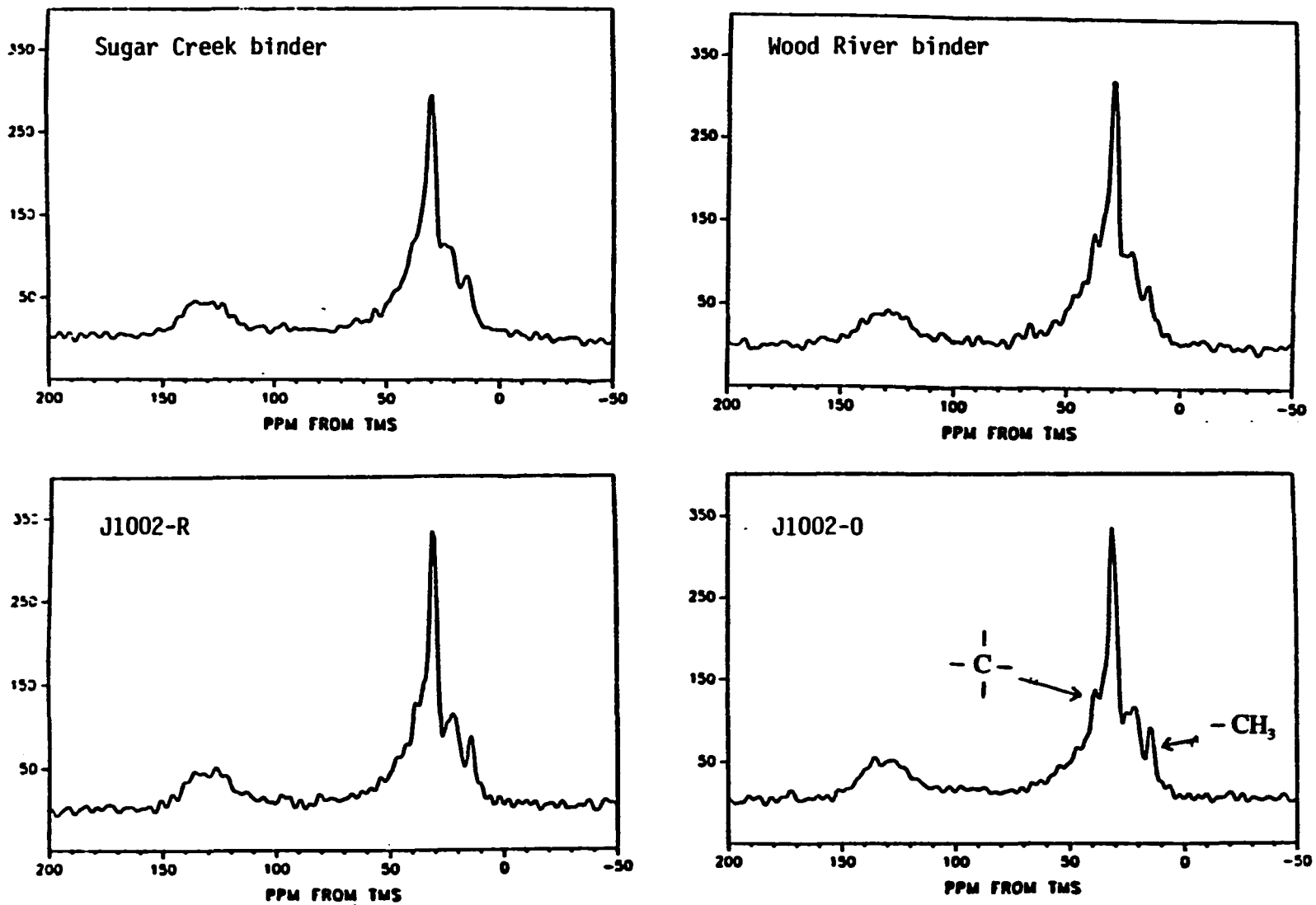

Figure 14. Proton NMR spectra

only increased the intensities of aromatic peaks relative to aliphatic peaks. Solvent effects were examined by using three different solvents, deutrated chloroform, deutrated tetrahydrofuran, and deutrated toluene; however, no noticeable effect on ^{13}C solution NMR was found. Measurement of relaxation constant, $T_{1\rho}$, indicated that 7PO with $T_{1\rho}$ of 1.50 ms was slightly harder than 7PAO with $T_{1\rho}$ of 1.40 ms. However, this difference could not be considered as significant when the instrumental error was considered.

The application of the NMR technique to study asphalt has been found to be useful [38,88,102]. However, due to the nature of asphalt, a complex mixture of many different molecular structures, characterizing asphalt using the NMR technique seems to be problematic for engineers who do not have the necessary expertise.

5. Water sensitivity of mixes

As an indirect performance measurement of each project, resistance to moisture-induced damage of one year old cores was evaluated by using the retained tensile strength ratio and the retained resilient modulus ratio after accelerated Lottman moisture conditioning. The results are presented in Table 23. The cores taken from project 11 showed the least resistance to moisture induced damage in terms of retained resilient modulus (RM) and retained indirect tensile strength (ITS). Also, the cores taken from project 10, with the highest air void percentage among those of all the projects, could be considered as susceptible to moisture damage in terms of retained indirect tensile strength.

Table 23. Water sensitivity of one year old core samples

Project	% Air Void	RM ratio	ITS ratio
(AC-5)			
4	5.26	1.05	0.93
5	4.91	0.95	0.95
7	2.81	1.29	1.26
8	2.77	1.38	1.31
(AC-10)			
1	3.83	1.10	1.16
11	4.04	0.39	0.52
(AC-20)			
2	6.43	0.96	1.05
3	5.52	1.10	1.09
10	7.19	1.04	0.75
12	5.46	1.26	1.00

Accelerated moisture conditioning is expected to reduce the structural soundness of specimens. However, as seen in Table 23, some specimens showed increased RM and ITS (e.g., larger than a ratio of 1). This increase also has been observed in another study [66]. This phenomenon could be explained by the contribution of water trapped in the pores of a mix. During the severe vacuum saturation procedure, most pores of a mix would be filled with water. If the mix survives the moisture conditioning procedure, the water trapped in the pores would behave as a structurally reinforcing material during RM and ITS measurements.

6. Aging characteristics

Levels of aging or property changes due to the thin film oven test (TFOT) were compared with those due to actual construction operations. This was done by comparing the rheological properties of TFOT residues (PAR), asphalt samples recovered from plant mixes (PM), cores taken right after construction (PC), and lab mixes (LM). In general, TFOT caused more hardening for softer asphalts (AC-5) than for harder asphalts (AC-10 or AC-20). In AC-20 asphalts, TFOT caused about the same hardening as hot mixing in terms of P5, P25, P4, and VIS25. However, in other properties, TFOT caused larger changes than the hot mixing process. Examination of CF and SI revealed that TFOT residues showed less hardening (higher CF and lower SI) than asphalts mixed and recovered (PM, PC, and LM).

Pressure-oxidation treatment for 5 hours and 46 hours is considered to be equivalent to 1 year and 5 years, respectively, of field aging under Iowa climatic

conditions. Based on data derived from these tests, rheological properties and HP-GPC parameters were predicted for 10, 20, and 30 year field service using the method suggested by Brown et al. [15] as given in Tables 24 and 25.

Predictive equations of penetration at 4°C and R&B softening point for AC-5 asphalts were plotted in Figures 15 and 16. In some cases, the prediction based on two point measurements resulted in mathematical expressions which were physically meaningless. As can be seen from Table 24, changes in penetrations at 5 and 4°C with time were in similar pattern for all asphalt samples. In terms of peneration at 25°C, the asphalt sample from project 7 showed the biggest age-hardening for prediction of 10 year service (Y10). For predictions of 5 and 10 year services (Y5 and Y10), asphalt samples from projects 2 and 3 showed the greatest hardening in terms of ring and ball softening point, sample from project 12 became the most viscous at 25°C, and sample from project 2 was the most viscous at 60 and 135°C. In this study, as will be discussed later, it was found that the percentage of the second and seventh size fractions (X2 and X7) of HP-GPC profiles, based on the 8-slice method, were very closely related to most asphalt properties. Table 25 gives the predicted percentage of these two slices along with that of X1. The project 2 asphalt will yield high X1 and X2 values and the lowest X7 value based on the long term prediction. This prediction indicates that this asphalt would become too stiff to perform well. Predicted values for the project 3 asphalt gave the highest X1 and the second lowest X7 after 10 year field service. The asphalt used in the project 12 gave the highest X2 at the ultimate stage. These three asphalts could be categorized as susceptible asphalts, especially as far as low

Table 24. Predicted rheological properties from lab aging test

Project	PAO	PC1	Y1	Y5	Y10	Y20	Y30	Ult.Prop.
Penetration at 5°C, 1/10 mm								
4	19	11	11	10	10	10	10	10
5	18	11	--	11	--	--	--	--
7	16	14	11	10	10	10	9	9
8	17	15	11	10	10	10	10	10
1	8	7	6	6	6	6	6	6
11	15	11	8	7	7	7	7	7
2	7	7	5	6	6	6	6	6
3	9	11	5	6	6	6	6	6
10	9	6	5	5	5	5	5	5
12	8	9	5	4	4	4	3	3
Penetration at 25°C, 1/10 mm								
4	181	98	86	52	31	12	3	--
5	191	83	--	53	--	--	--	--
7	193	105	84	46	3	--	--	--
8	196	107	83	46	15	--	--	--
1	82	52	44	27	14	1	--	--
11	133	91	58	35	23	13	9	--
2	54	45	36	25	--	--	--	--
3	75	89	41	26	18	11	8	1
10	82	36	40	24	15	7	3	--
12	82	67	40	23	13	3	--	--
Penetration at 4°C, 1/10 mm								
4	64	35	31	25	24	23	23	23
5	68	33	--	25	--	--	--	--
7	60	41	32	24	21	19	19	17
8	58	43	30	25	24	23	23	23
1	29	21	16	14	14	13	13	13
11	44	36	24	21	20	20	20	20
2	15	19	14	14	14	14	14	14
3	30	36	16	14	14	13	13	13
10	29	18	16	14	14	13	13	13
12	28	27	15	14	14	14	14	14
R&B softening point, °C								
4	41.5	44.6	48.8	54.0	56	58	58	60
5	41.5	49.3	--	54.0	--	--	--	--
7	39.0	45.3	49.3	56.0	58	59	60	61
8	38.5	44.5	50.2	56.0	58	60	61	62
1	47.5	51.4	54.1	61.5	69	80	88	--
11	44.0	49.0	53.2	59.5	67	80	92	--
2	49.0	55.8	52.6	67.0	--	--	--	--
3	47.0	47.2	55.8	63.0	85	--	--	--
10	49.0	59.0	56.5	62.5	64	65	66	67
12	47.0	49.6	56.2	63.0	68	72	74	80

Table 24. continued

Project	PAO	PC1	Y1	Y5	Y10	Y20	Y30	Ult.Prop.
Viscosity at 25°C, x 10,000 Pa·s								
4	1.5	9.0	11.1	41.5	--	--	--	--
5	1.9	16.0	--	47.5	--	--	--	--
7	2.5	5.4	15.0	52.5	134	1230	--	--
8	1.9	7.0	11.0	42.0	--	--	--	--
1	9.1	32.0	65.0	155.0	227	309	355	515
11	4.0	10.9	25.7	95.0	--	--	--	--
2	34.0	43.0	80.0	195.0	--	--	--	--
3	11.7	14.5	57.0	194.0	892	--	--	--
10	10.1	71.0	60.0	185.0	520	--	--	--
12	10.4	27.0	65.0	205.0	1010	--	--	--
Viscosity at 60°C, x 100 Pa·s								
4	0.58	1.73	2.05	4.68	11.7	--	--	--
5	0.63	2.35	--	4.51	--	--	--	--
7	0.73	0.85	2.37	6.38	25.7	--	--	--
8	0.67	1.28	2.43	5.08	9.1	21.0	44.1	--
1	1.58	4.02	5.60	13.21	22.9	43.0	64.0	--
11	1.11	2.02	4.60	10.43	26.2	--	--	--
2	3.57	5.49	10.98	39.72	151.0	--	--	--
3	2.73	2.49	8.95	21.41	40.0	92.2	183.4	--
10	2.11	14.55	7.98	18.36	63.6	--	--	--
12	2.34	2.54	9.54	22.62	41.4	89.9	162.2	--
Viscosity at 135°C, 10^{-6} m^2/s								
4	250	343	394	553	1219	--	--	--
5	248	540	--	500	--	--	--	--
7	251	346	414	619	--	--	--	--
8	253	380	429	550	793	2707	--	--
1	369	581	552	788	1917	--	--	--
11	444	452	592	770	1210	--	--	--
2	889	817	1080	1655	3891	--	--	--
3	477	495	810	1202	1702	2742	3837	--
10	460	1030	799	1091	1530	2789	5078	--
12	470	440	828	1140	2132	--	--	--

Table 25. Predicted HP-GPC properties from lab aging test

Project	PAO	PC1	Y1	Y5	Y10	Y20	Y30	Ult.Prop.
X1, 8-slice, %								
4	13.80	16.69	18.71	19.20	19.3	19.3	19.4	19.4
5	13.30	15.77	--	19.52	--	--	--	--
7	7.39	13.81	17.11	19.29	20.6	21.8	22.3	23.8
8	13.24	17.37	17.02	18.27	19.4	20.8	21.6	25.1
1	11.65	14.24	14.44	16.04	17.3	18.6	19.3	21.6
11	13.25	17.72	17.50	18.71	19.5	20.2	20.5	21.5
2	14.87	17.95	18.22	20.53	--	--	--	--
3	14.32	17.17	18.36	20.15	21.9	24.5	26.3	36.0
10	13.46	16.08	17.75	19.10	20.4	22.1	23.3	28.6
12	14.34	15.55	17.91	19.42	--	--	--	--
X2, 8-slice, %								
4	14.68	15.65	14.74	15.07	15.0	15.0	15.0	15.0
5	14.42	16.30	--	15.04	--	--	--	--
7	12.78	15.40	15.04	15.11	15.1	15.1	15.1	15.1
8	14.83	15.95	15.02	15.04	15.1	15.1	15.1	15.1
1	13.44	15.66	14.32	14.66	14.8	14.9	15.0	15.1
11	14.88	15.09	15.23	15.31	15.4	15.4	15.4	15.5
2	16.42	16.85	17.20	17.61	17.9	18.1	18.3	18.6
3	15.13	15.36	15.38	15.68	15.6	15.6	15.6	15.5
10	15.04	16.00	15.20	15.32	15.3	15.3	15.3	15.3
12	15.29	14.98	15.43	15.54	15.7	15.9	16.1	19.5
X7, 8-slice, %								
4	7.87	6.96	7.27	7.24	7.2	7.2	7.2	7.2
5	8.06	6.36	--	7.18	--	--	--	--
7	10.21	6.95	7.34	7.15	7.1	7.1	7.1	7.1
8	7.85	7.01	7.37	7.29	7.3	7.3	7.3	7.3
1	8.16	7.28	7.52	7.23	7.1	7.1	7.1	7.0
11	7.75	7.17	7.14	7.06	7.1	7.0	7.0	7.0
2	5.92	5.74	5.39	5.09	4.9	4.6	4.5	4.0
3	7.27	6.94	6.76	6.40	5.4	--	--	--
10	7.46	6.98	6.90	6.82	6.8	6.8	6.8	6.8
12	7.27	7.50	6.83	6.69	6.6	6.5	6.5	6.4
X1 + X2, 8-slice, %								
4	28.48	32.34	33.45	34.27	34.3	34.3	34.4	34.4
5	27.72	32.07	--	34.56	--	--	--	--
7	20.17	29.21	32.15	34.40	35.7	36.9	37.5	39.0
8	28.07	33.32	32.04	33.31	34.4	35.8	36.7	40.1
1	25.09	29.90	28.76	30.70	32.1	33.5	34.3	36.7
11	28.13	32.81	32.73	34.02	34.8	35.6	36.0	37.0
2	31.29	34.80	35.42	38.14	--	--	--	--
3	29.45	32.53	33.74	35.83	37.5	40.1	41.8	51.5
10	28.50	32.08	32.95	34.42	35.7	37.5	38.6	43.9
12	29.63	30.53	33.34	34.96	--	--	--	--

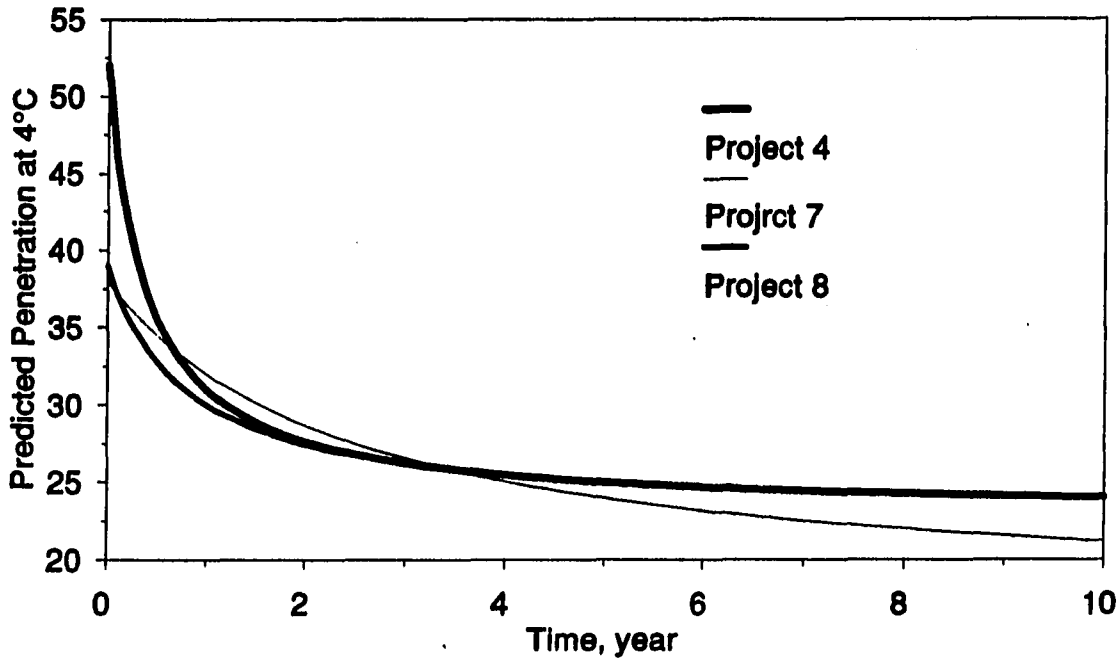

Figure 15. Predictive penetration at 4°C versus time

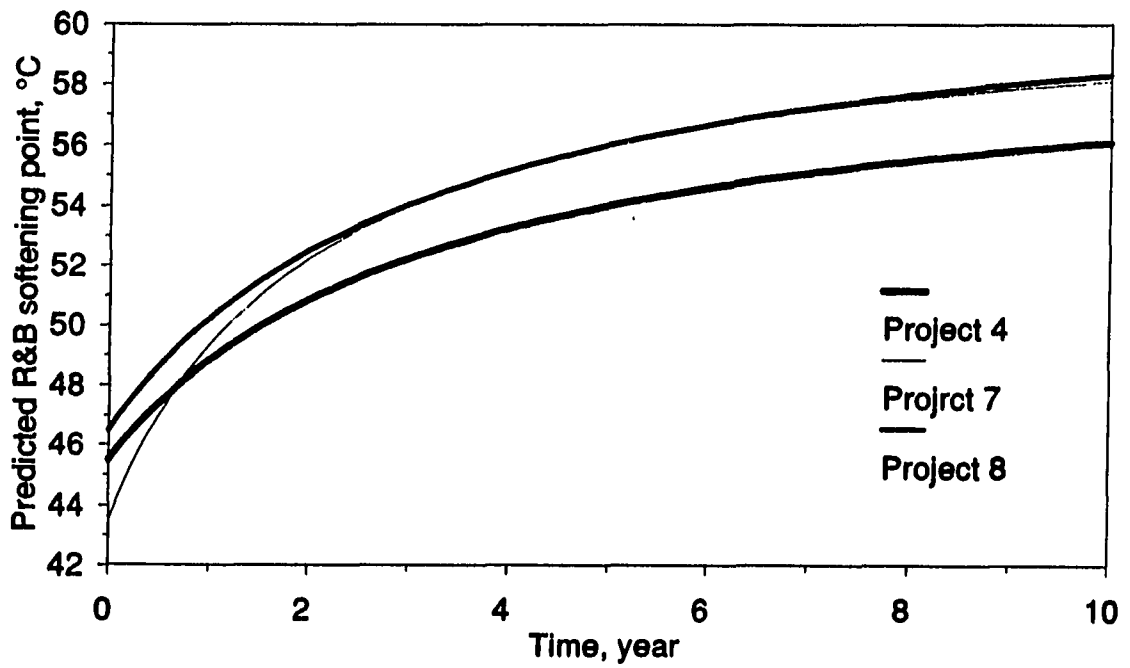

Figure 16. Predictive ring and ball softening point versus time

-temperature cracking properties are concerned.

Generally, an asphalt in a mix with high air voids ages faster than an asphalt in a mix with low air voids. In this study, air voids of lab mixes, compacted by 75 blows per side (L75 mixes), ranged from 3.37 to 7.11% and air voids of mixes, compacted by 35 blows per side (L35 mixes), ranged from 6.57 to 9.69%. The L75 mixes had 0.58 to 4.08% less air voids than the L35 mixes. The overall relationship between air voids and age-hardening, as determined by penetrations and viscosities, was not consistent. The level of aging for recovered asphalts from L35 and L75 mixes were about the same in terms of penetrations and viscosities, except for the sample from project 10. In this aging test on compacted mixes, aging measurement involved several procedures,e.g., mixing, compaction, aging, extraction, and recovery using an organic solvent. Because of this long procedure, it is likely that the laboratory measurement of aging using compacted mixes will contain more unknown variability than a laboratory aging test using neat asphalt.

The rheological properties of TFOT residues (PAR) and recovered asphalts after one year of field aging (PC1) are compared in Tables 11 and 12. The recovered asphalts of the projects 4, 5, and 10 were found to have aged more than the related TFOT residues in all properties. The recovered asphalts from the rest of the projects were aged less than the related TFOT residues in all properties except CF and SI. As seen in Table 23, the cores from these three projects showed the highest air voids among the projects of the same grade of asphalt. This observation is in agreement with Goode and Lufsey's conclusion [33] that air permeability, air voids, and asphalt film

thickness were major factors affecting age hardening of asphalt pavement.

In terms of rheological properties, asphalts pressure-oxidized for 5 hours (PO5) had aged more severely than asphalts recovered from one year old cores (PC1). The order of aging for an asphalt, in general, was PAO < PC1 < PO5 < PO in terms of rheological and HP-GPC properties. However, in TMA, only three aged asphalts showed a general trend as PC1 < PO5 < PO in terms of T_g, Tsp, and ML.

Previous studies have shown that the aging characteristics of asphalt during high temperature plant mixing (short-term aging), as with TFOT, may or may not reflect the aging characteristics of asphalt during low temperature aging in pavement (long-term aging) and in low temperature pressure-oxidation tests. This is demonstrated in Figure 17, in which the long term rate of age-hardening or long term aging index (defined as the ratio of the viscosity of 46 hour pressure-oxidized asphalt (PO) determined at 60°C to the viscosity of TFOT residue (PAR) at 60°C) is compared with the short-term aging index (which is the ratio of viscosity of PAR at 60°C to viscosity of PAO at 60°C). The project 2 asphalt showed a drastic difference between short-term and long-term aging indices; it was the least aged in terms of short-term aging index and the most aged in terms of long-term aging index.

7. Correlations

In this section, the discussion will be confined to correlations among physical properties, TMA parameters, and HP-GPC parameters of all samples related to the 10 projects.

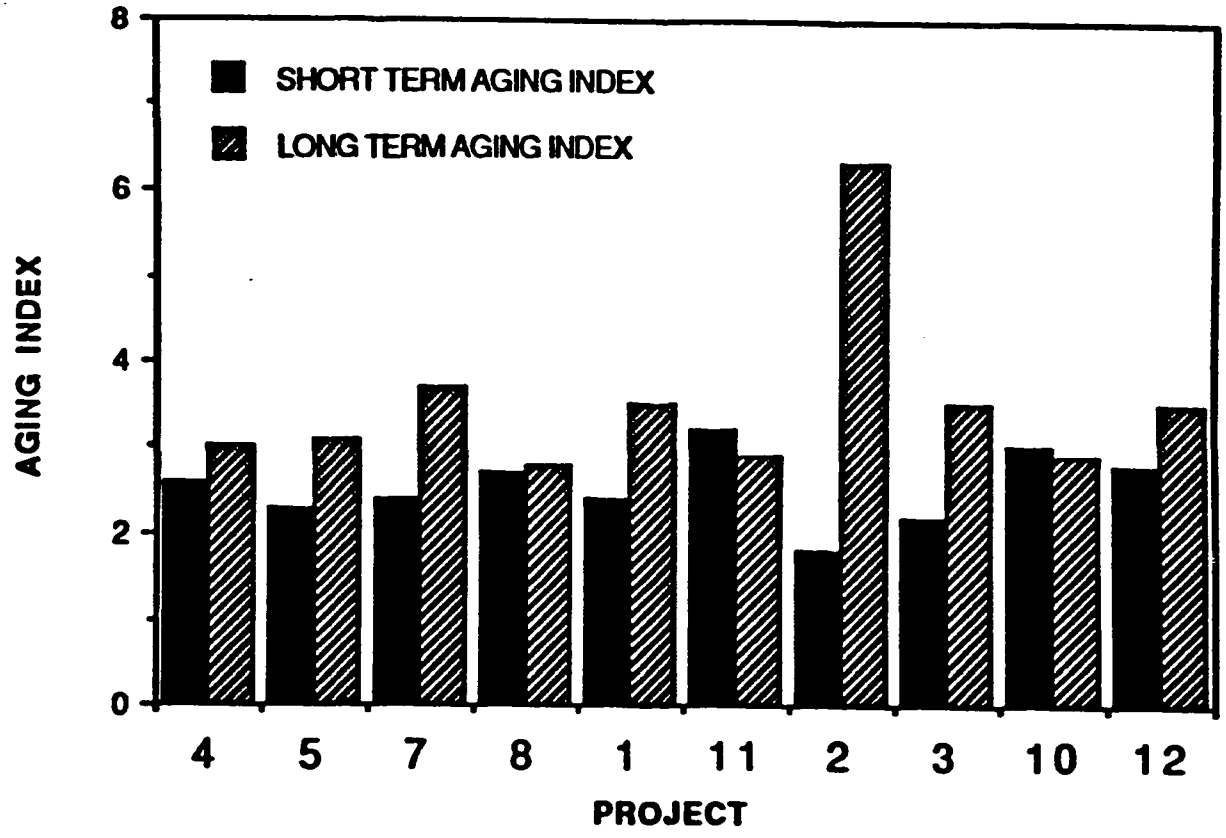

Figure 17. Short-term and long-term aging indices

Regression analyses were performed among physical parameters, TMA parameters, and molecular weight profile derived from HP-GPC tests. Table 26 gives the results of regression analyses between TMA parameters and HP-GPC parameters for 73 samples. The results indicate that TMA parameters, Tsp and ML, correlate with HP-GPC parameters, obtained using the 8-slice method, fairly well. Results of multiple linear regression between physical properties and TMA parameters are given in Table 27. These results show significant correlations between TMA parameters and almost all the physical properties with the exception of temperature susceptibility. Among the temperature susceptibility parameters only penetration ratio (PR) and penetration-viscosity number at 60°C (PVN60) significantly correlate with Tsp and ML. Tsp also correlates well with both rheological and low-temperature properties while T_g correlates well only with low-temperature properties. Between the two expansion slopes defined in a TMA thermogram, the low temperature expansion slope, ML, appears to be a better predictor for rheological properties than MH. Results from the multiple linear regression analyses performed between physical properties and HP-GPC parameters are given in Table 28. Molecular size distributions are best characterized by the 8-slice method thus correlating well with almost all physical properties. These results support findings by others [29,61] that molecular size profiles derived from HP-GPC can be used to predict many physical properties. However, HP-GPC parameters do not correlate well with temperature susceptibility in terms of PI, CN, and VTS.

Both TMA and HP-GPC parameters were significantly related to rheological properties while TMA parameters and HP-GPC parameters had less significant

Table 26. Regression analyses between TMA and HP-GPC parameters (n=73)

Dependent Variables	LMS+MMS1 P-value	r^2	LMS P-value	r^2	3-SLICE P-value	r^2
T_g	0.3710	0.011	0.1655	0.027	0.7365	0.018
Tsp	0.0022	0.124	0.1233	0.033	0.0160	0.138
ML	0.0475	0.054	0.1597	0.028	0.1046	0.085
MH	0.6908	0.002	0.8232	0.001	0.2022	0.064

Dependent Variables	4-SLICE P-value	r^2	8-SLICE P-value	r^2	MWT+POLYIDX P-value	r^2
T_g	0.3455	0.063	0.0381	0.216	0.3836	0.027
Tsp	0.0081	0.181	0.0033	0.292	0.0004	0.202
ML	0.0517	0.127	0.0037	0.289	0.1665	0.050
MH	0.3904	0.058	0.3786	0.120	0.4485	0.023

Dependent Variables	Selected variables by stepwise regression
T_g	None
Tsp	LMS+MMS1, MMS1, X2, MWT, POLYIDX
ML	MMS2, LMS, MMS2, X5, MWT
MH	None

Table 27. Regression analyses between Physical properties and TMA parameters (n=80)

Dependent Variables	Tg P-value	Tg r^2	Tsp P-value	Tsp r^2	ML P-value	ML r^2	MH P-value	MH r^2	All 4 Parameters P-value	All 4 Parameters r^2	Selected variables from stepwise regression
Rheological properties											
P5	0.0003	0.152	0.0001	0.228	0.0106	0.081	0.6021	0.004	0.0001	0.357	ALL
P25	0.0125	0.077	0.0001	0.207	0.0027	0.110	0.9885	0.000	0.0001	0.292	Tsp
P4	0.0016	0.121	0.0001	0.246	0.0057	0.094	0.8209	0.001	0.0001	0.340	ALL
VIS25	0.0037	0.103	0.0001	0.399	0.0003	0.157	0.7735	0.001	0.0001	0.474	Tsp
CF	0.9515	0.000	0.0001	0.249	0.0001	0.173	0.7922	0.001	0.0001	0.487	ALL
SI	0.9571	0.000	0.0001	0.249	0.0013	0.125	0.5032	0.006	0.0001	0.465	ALL
VIS60	0.2055	0.020	0.0001	0.297	0.0009	0.133	0.6978	0.002	0.0001	0.430	Tsp, ML, MH
VIS135	0.0520	0.048	0.0001	0.358	0.0001	0.173	0.7772	0.001	0.0001	0.508	Tsp, ML, MH
SP	0.0372	0.054	0.0001	0.336	0.0003	0.158	0.8249	0.001	0.0001	0.426	Tsp, ML, MH
Temperature susceptibility											
PR	0.5794	0.004	0.0004	0.150	0.0008	0.135	0.4413	0.008	0.0002	0.249	ALL
PI	0.1248	0.030	0.1208	0.031	0.3939	0.009	0.6061	0.003	0.0569	0.114	Tg, Tsp
CN	0.8330	0.001	0.0376	0.054	0.0960	0.035	0.6208	0.003	0.0497	0.118	Tsp
VTS	0.9091	0.000	0.5999	0.004	0.6046	0.003	0.8512	0.000	0.9374	0.011	None
PVN60	0.9802	0.000	0.0107	0.081	0.0413	0.052	0.7488	0.001	0.0083	0.165	Tsp
PVN135	0.9441	0.000	0.0970	0.035	0.2008	0.021	0.8359	0.001	0.2380	0.070	Tsp
Low-temperature cracking properties											
CT	0.0036	0.104	0.2035	0.021	0.9654	0.000	0.2546	0.017	0.0125	0.155	Tg, MH
TES	0.0016	0.120	0.0022	0.114	0.0216	0.066	0.8811	0.000	0.0008	0.221	Tg, Tsp
S23	0.0002	0.161	0.0001	0.280	0.0006	0.140	0.9183	0.000	0.0001	0.402	ALL
S29	0.0009	0.133	0.0001	0.211	0.0009	0.133	0.9954	0.000	0.0001	0.345	ALL

Table 28. Regression analyses between Physical properties and HP-GPC parameters (n=73)

Dependent Variable	LMS P-value	LMS r^2	LMS+MMS1 P-value	LMS+MMS1 r^2	3-SLICE P-value	3-SLICE r^2	4-SLICE P-value	4-SLICE r^2	8-SLICE P-value	8-SLICE r^2	Selected variables from stepwise regression
Rheological properties											
P5	0.0004	0.161	0.0001	0.245	0.0001	0.333	0.0001	0.356	0.0001	0.568	X2,X4,X5,X7,X8
P25	0.0001	0.248	0.0001	0.385	0.0001	0.432	0.0001	0.429	0.0001	0.549	X4,X6,X7,X8
P4	0.0001	0.191	0.0001	0.298	0.0001	0.378	0.0001	0.389	0.0001	0.560	X2,X7
VIS25	0.0012	0.139	0.0001	0.253	0.0001	0.302	0.0002	0.278	0.0001	0.462	X4,X6,X7,X8
CF	0.0500	0.053	0.0001	0.283	0.0001	0.339	0.0001	0.475	0.0001	0.546	X2
SI	0.0173	0.077	0.0001	0.311	0.0001	0.369	0.0001	0.457	0.0001	0.509	X2,X4
VIS60	0.0421	0.057	0.0001	0.185	0.0006	0.221	0.0006	0.249	0.0001	0.325	X2
VIS135	0.0036	0.113	0.0001	0.361	0.0001	0.416	0.0001	0.475	0.0001	0.588	X7,X8
SP	0.0001	0.208	0.0001	0.353	0.0001	0.391	0.0001	0.367	0.0001	0.505	X4,X6,X7,X8
Temperature susceptibility											
PR	0.0004	0.161	0.0001	0.258	0.0001	0.278	0.0001	0.307	0.0001	0.420	X5
PI	0.2533	0.018	0.1021	0.037	0.0523	0.105	0.0282	0.146	0.0366	0.218	X3,X4,X6
CN	0.1110	0.035	0.0208	0.073	0.1480	0.074	0.1827	0.086	0.1447	0.166	X5
VTS	0.1798	0.025	0.6095	0.004	0.8754	0.010	0.4803	0.049	0.2465	0.142	X3
PVN60	0.2874	0.016	0.0099	0.090	0.0700	0.097	0.0061	0.188	0.0076	0.268	X2,X8
PVN135	0.7255	0.002	0.0619	0.048	0.2190	0.062	0.0001	0.301	0.0001	0.433	X2,X8
Low-temperature cracking properties											
CT	0.2700	0.017	0.2242	0.021	0.0515	0.106	0.0103	0.174	0.0001	0.311	X1,X2,X7
TES	0.0001	0.205	0.0001	0.273	0.0001	0.317	0.0001	0.354	0.0001	0.432	X2,X7
S23	0.0032	0.116	0.0001	0.236	0.0001	0.334	0.0001	0.326	0.0001	0.411	X2,X7
S29	0.0099	0.090	0.0001	0.211	0.0001	0.319	0.0001	0.316	0.0001	0.467	X1,X2,X7,X8

correlation to each other. Therefore, it would be meaningful to use both TMA and HP-GPC parameters to predict rheological properties. Table 29 gives a summary of the regression analyses performed on physical properties versus TMA and HP-GPC parameters combined. These regression analyses give considerably higher r^2 values than the regression analyses using TMA or HP-GPC parameters alone. The regression coefficient matrix for Table 29 is given in Appendix A. The comparison of the actual physical properties with predicted properties obtained using regression equations in Appendix A is shown in Appendix B.

Among TMA and HP-GPC parameters, more significant parameters were identified by use of the stepwise linear regression technique. While, as indicated above, Tsp, of the TMA parameters, was significantly correlated with rheological properties, X2 and X7, among HP-GPC parameters, most dominantly relate to rheological and low-temperature properties. Slices X2 and X7 seem to be the most important among the eight slices. Slice X2 may best represent large size molecules and their increase in number upon aging while slice X7 may best represent small size molecules and their decrease in number upon aging.

C. Proposed Asphalt Specifications for the State of Iowa

The selection of the proper grade of asphalt for a given paving project must be based on consideration of climate (temperature), traffic, pavement thickness, and the prevailing construction conditions. The selection of an asphalt within a given grade must be based on its temperature susceptibility and predicted durability. The

Table 29. Regression analyses: physical properties against TMA and HP-GPC parameters (n=73)

Dependent Variables	TMA & HP-GPC parameters P-value	r^2	Selected variables from stepwise reg. TMA parameter	HP-GPC parameter
Rheological properties				
P5	0.0001	0.666	**Tsp**	**X2**,X6,**X7**
P25	0.0001	0.669	Tsp,ML,MH	**X4**,X6,**X7**
P4	0.0001	0.667	Tsp	**X2**,X4,X6,**X7**,X8
VIS25	0.0001	0.766	**Tsp**	**X2**,X4,X6,**X7**,MWT,PIDX
CF	0.0001	0.741	Tg,Tsp,**ML**,MH	**X2**
SI	0.0001	0.719	Tg,**Tsp**,ML,MH	**X2**
VIS60	0.0001	0.583	**Tsp**	X8
VIS135	0.0001	0.773	**Tsp**,ML,MH	**X7**
SP	0.0001	0.208	**Tsp**,ML,MH	**X1**,**X3**,**X6**,MWT
Temperature susceptibility				
PR	0.0001	0.636	Tsp	X2,**X4**,X5
PI	0.0517	0.309	Tg,Tsp	**X4**,PIDX
CN	0.2076	0.246	Tsp	X5
VTS	0.5121	0.187		X3
PVN60	0.0098	0.368		X2,X8
PVN135	0.0001	0.496		**X2**,**X8**
Low-temperature cracking properties				
CT	0.0008	0.438	Tg	X2,**X5**,**X7**,X8
TES	0.0001	0.564	Tg	X2,**X7**
S23	0.0001	0.655	**Tsp**,ML,MH	**X2**,X4,**X7**,PIDX
S29	0.0001	0.588	Tsp,ML,MH	X2,X5,**X7**

Note: Bold face indicates more significantly correlated variables

temperature susceptibility of an asphalt influences the mixing, placing, and compaction of paving mixtures as well as the high and low temperature performance of the pavement. The durability of an asphalt or its resistance to hardening and aging, both during construction and in-service, affects the pavement life.

It is generally accepted that the major causes of asphalt hardening are volatilization during mixing at high temperatures (short-term aging) and oxidation during service in pavement (long-term aging). Current asphalt specifications, while containing requirements for indirect control of temperature susceptibility and asphalt hardening during hot-plant mixing, offer no prediction over long-term durability. Trial specifications based on the Iowa pressure oxidation test are proposed. This procedure was developed based on consideration of the two stages of hardening processes of asphalt in their logical order and of the differences in aging mechanisms and their effects.

Trial asphalt specifications for Iowa conditions have been developed based on a realistic durability test, performance related physical properties, compositional properties from HP-GPC, and low-temperature properties from TMA. Many researchers have proposed certain physical properties of asphalts and their critical limits for acceptable pavement performance. Some of these suggested properties are penetration at 25°C, R&B softening point, viscosity at 25°C, shear index, penetration-viscosity number, and stiffness at low temperature, as summarized in Table 30. Although, due to insufficient field performance data, direct correlations between HP-GPC and TMA parameters and field performance are not yet available at this stage, critical values of HP-GPC and

Table 30. Critical values for performance related parameters and their corresponding HP-GPC and TMA parameters

			Corresponding HP-GPC parameters		Corresponding TMA parameters		
Paramter	Critical Values	Reference	X2, %	X7, %	Tg, °C	Tsp, °C	ML, μm/°C
P25	> 20	28	< 18.0	> 5.0	< -18.5	< 31.0	< 0.39
SI	< 0.55	58	< 18.1	> 4.6		< 36.0	< 0.60
R&B SP	< 65.5°C	28	< 18.7	> 4.6		< 31.2	< 0.45
VIS25	< 2 mega Pa·s	28	< 18.2	> 5.2	< -17.5	< 28.0	< 0.42
PVN60	> -1.3	35	> 9.8	< 13.6			
PVN135	> -1.0	76	> 11.9	< 12.7			
S23	> 138 MPa	57	< 19.5	> 3.7	< -17.0	< 32.5	< 0.47

TMA parameters were indirectly estimated from correlations with the performance related physical properties given in Table 30. Since changes of asphalt properties beyond five years of aging are usually small, the critical values discussed above are recommended as limiting values in specifications for an asphalt pressure-oxidized for 46 hours at 65.6°C and at a pressure of 20 atm of oxygen which simulates five year field aging under Iowa conditions.

Cracking temperature criteria have been suggested in pavement design to prevent a low-temperature asphalt pavement transverse cracking problem [5]. In this design method, the cracking temperature determined from penetrations at 5°C and 25°C should be lower than the minimum pavement design temperature. For Iowa climates, a minimum pavement temperature of -35°C was estimated. The minimum penetrations at 5°C for AC-5, AC-10, and AC-20 and this cracking temperature were determined from the cracking temperature nomograph as 10, 8, and 7, respectively.

To assure long term durability, it seems necessary to limit the long term aging index, i.e. the ratio of viscosity at 60°C after pressure-oxidation for 46 hours to viscosity at 60°C after TFOT. The long term aging indices for the 10 project asphalts range from 2.9 to 3.5 except the project 2 asphalt which has a long term aging index of 6.3. Based on this observation, a critical maximum long term aging index of 5 is tentatively suggested. This criterion limits the maximum allowable viscosity at 60°C after the pressure oxidation to 1,000 to 4,000 Pa·s. These values are in agreement with Sisko and Brunstrum's observation [99]. They reported that, for cracked pavements, the viscosities of recovered asphalts were higher than 1,000 to 4,000 Pa·s.

The proposed specifications, based on the pressure oxidation test and existing AASHTO M226, Table 2, is given in Table 31. Limiting values can be increased or decreased as more field performance data become available.

The usefulness of the percentage of the LMS fraction in the original asphalt and its change after laboratory aging to predict asphalt pavement performance has been recognized [50,54]. Although they are not included in the trial specifications due to insufficient performance data, it is recommended that they be included when long-term performance data become available.

Table 31. Proposed trial specification for asphalt cements

Test	AC-5	AC-10	AC-20
Original asphalt			
Viscosity at 60°C, Pa·s [1]	50±10	100±20	200±40
Viscosity at 135°C, 10^{-6} m^2/s, min. [1]	175	250	300
Penetration at 25°C, 0.1mm, min. [1]	140	80	60
Flash point, °C, min. [1]	177	219	232
Solubility in trichloroethylene, %, min. [1]	99.0	99.0	99.0
Residue from thin film oven test			
Viscosity at 60°C, Pa·s, max. [1]	200	400	800
Residue from pressure-oxidation (46 hour Iowa durability test)			
Viscosity at 60°C, Pa·s, max.	1,000	2,000	4,000
Penetration, 25°C/100g/5s, 0.1mm, min.	20	20	20
Penetration, 4°C/200g/60s, 0.1mm, min.	5	5	5
Penetration, 5°C/100g/5s, 0.1mm, min.	10	8	7
R&B softening point, °C, max.	65.5	65.5	65.5
Stiffness, -23°C/10,000s, MPa, max.	138	138	138
Viscosity, 25°C, mega Pa·s, max.	2	2	2
Shear susceptibility, max.	0.55	0.55	0.55
X2 (HP-GPC), %, max.	20	20	20
X7 (HP-GPC), %, min.	5	5	5
T_g (TMA), °C, max.	-10	-10	-10
Tsp (TMA), °C, max.	28	28	28
ML (TMA), μm/°C, max.	0.4	0.4	0.4

[1] AASHTO M226, Table 2

VI. SUMMARY AND CONCLUSIONS

Three groups of asphalt samples were tested during this investigation including: (a) 12 samples from local asphalt suppliers and their TFOT residues, (b) six core samples of known service records, and (c) a total of 79 asphalts from 10 pavement projects including original, lab aged, and recovered asphalts from lab mixes, field mixes, and pavement cores. They were studied by physical and physicochemical tests including standard rheological tests, HP-GPC, and TMA. Some specific viscoelastic tests were run at 5°C on the (b) samples and on some (a) samples. DSC and XRD studies were also performed on the (a) and (b) samples. In addition, NMR techniques were applied to some (a), (b), and (c) samples.

Efforts were made to identify physicochemical properties which correlated to physical properties known to affect field performance. The significant properties formed the basis for the recommended performance-based trial specifications for Iowa to ensure better pavement performance.

Conclusions of a general nature are summarized below:

(1) With each viscosity grade of asphalt available in Iowa and meeting AASHTO specification M226, there were differences in temperature susceptibility between the samples supplied by different suppliers and between samples from the same supplier taken at different times.

(2) Distinctly different HP-GPC chromatograms, TA results, XRD patterns were obtained for asphalts of the same grade, from the same supplier, but supplied at different times.

(3) The greatly different effect of a cold shock at -30°C on the viscoelastic properties of the core asphalt from the Sugar Creek surface course from the other samples might have important bearing on its poor field performance.

(4) No decisive correlation is observed among HP-GPC, DSC, and XRD results.

(5) The HP-GPC technique is very sensitive for monitoring aging and can also be used to predict behavior and performance of asphalts.

(6) The endothermic peaks in a DSC thermogram indicate the presence of crystallizable components and can be used to evaluate the low-temperature performance of asphalts. The enthalpy changes (ΔH) are, on the whole, more pronounced in virgin asphalts of Jebro origin than in the Koch asphalts.

(7) Asphalts used in the 1988 construction season came from a limited number of sources in Iowa and showed differences not obvious by either physical or physicochemical tests alone. For example, the asphalt used in Project 7 had a large percent increase in LMS due to aging but this was not reflected by changes in physical properties, e.g. viscosity ratio. On the other hand, the asphalt used in Project 11 had a high viscosity ratio after TFOT aging, but this was not reflected in an increase in LMS.

(8) The ratio of changes in %LMS to changes in physical properties upon aging could be used as compatibility index for asphalts.

(9) Of two accelerated laboratory aging procedures for long term performance, the pressure-oxidation procedure seems to be superior to the mix aging procedure. The pressure-oxidation test is a simpler, faster, less expensive, and more reliable

procedure.

(10) Aging, both in the field and in the laboratory, is accompanied by hardening, a reduction in temperature susceptibility by most measures, an increase in shear susceptibility, a decrease in complex flow, an increase in temperature for limiting stiffness, an increase in stiffness at low temperatures, an increase in LMS, and a decrease in SMS. For some asphalts, aging characteristics at high-temperature (short-term aging) and at service temperature (long-term aging) were very different.

(11) The glass transition temperatures determined by TMA correlated weakly with those determined by DSC but correlate fairly well with low-temperature cracking properties.

(12) Both TMA and HP-GPC parameters correlated well with physical properties. Tsp correlates well with both rheological and low-temperature properties, T_g correlates well with low-temperature properties, and ML is a strong predictor of rheological properties. Molecular size distribution based on HP-GPC and the 8-slice method can be used to predict many physical properties.

(13) While TMA parameters and HP-GPC parameters did not correlate well, physical and low-temperature properties can be predicted by combinations of these two sets of parameters, especially using Tsp, ML, X2, and X7.

(14) Asphalt specifications for Iowa climates were developed based on consideration of the long-term durability test and performance related physicochemical properties.

VII. RECOMMENDATIONS

1. A tentative specification for paving asphalts, including IDT durability requirements, as well as chemical and low-temperature requirements, is recommended.
2. Continued observations and tests of the 10 pavements are recommended because of a lack of sufficient data on critical values of critical properties under Iowa weathering and traffic conditions. The critical values for Iowa conditions are needed so the specifications can be refined to yield a truly performance-based asphalt specification.
3. No critical values for physical or chemical properties are available in the literature nor are given in the tentative specification concerning moisture sensitivity of asphalt-aggregate mixes. Research investigating the relationship between asphalt composition and asphalt-aggregate-moisture interaction is needed so that moisture related distresses can be addressed in the specification.
4. In addition to the size characterization of asphalt by HP-GPC, development of simple and reliable tools better characterizing the polarity distribution and the aromaticity of asphalts are needed in order to obtain complete chemical information on asphalts and, therefore, to further refine the tentative specification.

BIBLIOGRAPHY

1. Albert, M., F. Bosselet, P. Claudy, J. M. Letoffe, E. Lopez, B. Damin, and B. Neff. "Comportement thermique des bitumes routiers. Determination du taux de fractions cristallisees par analyse calorimetrique differentielle." Thermochimica Acta. 84 (1985): 101-110.

2. Alexander, L. E. X-ray diffraction methods in polymer science. New York: John Wiley & Sons, Inc., 1969.

3. Altgelt, K. H. and O. L. Harle. "The effect of asphaltenes on asphalt viscosity." Industrial and Engineering Chemistry, Product Research and Development, 14(4) (1975): 240-246.

4. Anderson, D. A. and E. L. Dukatz. "Finger printing versus field performance of paving grade asphalts." Report No. FHWA/RD-84/095, FHWA, Washington, D. C., 1985.

5. The Asphalt Institute. "Design technique to minimize low temperature asphalt pavement transverse cracking." Research Report No. 81-1, College Park, Maryland, 1981.

6. The Asphalt Institute. The asphalt hand book. Manual Series No. 4, 1989.

7. Bell, C. A. "Use of Shell bitumen test data chart in evaluation and classification of asphalts." AAPT 52 (1983): 1-31.

8. Bishara, W. and E. Wilkins. "Rapid method for the chemical analysis of asphalt cement: quantitative determination of the naphthene aromatic and polar aromatic fractions using high performance liquid chromatography." TRR 1228 (1989): 183-190.

9. Blokker, P. C. and H. van Hoorn. "Durability of bitumen in theory and practice." Proc. of 5th World Petroleum Congress, Section IV (1959): 417.

10. Boduszynski, M. M. "Asphaltenes in petroleum asphalts; composition and formation." in Chemistry of Asphaltenes, eds. J.W. Bunger and N.C. Li American Chemical Society, Washington, D.C., 1981. 119-135.

11. Branthaver, J. F., S. S. Kim, M. W. Catalfomo, and D. C. Goray. "Isolation and Characterization of Amphoteric Components of SHRP Asphalts by Ion Exchange Chromatography." Am. Chem. Soc., Div. Fuel Chem. Preprints, 37(3) (1992): 1299-1311.

12. Breen, J. J. and J. E. Stephens. "The glass transition temperature and mechanical properties of asphalts." Proc. Canadian Technical Asphalt Association 12 (1967): 137-144.

13. Brodnyan, J. G. "Use of rheological and other data in asphalt engineering problems." HRB Bulletin 192 (1958): 1-19.

14. Brodnyan, J. G., F. H. Gaskins, W. Philippoff, and E. Thelen. "The rheology of asphalt III." Transactions of Society of Rheology 4 (1960): 279-296.

15. Brown, A. B., J. W. Sparks, and O. Larsen. "Rate of changes of softening point, penetration and ductility of asphalt in bituminous pavement." AAPT 26 (1957): 66-81.

16. Button, J. W., D. N. Little, and B. M. Gallaway. Influence of asphalt temperature susceptibility on pavement construction and performance. NCHRP Report 268, 1983.

17. Christensen, D. W., Jr. and D. A. Anderson. "Interpretation of dynamic mechanical test data for paving grade asphalt cements." AAPT 61 (1992): 67-116.

18. Claudy, P., F. Rondelez, L. Germanaud, G. King, and J. P. Planche. "A new interpretation of time-dependent physical hardening in asphalt based on DSC and optical thermoanalysis." Am. Chem. Soc., Div. Fuel Chem. Preprints, 37(3) (1992): 1408-11426.

19. Corbett, L. C. "Relationship between composition and physical properties of asphalt." AAPT 39 (1970): 481-491.

20. Davis, T. C. and J. C. Petersen. "An adaptation of inverse gas liquid chromatography to asphalt oxidation studies." Ana. Chem. 38 (1966): 1938-1940.

21. Davis, T. C., J. C. Petersen, and W. E. Haines. "Inverse gas-liquid chromatography. A new approach for studying petroleum asphalts." Ana. Chem. 38 (1966): 241-243.

22. Dobson, G. R. "The dynamic mechanical properties of bitumen." AAPT 38 (1969): 1-10.

23. Elder, A. C., M. M. Hattingh, V. P. Servas, and C. P. Marais. "Use of aging tests to determine the efficacy of hydrated lime additions to asphalt in retarding its oxidative hardening." AAPT 54 (1985): 118-139.

24. Ensley, E. K. "Multilayer adsorption with molecular orientation of asphalt on mineral aggregate and other substrates." J. of Applied Chemistry and Biotechnology 25 (1975): 671-682.

25. Enustun, B. V., S. S. Kim, and D. Y. Lee. "Correlation of locally-based performance of asphalts with their physicochemical parameters." Final Report, IDOT Project HR-298, Ames, Iowa, 1990.

26. Epps, J. A. and W. J. Kari "Factors to be considered in developing performance based specifications." AAPT 52 (1983): 271-291.

27. Ferry, J. D. Viscoelastic properties of polymers. Third Edition, John Wiley & Sons, 1980.

28. Finn, F. N. "Factors involved in the design of asphaltic pavement surfaces." NCHRP Report 39, 1967.

29. Garrick, N. W. and L. E. Wood. "Predicting asphalt properties from HP-GPC profiles." AAPT 57 (1988): 26-40.

30. Gaskins, F. H., J. G. Brodnyan, W. Philippoff, and E. Thelen. "The rheology of asphalt. II. -- Flow characteristics of asphalt." Transactions of Society of Rheology 4 (1960): 265-278.

31. Gaw, W. J. "The measurement and prediction of asphalt stiffness at low and intermediate pavement service temperatures." AAPT 47 (1978): 457-494.

32. Gerstein, B. C. "Nuclear Magnetic Resonance." An invited article for the Encyclopedia of Science, Academic Press, New York: 1986.

33. Goode, J. F. and L. A. Lufsey. "Voids permeability film thickness vs. asphalt hardening." AAPT 34 (1965): 430-463.

34. Goodrich, J. L. "Asphalt and polymer-modified asphalt properties related to the performance of asphalt concrete mixes." AAPT 57 (1988): 116-175.

35. Goodrich, J. L. and L. H. Dimpfl. "Performance and supply factors to consider in paving asphalt specifications." AAPT 55 (1986): 57-87.

36. Goodrich, J. L., J. E. Goodrich, and W. J. Kari. "Asphalt composition tests: their application and relation to field performance." TRR 1096 (1986): 146-167.

37. Griffin, R. L., T. K. Miles, and C. J. Penther. "Microfilm durability test for asphalt." AAPT 24 (1955): 31-62.

38. Hagen, A. P., M. P. Johnson, and B. B. Randolph. "^{13}C NMR studies on roadway asphalts." Fuel Science and Technology Int'l 7(9) (1989): 1289-1326.

39. Hall, G. and P. Herron. "Size characterization of petroleum asphaltenes and maltenes." in Chemistry of Asphaltenes, eds. J.W. Bunger and N.C. Li American Chemical Society, Washington, D.C., 1981. 137-153.

40. Halstead, W. J. "Relation of asphalt chemistry to physical properties and specifications." AAPT 54 (1985): 91-117.

41. Halstead, W. J. and J. Y. Welborn. "History of the development of asphalt testing apparatus and asphalt specifications." AAPT 43A (1974): 89-120.

42. Heithaus, J. J. "Measurement and significance of asphalt peptization." Am. Chem. Soc., Petroleum Chem. Div., Preprint 5(4-A) (1960): A23-38.

43. Heukelom, W. "An improved method of characterizing asphaltic bitumen with the aid of their mechanical properties." AAPT 42 (1973): 67-94.

44. Heithaus, J. J. and R. W. Johnson. "A microviscometer study of asphalt hardening in the field and laboratory." AAPT 27 (1958): 17-34.

45. Heukelom, W. "Observations on the rheology and fracture of bitumens and asphalt mixes." AAPT 35 (1966): 358-399.

46. Hills, J. F. "Predicting the fracture of asphalt mixes by thermal stress." J. of Institute of Petroleum IP 74-014 (1974): 1-11.

47. Hodgson, R. S. "Changes in asphalt." TRR 999 (1984): 10-12.

48. Hubbard, R. L. and K. E. Stanfield. "Determination of asphaltenes, oils, and resins in asphalt." Ana. Chem. 20 (May 1948): 460-465.

49. Hveem, F. N., E. Zube, and J. Skog. "Proposed new tests and specifications for paving grade asphalts." AAPT 32 (1963): 271-372.

50. Jennings, P. W. "Prediction of asphalt performance by HP-GPC." AAPT 54 (1985): 635-651.

51. Jennings, P. W., J. A. Pribanic, W. Campbell, K. R. Dawson, and R. B. Taylor. "High pressure liquid chromatography as a method of measuring asphalt composition." Research Report FHWA/MT-7930, Bozeman, Montana, 1980.

52. Jennings, P. W., J. A. S. Pribanic, and K. R. Dawson. "Use of high pressure liquid chromatography to determine the effects of additives and fillers on the characteristics of asphalt." Research Report FHWA/MT-82/001, Bozeman, Montana, 1982.

53. Jennings, P. W, J. A. S. Pribanic, and K. R. Dawson. "The expanded Montana asphalt quality study using high pressure liquid chromatography." Research Project FHWA/MT-85/001, Bozeman, Montana, 1985.

54. Jennings, P. W., J. A. S. Pribanic, J. Smith, and T. M. Mendes. "Predicting the performance of the Montana test sections by physical and chemical testing." TRR 1171 (1988): 59-65.

55. Jennings, P. W., J. A. S. Pribanic, J. A. Smith, and T. M. Mendes. "HP-GPC analysis of asphalt fractions in the study of molecular self-assembly in asphalt." Am. Chem. Soc., Div. Fuel Chem. Preprints 37 (3) (1992): 1312-1319.

56. Jongepier, R. and B. Kuilman. "Characteristics of the rheology of bitumens." AAPT 38 (1969): 98-122.

57. Kandhal, P. S. "Low temperature shrinkage cracking of pavements in Pennsylvania." AAPT 47 (1978): 73-114.

58. Kandhal, P. S., L. D. Sandvig, and M. E. Wenger. "Shear susceptibility of asphalts in relation to pavement performance." AAPT 42 (1973): 99-112.

59. Kandhal, P. S. and M. E. Wenger. "Asphalt properties in relation to pavement performance." TRR 544 (1975): 6-13.

60. Kennedy, T. D. "Characterization of asphalt pavement materials using the indirect tensile test." AAPT 46 (1977): 132-150.

61. Kim, K. W. and J. L. Burati Jr. "Use of GPC chromatograms to characterize aged asphalt cement." J. materials in Civil Engineering, American Society of Civil Engineering, Materials Engineering Division, 5(1) (1993): 41-52.

62. Lee, D. Y. "Development of laboratory durability test for asphalts." HRR 231 (1968): 34-41.

63. Lee, D. Y. "Durability and durability tests for paving asphalt: a state-of-the-art report." Special Report Submitted to Iowa State Highway Commission, HR-124, Ames, Iowa, 1969.

64. Lee, D. Y. "Development of durability test for asphalts." Final Report, IDOT Project HR-124, Ames, Iowa, 1972.

65. Lee, D. Y. "Asphalt durability correlations in Iowa." HRR 468 (1973): 43-60.

66. Lee, D. Y. and T. Demirel. "Beneficial effects of selected additives on asphalt cement mixes." Final Report for IDOT Project HR-278, Ames, Iowa, 1987.

67. Lee, D. Y. and B. V. Enustun. "Correlation of locally-based performance of asphalts with their physicochemical parameters." Task 1 Report, IDOT Project HR-298, Ames, Iowa, 1988.

68. Long, R. B. "The concept of asphaltenes." in Chemistry of Asphaltenes, eds. J.W. Bunger and N.C. Li American Chemical Society, Washington, D.C., 1981. 17-27.

69. Lottman, R. P. "Predicting moisture-induced damage to asphaltic concrete - field evaluation." NCHRP Report 246, 1982.

70. Mack, C. "Colloid chemistry of asphalts." J. of Physical Chemistry 30 (1932): 2901-2914.

71. Marks, V. J. and C. L. Huisman. "Reducing the adverse effects of transverse cracking." TRR 1034 (1985): 80-86.

72. Majidzadeh, K. and H. E. Schweyer. "Non-Newtonian behavior of asphalt cements." AAPT 34 (1965): 20-44.

73. Mascia, L. Thermoplastics. Elsevier Applied Science. 1989.

74. McLeod, N. W. "A 4-year study of low temperature transverse pavement cracking on three Ontario test roads." AAPT 41 (1972): 424-493.

75. McLeod, N. W. "Asphalt cements: pen-vis number and its application to moduli of stiffness ." J. of Testing and Evaluation 4(4) (1976): 275-282.

76. McLeod, N. W. "Relationship of paving asphalt temperature susceptibility as measured by PVN to paving asphalt specifications, asphalt paving mixture design and asphalt pavement performance." AAPT 58 (1989): 410-489.

77. Moavenzadeh, F. and R. R. Stander, Jr. "On flow of asphalt." HRR 134 (1966): 8-35.

78. NCHRP Synthesis 59. "Relationship of asphalt cement properties to pavement durability" TRB, National Research Council, Washington, D. C., 1979.

79. Noel, F. and L. W. Corbett. "A study of the crystalline phases in asphalt." J. of the Institute of Petroleum 56 (1970): 261-268.

80. Noureldin, A. S. and L. E. Wood. "Variation in molecular size distribution of virgin and recycled asphalt binders associated with aging." TRR 1228 (1989): 191-197.

81. Page, G. C., K. H. Murphy, B. E. Ruth, and R. Roque. "Asphalt binder hardening - causes and effects." AAPT 54 (1985): 140-161.

82. Petersen, J. C. "Chemical composition of asphalt as related to asphalt durability: state-of-the-art." TRR 999 (1984): 13-30.

83. Pfeiffer, J. Ph. and P. M. van Doormaal. "The rheological properties of asphalt bitumen." J. of Institute of Petroleum Technologists 22 (1936): 414.

84. Pfeiffer, J. Ph. and R. N. J. Saal. "Asphaltic bitumen as colloid system." J. of Physical Chemistry 44 (1940): 139-149.

85. Plancher, H., E. L. Green, and J. C. Petersen. "Reduction of oxidative hardening of asphalt by treatment with hydrated lime -- a mechanistic study." AAPT 45 (1976): 1-24.

86. Pribanic, J. A. S., M. Emmelin, and G. King. "Use of multiwavelength UV-Vis HP-GPC to give a three-dimensional view of bituminous materials." TRR 1228 (1989): 168-176.

87. Robert F. L., P. S. Kandhal, E. R. Brown, D. Y. Lee, and T. W. Kennedy. Hot mix asphalt materials, mixture design, and construction. NAPA Education Foundation, 1991.

88. Rose, K. D. and M. A. Francisco. "Characterization of acidic heteroatoms in heavy petroleum fractions by phase-transfer methylation and NMR spectroscopy." Energy & Fuels 1(3) (1987): 233-239.

89. Rostler, F. S. and R. M. White. "Composition and changes in composition of highway asphalts, 85-100 penetration grade." AAPT 31 (1962): 35-89.

90. Schmidt, R. J. "A practical method for measuring the resilient modulus of asphalt-related mixes." HRR 404 (1972): 22-32.

91. Schmidt, R. J. and L. E. Santucci "A practical method for determining the glass transition temperature of asphalts and calculation of their low-temperature viscosities." AAPT 35 (1966): 61-90.

92. Schweyer, H. E. "Asphalt rheology in the near-transition temperature range." HRR 468 (1973): 1-15.

93. Schweyer, H. E. "A pictorial review of asphalt rheology." AAPT 43A (1974): 121-157.

94. Schweyer, H. E. and R. N. Traxler. "Separating asphalt materials -- butanol-acetone method." Oil Gas J. 52 (1953): 133.

95. Schweyer, H. E., L. L. Smith, and G. W. Fish. "A constant stress rheometer for asphalt cements." AAPT 45 (1976): 53-77.

96. Shoor, S. K., K. Majidzadeh, and H. E. Schweyer. "Temperature-flow functions for certain asphalt cements." HRR 134 (1966): 63-74.

97. Simpson W. C., R. L. Griffin, and T. K. Miles. "Correlation of the microfilm durability test with field hardening observed in the Zaca-Wigmore experimental project." ASTM STP 277, American Society for Testing and Materials (1960): 52-63.

98. Sisko, A. W. "Determination and treatment of asphalt viscosity data." HRR 67 (1965): 27-37.

99. Sisko, A. W. and L. C. Brunstrum. "The rheological properties of asphalts in relation to durability and pavement performance." AAPT 37 (1968): 448-473.

100. Speight, J. G. "On the molecular nature of petroleum asphaltenes." in Chemistry of Asphaltenes, eds. J.W. Bunger and N.C. Li American Chemical Society, Washington, D.C., 1981. 1-15.

101. Strategic Highway Research Program. "Binder characterization and evaluation." Final Report, SHRP A-002A, National Research Council, Washington, D. C., 1992.

102. Strategic Highway Research Program. "Binder characterization and evaluation by NMR spectroscopy." Final Report, SHRP A-002C, National Research Council, Washington, D. C., 1991.

103. Tia, M. and B. E. Ruth. "Basic rheology and rheological concepts established by H.E. Schweyer." ASTM STP 941, American Society for Testing and Materials (1987): 118-145.

104. Traxler, R. H. "Durability of asphalt cements." AAPT 32 (1963): 44-63.

105. Traxler, R. H., H. E. Schweyer, and J. N. Romberg. "Rheological properties of asphalts." Industrial and Engineering Chemistry 36 (1944): 823-829.

106. Vallerga, B. A., C. L. Monismith, and K. Granthem. "A study of some factors influencing the weathering of paving asphalts." AAPT 26 (1957): 126-150.

107. Van der Poel, C. "A general system describing the viscoelastic properties of bitumens and its relationship to routine test data." J of Applied Chemistry 4 (1954): 221-236.

108. Wada, Y. and H. Hirose. "Glass transition phenomena and rheological properties of petroleum asphalt." J. of Physical Society of Japan 15(10) (1960): 1885-1894.

109. Welborn, J. Y. "The philosophy of using viscosity for grading asphalt cements", ASTM STP 424, American Society for Testing and Materials (1967): 3-13.

110. Welborn, J. Y. "Physical properties as related to asphalt durability." TRR 999 (1984): 31-36.

111. Welborn, J. Y., E. R. Oglio, and J. A. Zenewitz. "A study of viscosity graded asphalt cements." AAPT 35 (1966): 19-60.

112. Williams, M. L., R. F. Landel, and J. D. Ferry. "The temperature dependence of relaxation mechanisms in amorphous polymers and other glass-forming liquids." J. of American Chemical Society 77 (1955): 3701-3707.

113. Williford, C. L. "X-ray studies of paving asphalts." Texas Engr. Exp. Station Bulletin 73. A & M College of Texas, College Station, Texas, 1943.

114. Yen, T.F. "Structural differences between asphaltenes isolated from petroleum and from coal liquid." in Chemistry of Asphaltenes, eds. J.W. Bunger and N.C. Li American Chemical Society, Washington, D.C., 1981. 39-51.

115. Zenewitz, J. A. and K. T. Tran. "A further statistical treatment of the expanded Montana asphalt quality study." Public Roads 51(3) (1987): 72-81.

APPENDIX A. REGRESSION COEFFICIENT MATRIX

	P5 0.1mm	P25 0.1mm	P4 0.1mm	R&B SP °C	VIS25 Pa·s
Intercept	3.76E+02	7.19E+03	1.79E+03	-5.54E+02	4.81E+07
X1	-5.61E+00	-1.05E+02	-2.48E+01	1.23E+01	-5.88E+04
X2	-1.29E+00	-3.05E+01	-8.17E+00	-2.53E+00	-1.00E+06
X3	-4.46E+00	-1.11E+02	-2.38E+01	1.60E+01	1.79E+04
X4	-9.87E-01	-4.11E+01	-1.22E+01	-4.81E+00	-1.33E+06
X5	-7.80E+00	-4.53E+01	-1.53E+01	9.73E-01	-5.76E+05
X6	-9.07E+00	-1.79E+02	-4.98E+01	2.67E+01	1.06E+06
X7	9.03E+00	6.30E+01	3.27E+01	-1.44E+01	-2.04E+06
X8	-6.73E+00	-7.38E+01	-2.40E+01	8.01E+00	-1.21E+05
MWT	1.91E-03	6.51E-02	1.46E-02	-4.66E-03	2.59E+02
POLYIDX	4.35E-02	-1.95E+01	-5.49E+00	-1.96E+00	-5.56E+05
T_g	-6.94E-02	6.80E-01	1.82E-02	-2.63E-01	-2.75E+03
Tsp	-1.71E-01	-1.94E+00	-7.46E-01	4.95E-01	4.03E+04
ML	-1.58E+01	-2.88E+02	-7.20E+01	4.59E+01	2.34E+06
MH	1.23E+01	1.64E+02	4.79E+01	-2.60E+01	-1.42E+06

	CF	SI	VIS60 Pa·s	VIS135 10^{-6} m^2/s	PR
Intercept	-8.79E-01	5.40E+00	-7.89E+04	-2.26E+04	-7.23E+00
X1	-7.25E-02	3.31E-02	1.22E+03	3.81E+02	1.78E-01
X2	1.55E-01	-1.86E-01	1.93E+02	-8.14E+01	-4.31E-02
X3	-1.79E-01	1.25E-01	1.77E+03	7.44E+02	2.39E-01
X4	2.96E-01	-2.97E-01	-7.66E+02	-3.51E+02	-8.88E-02
X5	-6.26E-02	-4.65E-03	2.14E+02	2.14E+01	-3.30E-02
X6	-1.45E-01	1.18E-01	3.32E+03	1.05E+03	3.07E-01
X7	2.95E-01	-2.95E-01	-9.83E+02	-6.63E+02	-1.24E-02
X8	-9.97E-02	4.52E-02	8.85E+02	5.14E+02	4.30E-02
MWT	-4.15E-05	6.80E-05	7.80E-01	3.49E-01	-6.01E-05
POLYIDX	1.21E-01	-1.30E-01	-9.62E+02	-3.66E+02	-5.18E-02
T_g	1.01E-02	-9.80E-03	-2.97E+01	-2.43E+00	-3.93E-03
Tsp	-5.29E-03	6.07E-03	8.17E+01	1.80E+01	3.78E-03
ML	-8.76E-01	6.78E-01	7.82E+03	1.64E+03	6.47E-01
MH	3.50E-01	-3.28E-01	-4.60E+03	-9.90E+02	-2.85E-01

	PI	CN	VTS	PVN60	PVN135
Intercept	-8.23E-01	1.57E+03	-1.41E+01	-5.26E+01	-2.46E+00
X1	3.69E-01	-1.72E+01	2.28E-01	5.00E-01	-8.38E-02
X2	-6.42E-01	-1.56E+01	1.92E-01	5.30E-01	-1.96E-02
X3	1.06E+00	-2.28E+01	1.16E-01	9.90E-01	5.02E-01
X4	-1.05E+00	5.28E+00	5.13E-02	-5.45E-01	-5.30E-01
X5	-4.56E-01	-1.51E+01	2.18E-01	6.07E-01	-4.85E-02
X6	6.83E-01	-3.84E+01	4.57E-01	1.16E+00	2.59E-02
X7	3.76E-02	6.30E-01	9.67E-03	8.34E-02	-5.68E-02
X8	-7.71E-02	-1.81E+01	1.06E-01	7.88E-01	3.70E-01
MWT	-6.81E-05	-8.25E-03	-6.05E-05	7.23E-04	6.27E-04
POLYIDX	-2.78E-01	7.59E+00	-6.28E-03	-5.14E-01	-3.59E-01
T_g	-4.48E-02	3.76E-02	-3.40E-03	1.00E-03	9.44E-03
Tsp	2.35E-02	-1.51E-01	4.32E-03	2.34E-03	-8.61E-03
ML	5.31E-01	-4.79E+01	9.50E-01	8.97E-01	-1.20E+00
MH	-1.43E-01	3.52E+01	-5.86E-01	-7.25E-01	5.38E-01

	CT °C	TES °C	S23 MPa	S29 MPa
Intercept	-1.25E+02	-1.37E+03	1.86E+03	4.82E+03
X1	7.38E-01	1.70E+01	-2.78E+00	-2.91E+01
X2	1.51E+00	9.81E+00	-4.44E+01	-9.06E+01
X3	-2.90E+00	1.39E+01	-1.75E+00	-2.46E+01
X4	1.34E+00	1.34E+01	-3.22E+01	-5.43E+01
X5	1.12E+01	1.13E+01	-6.97E+00	-7.62E+00
X6	-3.34E+00	2.83E+01	1.64E+01	-3.34E+01
X7	-6.54E+00	-1.14E+01	-8.43E+01	-1.38E+02
X8	6.56E+00	1.99E+01	4.36E-02	-1.55E+01
MWT	3.05E-03	-2.21E-03	3.17E-03	1.45E-02
POLYIDX	-1.83E+00	-1.03E+00	-1.39E+01	-2.09E+01
T_g	3.26E-01	2.61E-01	6.72E-01	1.39E+00
Tsp	-7.60E-02	3.50E-02	1.31E+00	1.72E+00
ML	-1.26E+01	2.01E+01	1.17E+02	2.56E+02
MH	-9.09E-01	-1.50E+01	-5.99E+01	-9.88E+01

APPENDIX B. PREDICTED VS. MEASURED PROPERTIES

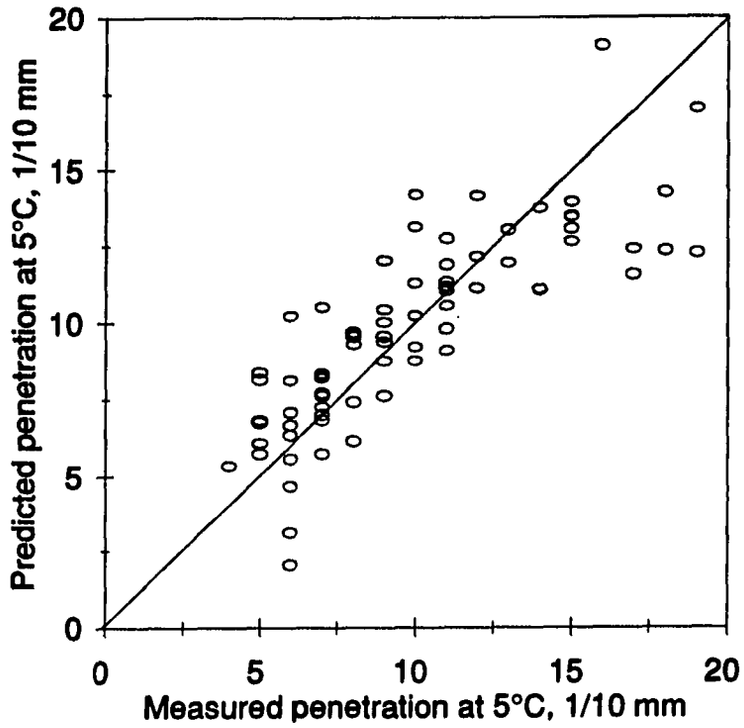
Predicted penetration at 5°C, 1/10 mm
Measured penetration at 5°C, 1/10 mm
0
5
10
15
20

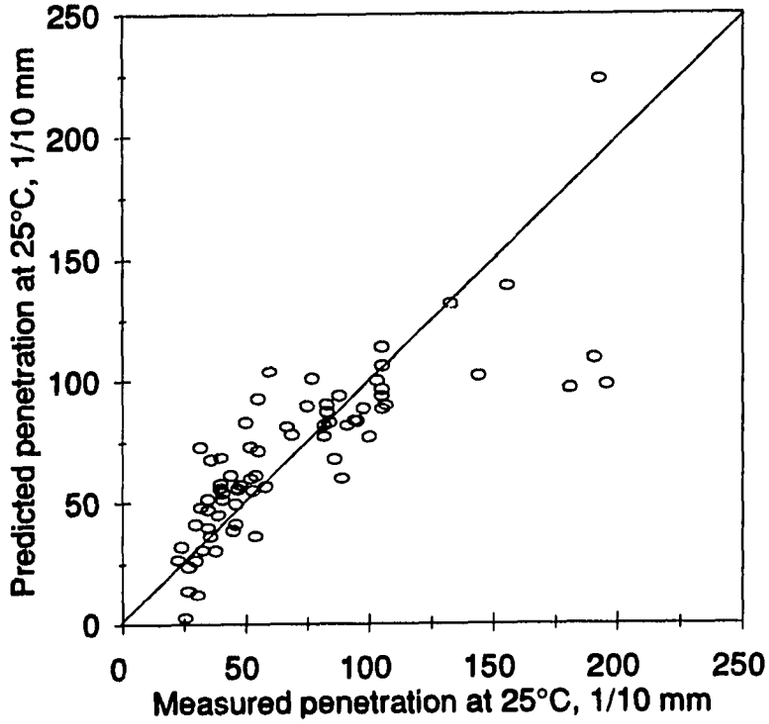
Predicted penetration at 25°C, 1/10 mm
Measured penetration at 25°C, 1/10 mm
0
50
100
150
200
250

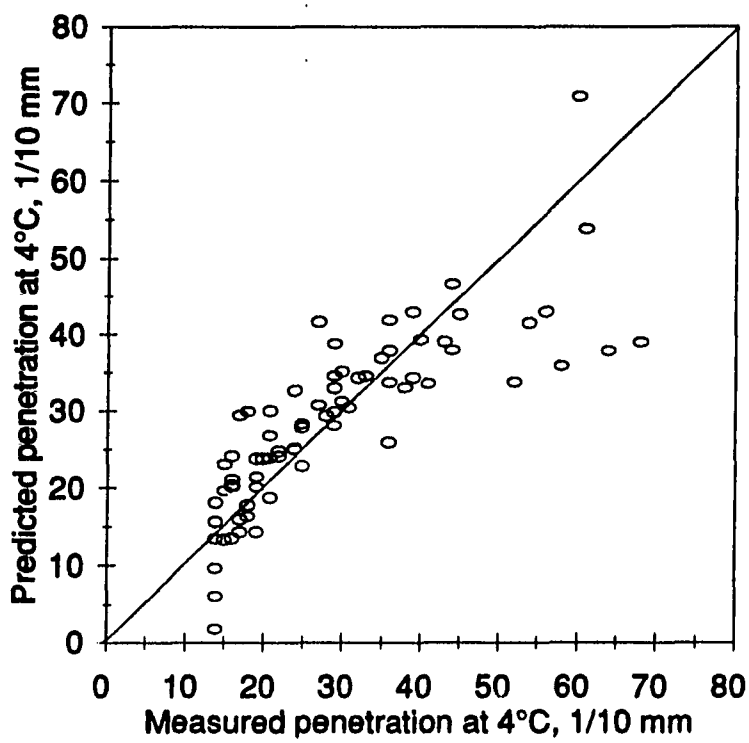
Predicted penetration at 4°C, 1/10 mm
0
10
20
30
40
50
60
70
80
Measured penetration at 4°C, 1/10 mm

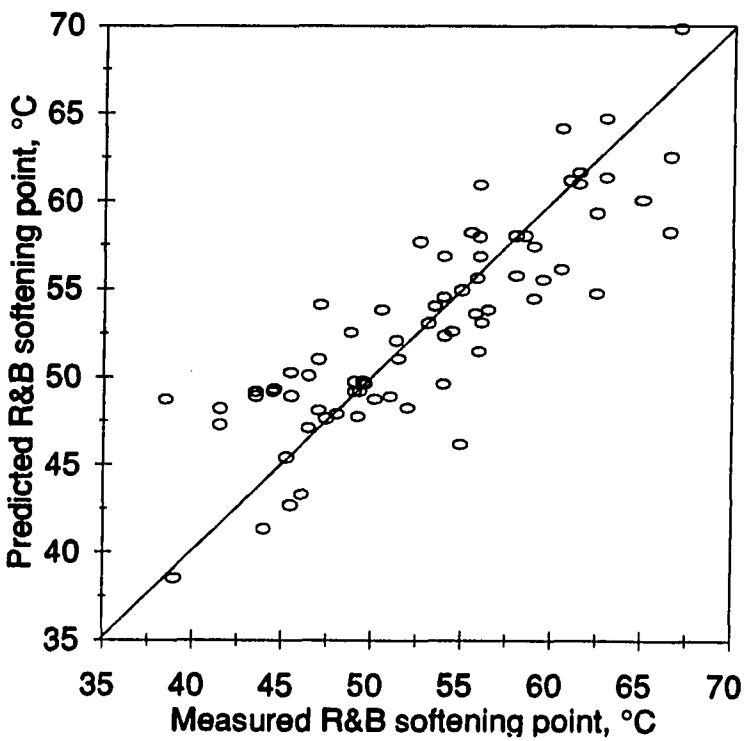
Predicted R&B softening point, °C
35
40
45
50
55
60
65
70
Measured R&B softening point, °C

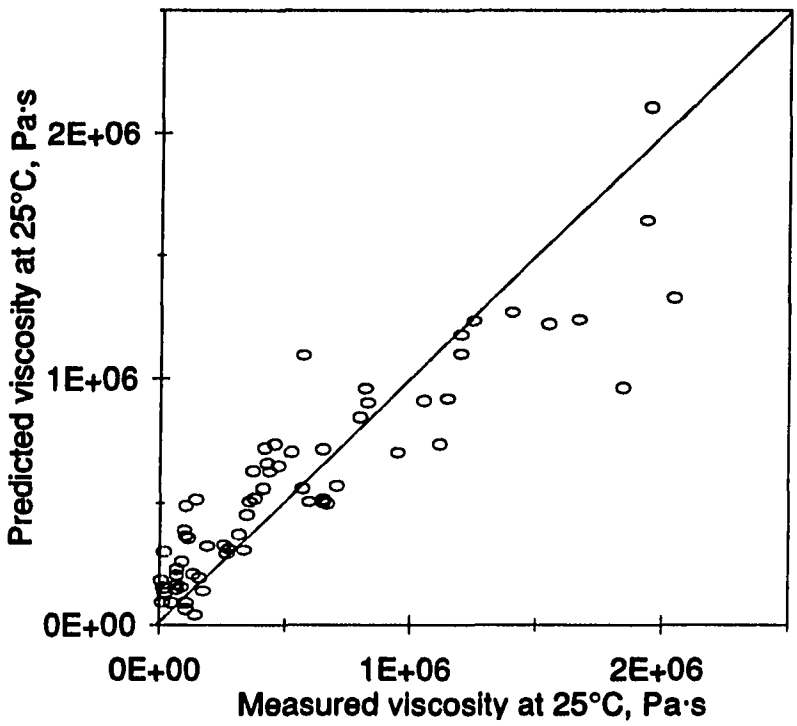
Predicted viscosity at 25°C, Pa·s
2E+06
1E+06
0E+00
0E+00
1E+06
2E+06
Measured viscosity at 25°C, Pa·s

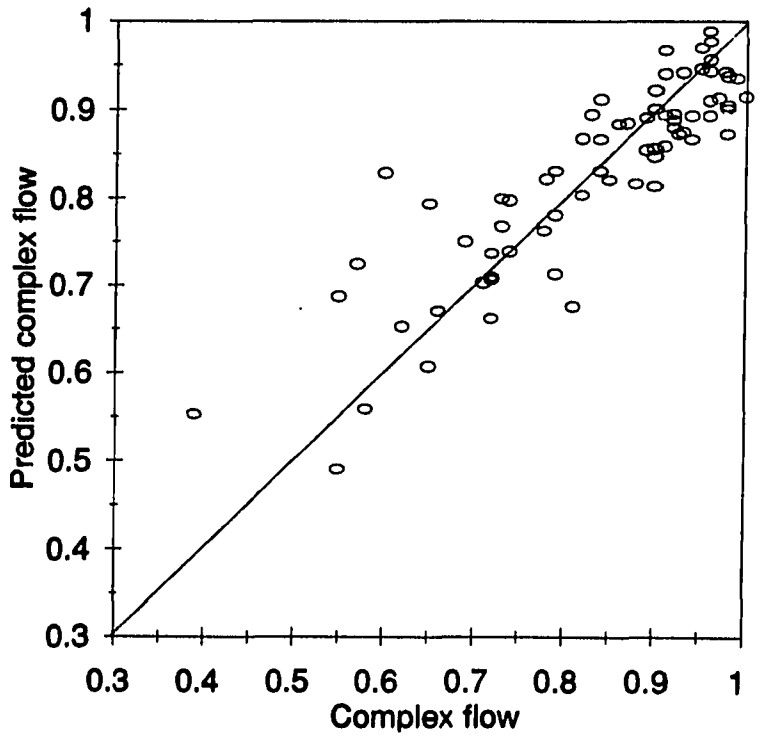
Predicted complex flow
1
0.9
0.8
0.7
0.6
0.5
0.4
0.3
0.3
0.4
0.5
0.6
0.7
0.8
0.9
1
Complex flow

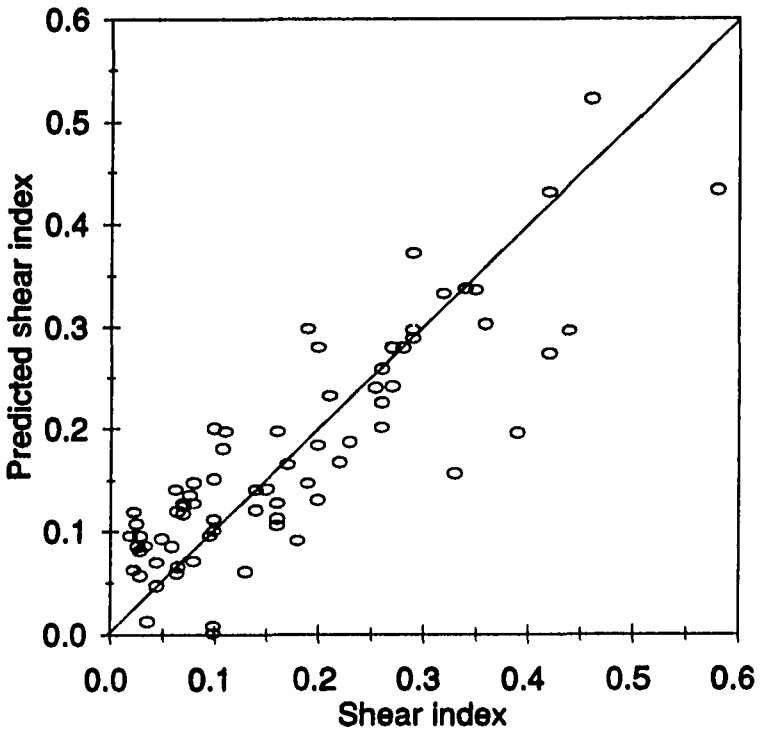
Predicted shear index
0.0
0.1
0.2
0.3
0.4
0.5
0.6
Shear index

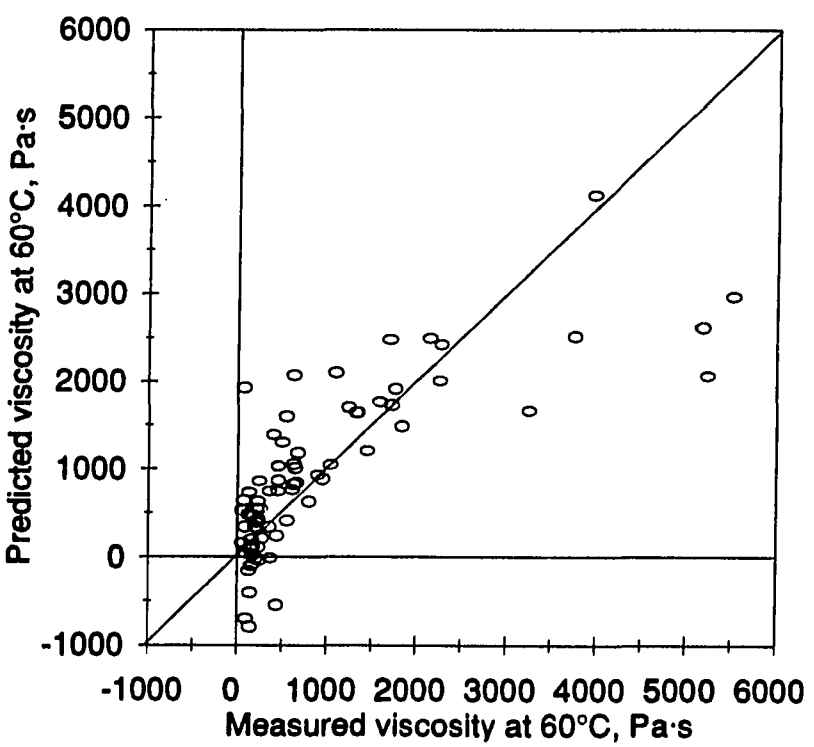
Predicted viscosity at 60°C, Pa·s
6000
5000
4000
3000
2000
1000
0
-1000
-1000 0 1000 2000 3000 4000 5000 6000
Measured viscosity at 60°C, Pa·s

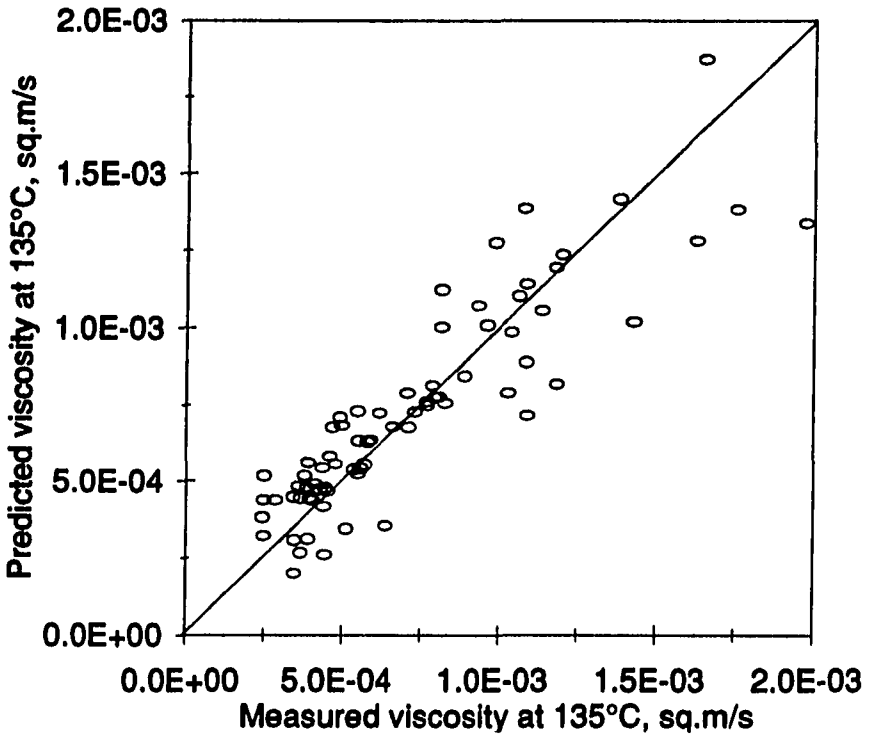
2.0E-03
1.5E-03
1.0E-03
5.0E-04
0.0E+00
Predicted viscosity at 135°C, sq.m/s
0.0E+00
5.0E-04
1.0E-03
1.5E-03
2.0E-03
Measured viscosity at 135°C, sq.m/s

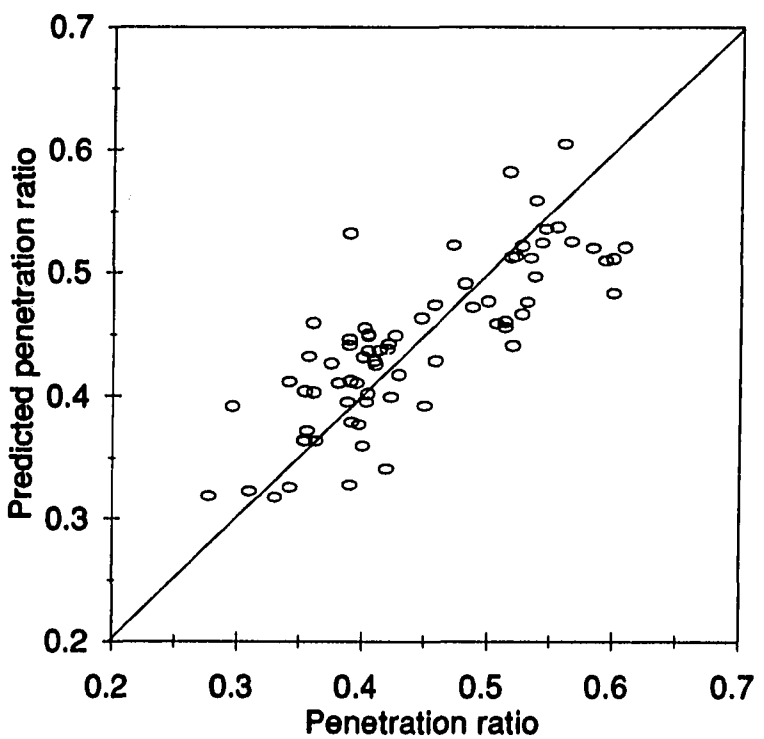
0.7
0.6
0.5
0.4
0.3
0.2
Predicted penetration ratio
0.2
0.3
0.4
0.5
0.6
0.7
Penetration ratio

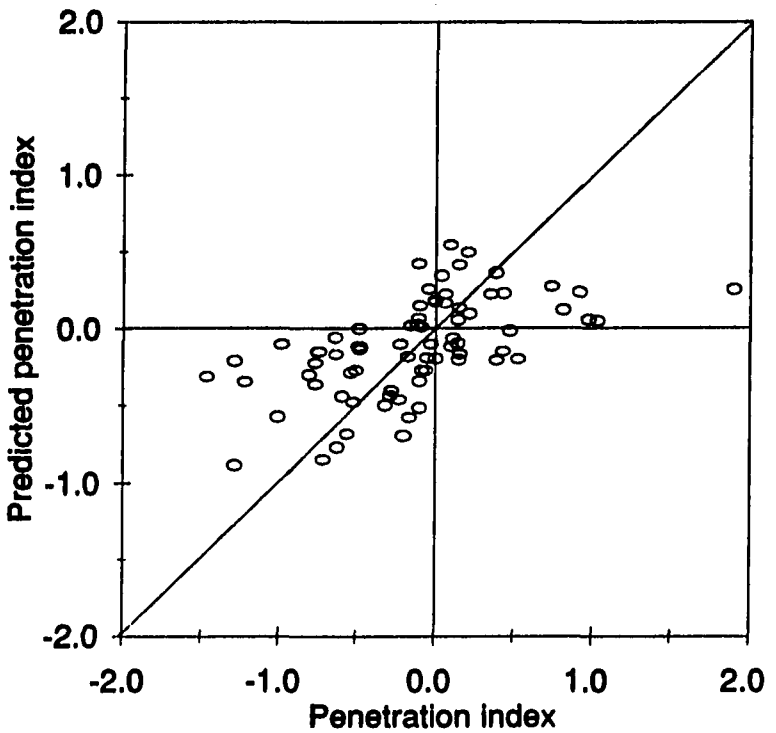
2.0
1.0
0.0
-1.0
-2.0
Predicted penetration index
-2.0
-1.0
0.0
1.0
2.0
Penetration index

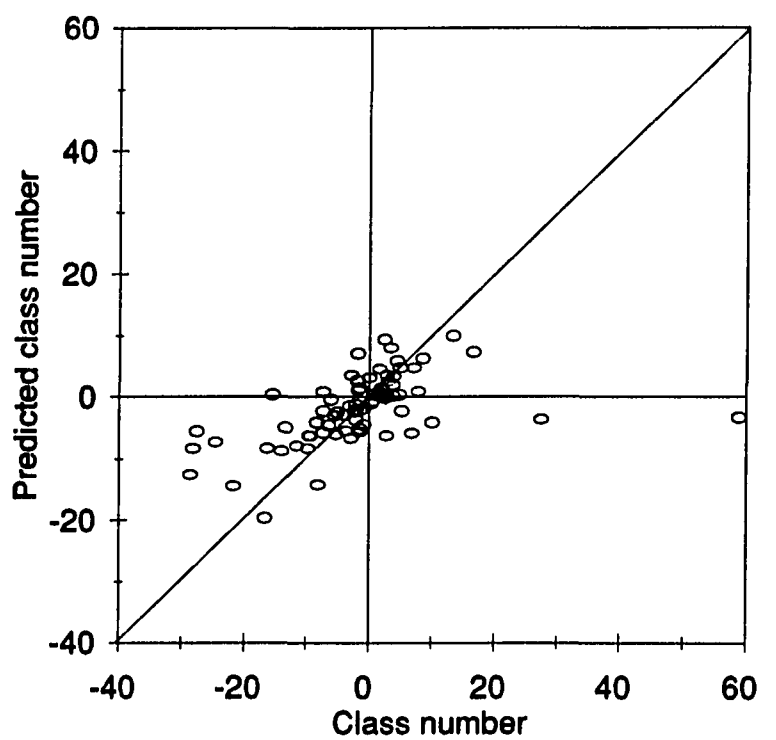
60
40
20
0
-20
-40
Predicted class number
-40
-20
0
20
40
60
Class number

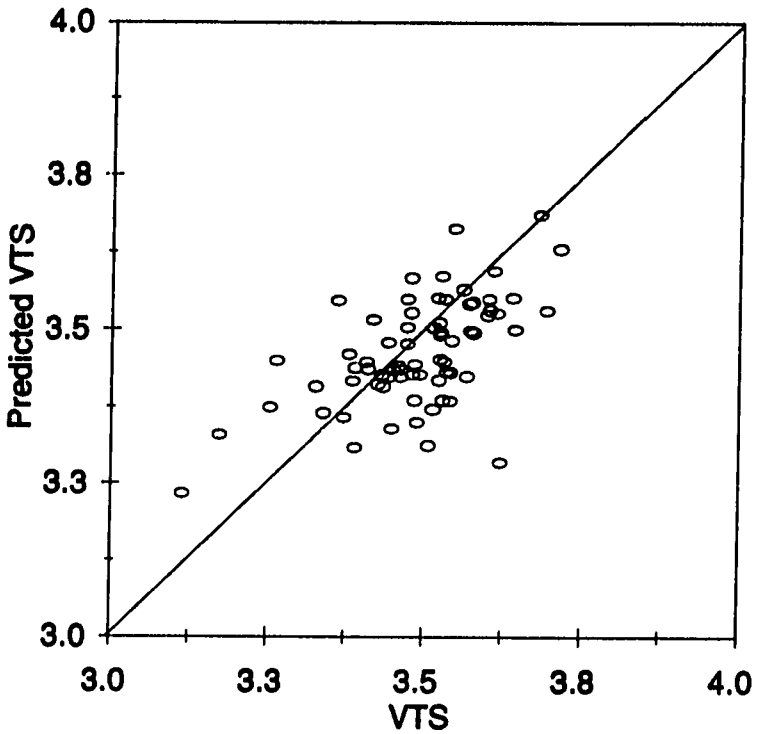
4.0
3.8
3.5
3.3
3.0
Predicted VTS
3.0
3.3
3.5
3.8
4.0
VTS

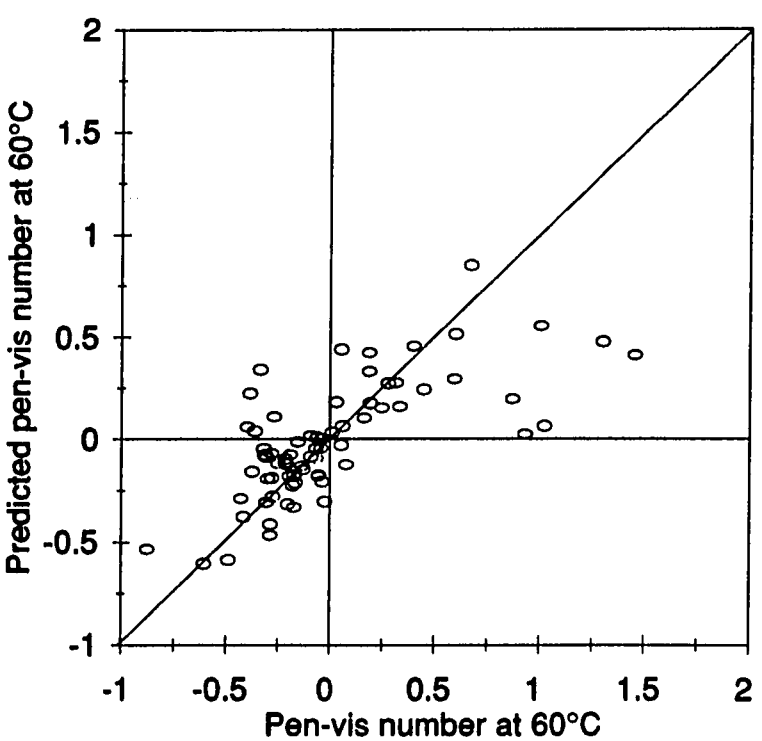
2
1.5
1
0.5
0
-0.5
-1
Predicted pen-vis number at 60°C
-1
-0.5
0
0.5
1
1.5
2
Pen-vis number at 60°C

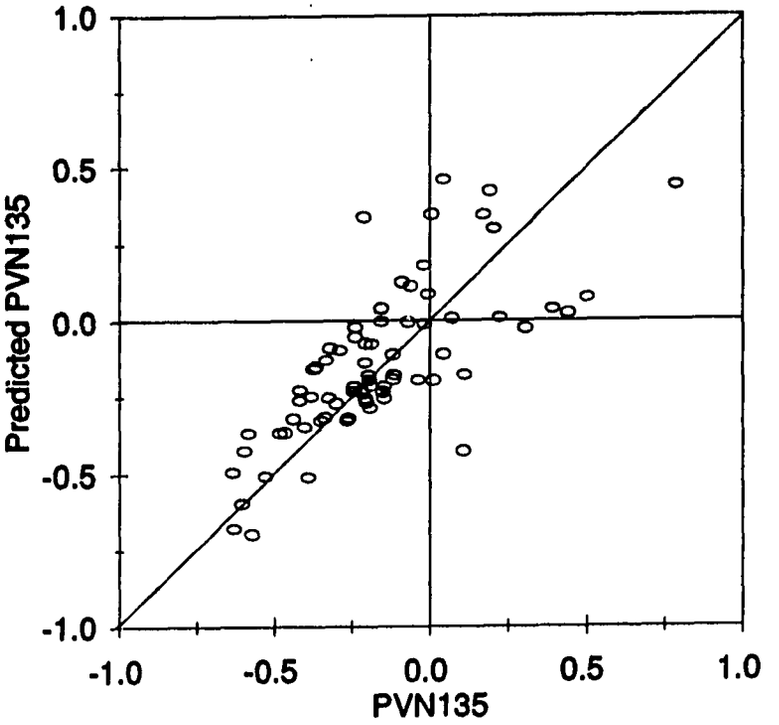
1.0
0.5
0.0
-0.5
-1.0
Predicted PVN135
-1.0
-0.5
0.0
0.5
1.0
PVN135

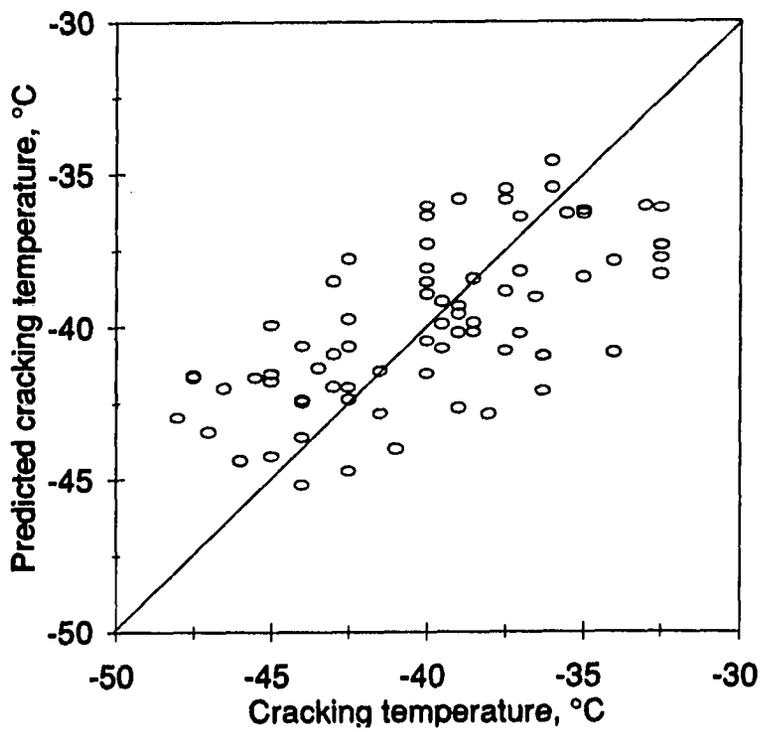
-30
-35
-40
-45
-50
Predicted cracking temperature, °C
-50
-45
-40
-35
-30
Cracking temperature, °C

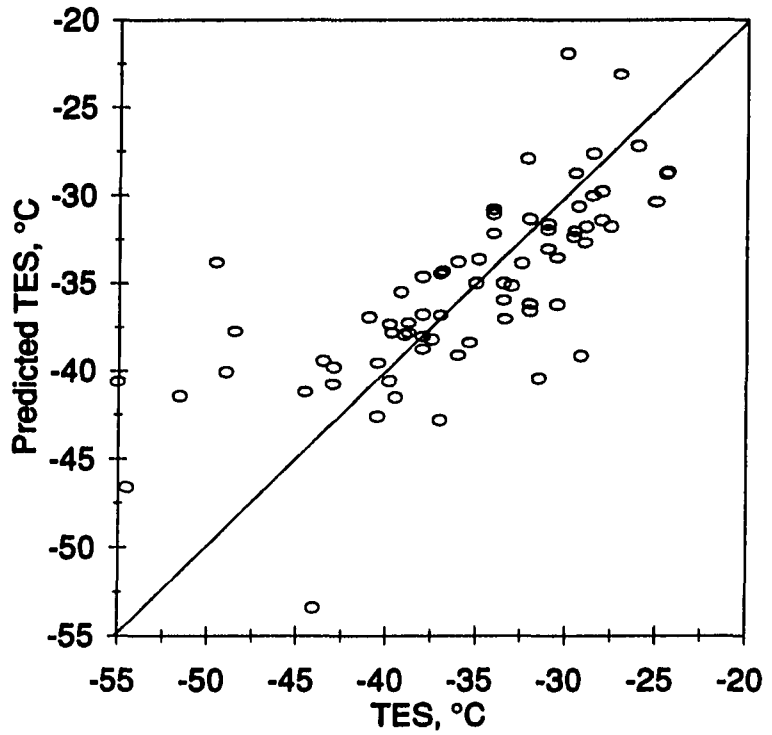
-20
-25
-30
-35
-40
-45
-50
-55
Predicted TES, °C
-55 -50 -45 -40 -35 -30 -25 -20
TES, °C

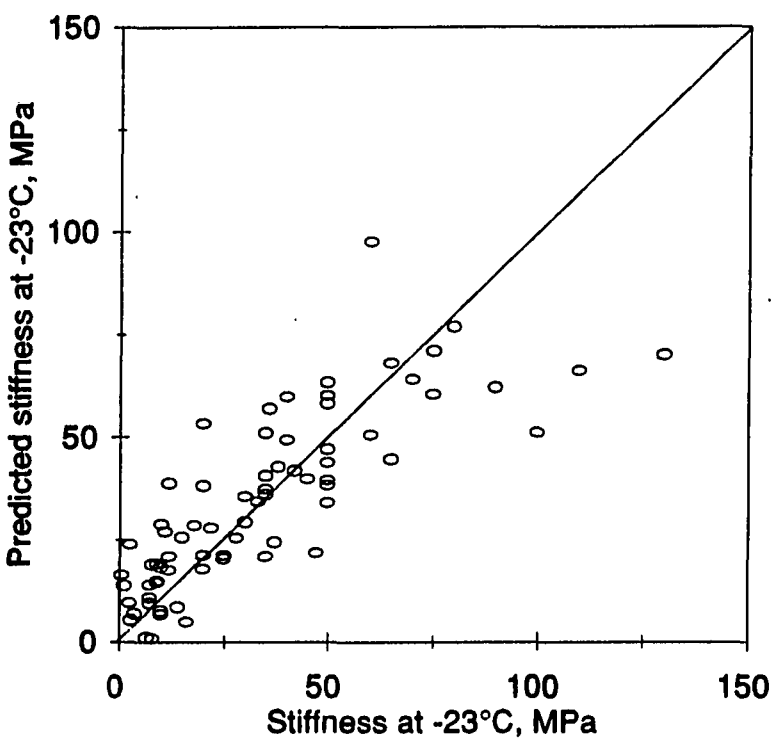
150
100
50
0
Predicted stiffness at -23°C, MPa
0 50 100 150
Stiffness at -23°C, MPa

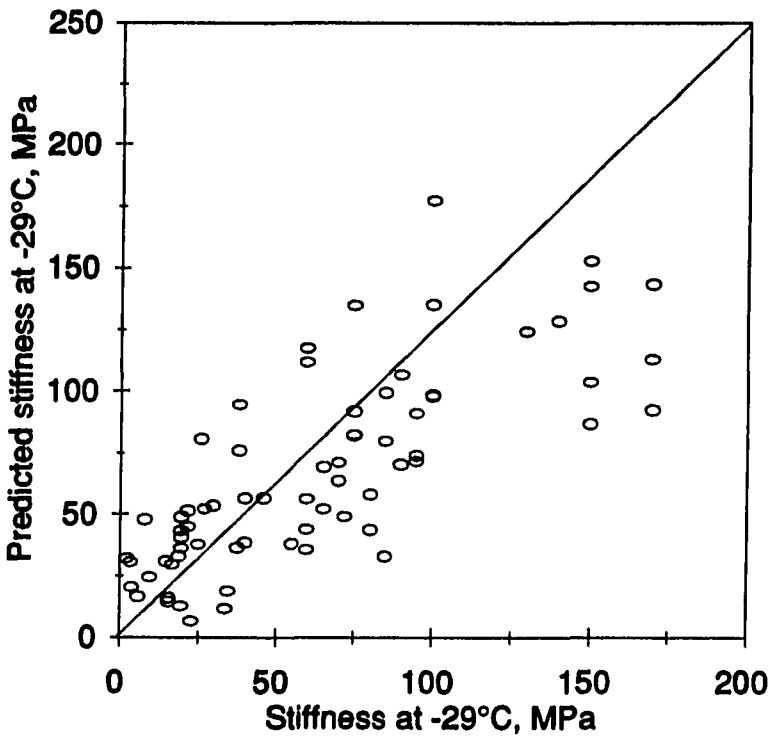
Predicted stiffness at -29°C, MPa
250
200
150
100
50
0
0
50
100
150
200
Stiffness at -29°C, MPa